Graduation thesis

March 2019

The modular post-earthquake shell

A multi-objective parametric structural design approach

Follow-up thesis to a previous graduation project in the field of architecture:

Opportunity in Chaos; Triggering revival of the damaged historic town centres of Italy

Author	Ir. J.D. Jimmink	
Graduation committee	Prof. Ir. R. Nijsse (chairman)	TU Delft
	Dr. Ir. G.J.P. Ravenshorst	TU Delft
	Dr. Ir. F.A. Veer	TU Delft
	Dr. H.M. Jonkers	TU Delft
	Dr. Ir. M. Palmieri	Arup NL

Delft University of Technology
Faculty of Civil Engineering and Geosciences
Department Structural Engineering
Stevinweg 1 | 2628 CN Delft
P.O. box 5048 | 2600 GA Delft

Arup Netherlands
Department Seismic Engineering
Department Computational Design
Beta Building
Naritaweg 118 | 1043 CA Amsterdam

© Joanne Jimmink, 2019. ALL RIGHTS RESERVED.

List of abbreviations

Latin upper-case letters

A	Cross-sectional area
A_{net}	Net cross-sectional area
$CHSH$	Circular Hollow Section Hot-rolled (steel)
E	Modulus of elasticity
$E_{m,0,k}$	5th-Percentile modulus of elasticity for bending parallel to the grain (timber)
$E_{m,0,mean}$	Mean modulus of elasticity for bending parallel to the grain (timber)
$E_{m,90,mean}$	Mean modulus of elasticity for bending perpendicular to the grain (timber)
$ETFE$	Ethylene tetrafluoroethylene, a fluorine-based plastic
F	Load
$F_{v,Ed}$	Design value of the load per bolt
$F_{v,Rd}$	Design value of the strength per bolt
$F_{v,Rk}$	Characteristic value of the strength per bolt
G	Shear modulus
G_{mean}	Mean shear modulus
I_{net}	Net moment of inertia
$K_{r,ser}$	Rotational stiffness of bolted connection
K_{ser}	Joint slip modulus
K_u	Ultimate joint slip modulus
M_{Ed}	Design value of bending moment
M_y	Bending moment around Y-axis
$M_{y,Rk}$	Characteristic yield moment of a bolt
M_z	Bending moment around Z-axis
N	Axial load
N_{Ed}	Design value of axial load
PL	Point load
SLS	Serviceability Limit State
SLO	*Stato Limite di Operatività* (seismic limit state, concerning immediate operativity)
SLD	*Stato Limite di Danno* (seismic limit state, concerning damage control)
SLV	*Stato Limite di salvaguardia della Vita* (seismic limit state, concerning life safety)
SLC	*Stato Limite di prevenzione del Collasso* (seismic limit state, concerning collapse prevention)
UDL	Uniformly distributed load
ULS	Ultimate Limit State
V_{Ed}	Design value of shear load
V_y	Shear load Y-axis
V_z	Shear load Z-axis
W_{net}	Net section modulus

X_d	Design value of any strength property (timber)
X_k	Characteristic value of any strength property (timber)

Latin lower-case letters

a	Acceleration
a_1	Required spacing between bolts, parallel to the element (timber)
a_2	Required spacing between bolts, perpendicular to the element (timber)
$a_{3,c}$	Required spacing next to bolt on unloaded side of member (timber)
$a_{3,t}$	Required spacing next to bolt on loaded side of member (timber)
$a_{4,c}$	Required spacing between bolt and unloaded side of member (timber)
$a_{4,t}$	Required spacing between bolt and loaded side of member (timber)
c_{pe}	External wind pressure coefficient
c_{pi}	Internal wind pressure coefficient
$c_{p,net}$	Net wind pressure coefficient
d	Bolt diameter
$f_{c,0,d}$	Design value of the compressive strength parallel to the grain (timber)
$f_{c,0,k}$	Characteristic value of the compressive strength parallel to the grain (timber)
$f_{c,90,d}$	Design value of the compressive strength perpendicular to the grain (timber)
$f_{c,90,k}$	Characteristic value of the compressive strength perpendicular to the grain (timber)
$f_{h,k}$	Characteristic value of the bearing strength (timber)
$f_{h,0,k}$	Characteristic value of the bearing strength parallel to the grain (timber)
$f_{h,\alpha,k}$	Characteristic value of the bearing strength at an angle α with the grain (timber)
$f_{m,y,d}$	Design value of the bending strength around the y-axis (timber)
$f_{m,z,d}$	Design value of the bending strength around the z-axis (timber)
$f_{m,y,k}$	Characteristic value of the bending strength around the y-axis (timber)
$f_{m,z,k}$	Characteristic value of the bending strength around the z-axis (timber)
$f_{t,0,d}$	Design value of the tensile strength parallel to the grain (timber)
$f_{t,0,k}$	Characteristic value of the tensile strength parallel to the grain (timber)
$f_{t,90,d}$	Design value of the tensile strength perpendicular to the grain (timber)
$f_{t,90,k}$	Characteristic value of the tensile strength perpendicular to the grain (timber)
f_u	Nominal tensile strength of the weakest connected part of a weld;
$f_{v,d}$	Design value of the shear strength (timber)
$f_{v,k}$	Characteristic value of the shear strength (timber)
f_y	Yield strength (steel)
$f_{y,d}$	Design value of the yield strength (steel)
k_{90}	Factor depending on the type of timber
k_m	Factor taking into account the stress redistribution and the heterogeneity of the material in its cross section (timber)
k_{mod}	Modification factor taking into account load duration and moisture content (timber)
m	Mass

t	Timber thickness on either side of the steel plate (connection design)
q_p	General wind pressure
z	Height above the ground (wind calculations)
z_{max}	Maximal distance from cross-section gravitational centre to outer fibre

Greek lower-case letters

α	Angle of the load with the grain (timber)
α_T	Coefficient of thermal expansion
β_w	Correlation factor depending on the steel strength of the connected parts of a weld;
γ	Specific weight
γ_M	Partial material factor
ρ_{mean}	Mean density
ρ_k	Characteristic density
$\sigma_\perp$	Axial stress perpendicular to the throat section of a weld
$\sigma_{c,0,d}$	Design value of the stresses due to compression parallel to the grain (timber)
$\sigma_{c,90,d}$	Design value of the stresses due to compression perpendicular to the grain (timber)
$\sigma_{m,y,d}$	Design value of stresses due to bending around the y-axis (timber)
$\sigma_{m,z,d}$	Design value of stresses due to bending around the z-axis (timber)
$\sigma_{t,0,d}$	Design value of the stresses due to tension parallel to the grain (timber)
$\sigma_{x,Ed}$	Axial stresses (steel)
σ_N	Axial stresses
$\tau_\perp$	Shear stress (in the throat section) perpendicular to the length-axis of the weld;
$\tau_\parallel$	Shear stress (in the throat section) parallel to the length-axis of the weld;
τ_d	Design value of the stresses due to shear (timber)
τ_{Ed}	Shear stresses (timber)

List of equations

Equation 1 56
Equation 2 57
Equation 3 57
Equation 4 57
Equation 5 57
Equation 6 58
Equation 7 58
Equation 8 58
Equation 9 59
Equation 10 59
Equation 11 88
Equation 12 88
Equation 13 88
Equation 14 88
Equation 15 89
Equation 16 89
Equation 17 89
Equation 18 89
Equation 19 89
Equation 20 90
Equation 21 90
Equation 22 90
Equation 23 102
Equation 24 137
Equation 25 137
Equation 26 138
Equation 27 138
Equation 28 138
Equation 29 138
Equation 30 138

List of figures

Figure 1: Architectural design xi
Figure 2: Workflow xi
Figure 3: Impression of structural variations xii
Figure 4: Top-ranking designs xii
Figure 5: Top-1 design xiii
Figure 6: Proposed connection design xiii
Figure 7: Horizontal elastic response spectrum xiv
Figure 8: Deflection envelope xiv
Figure 9: Location | L'Aquila, Italy 24
Figure 10: Current post-disaster approach 25
Figure 11: Alternative post-disaster approach 25
Figure 12: Community (recovery) centre 25
Figure 13: Location | Piazza del Duomo, L'Aquila 26
Figure 14: Piazza del Duomo 26
Figure 15: Architectural design 27
Figure 16: Triple-layered ETFE cushions for climate control 27
Figure 17: Natural ventilation through Venturi roof elements 28
Figure 18: Exploded view 28
Figure 19: Flexible room dividers 29
Figure 20: Different possible floor plans | Option A (top) & Option B (bottom) 29
Figure 21: Main load-bearing structure 30
Figure 22: General loads 30
Figure 23: Wind load distribution 31
Figure 24: Connection detail 31
Figure 25: Elevated floor module 32
Figure 26: Floor & Structure detail 32
Figure 27: Optimisation scope 33
Figure 28: Workflow graduation project 34
Figure 29: Grid size | Two variations with element size of 2.6m (left) and of 1.0m (right) 37
Figure 30: Basic geometry | Rigid connections (L) & Combined connections (R) 38
Figure 31: No in-plane additions 38
Figure 32: All horizontals 39
Figure 33: BESO-horizontals 39
Figure 34: Deformations 39
Figure 35: No out-of-plane additions 40
Figure 36: Two trusses (left) & Three trusses (right) 40
Figure 37: Self-weight 45
Figure 38: Exterior façade loads (left) & interior façade loads (right) 46
Figure 39: East zone, middle zone & West zone 46

Figure 40: East side & west side 46
Figure 41: Wind load 1, North | Middle zone 47
Figure 42: Wind load 1, North | East & West zone 47
Figure 43: Wind load 2, South | Middle zone 47
Figure 44: Wind load 2, South | East & West zone 48
Figure 45: Wind load 2, South | East & West side 48
Figure 46: Wind load 3, Side | East, Middle & West zone 48
Figure 47: Wind load 3, Side | East & West side 49
Figure 48: Snow load 1 | Before redistribution 49
Figure 49: Snow load 2 & 3 | After redistribution 50
Figure 50: Maintenance UDL | Middle & Side 50
Figure 51: Maintenance point load | Middle & Side 51
Figure 52: Zoning seismic loading 51
Figure 53: Seismic actions X-direction | Zone 1 (L) & Zone 2 (R) 52
Figure 54: Seismic actions X-direction | Zone 3 (L) & Zone 4 (R) 52
Figure 55: Seismic actions X-direction | Zone 5 (L) & Zone 6 (R) 52
Figure 56: Seismic actions X-direction | Zone 7 (L) & Zone 8 (R) 53
Figure 57: Seismic actions Y-direction | Zone 1 (L) & Zone 2 (R) 53
Figure 58: Seismic actions Y-direction | Zone 3 (L) & Zone 4 (R) 53
Figure 59: Seismic actions Y-direction | Zone 5 (L) & Zone 6 (R) 54
Figure 60: Seismic actions Y-direction | Zone 7 (L) & Zone 8 (R) 54
Figure 61: Fraction of D24 to be replaced 62
Figure 62: Fraction of D70 to be replaced 64
Figure 63: Annual environmental burden per kg structure 65
Figure 64: Environmental burden over lifetime of 50 years per kg of structure 66
Figure 65: Conceptual joint design steel structure (top) and timber structure (bottom) 67
Figure 66: Annual environmental burden per joint 69
Figure 67: Environmental burden over lifetime of 50 years per joint 70
Figure 68: Scatter plot of the full database (10 836 models) 72
Figure 69: Scatter plot | Steel configurations (S235) 73
Figure 70: Scatter plot | Steel configurations (S355) 73
Figure 71: Scatter plot | Timber configurations (D70) 74
Figure 72: Scatter plot | Combined configurations (D70 & S355) 74
Figure 73: First round of exclusion | Unity check > 1.0 76
Figure 74: Remainder of models after first round of exclusion 77
Figure 75: Second round of exclusion | Element weight > 40kg 77
Figure 76: Remainder of models after second round of exclusion 78
Figure 77: Extracting the environmental top-scorers 78
Figure 78: Most environmentally friendly models 79
Figure 79: Top 28 designs 80
Figure 80: Structural design (Rank 1 out of 28) 82
Figure 81: Stresses in the timber structure (the steel trusses are hidden) 84

Figure 82: Stresses in the trusses (the timber structure is hidden)........85
Figure 83: Conceptual joint design........86
Figure 84: Spacing requirements bolts in timber........87
Figure 85: Possible failure mechanisms connection (EN 1995-1-1, 2011)........88
Figure 86: Stresses in weld throat........90
Figure 87: Local axes | Diagonals (left) and horizontals (right)........91
Figure 88: Redefinition interaction between trusses and main structure........91
Figure 89: Connection design........92
Figure 90: Spacing requirements bolt configuration........93
Figure 91: Horizontal elastic response spectrum of L'Aquila, Italy........100
Figure 92: Mode 47 (top) & Mode 57 (bottom)........101
Figure 93: Mode 1........101
Figure 94: Deflection response spectrum analysis 1........102
Figure 95: Deflection response spectrum analysis 2........103
Figure 96: Final design selection........107
Figure 97: Final structural design | Perspective (top) & top view (bottom)........108
Figure 98: High loads (black) vs. low loads (grey)........109
Figure 99: Stresses in truss........109
Figure 100: Truss | Members inner layer (left) & outer layer (right)........109
Figure 101: Truss | Supporting members (left) and connecting members A (right)........110
Figure 102: Truss | Connecting members B........110
Figure 103: Perspective and top view of the structural concept (top) and the final structural design (bottom).112
Figure 104: Weak direction........112
Figure 105: Integrated trusses (left) & separate trusses (right)........113
Figure 106: Big joints (black) vs. small joints (grey)........113
Figure 107: Success rate of different cross sections........116
Figure 108: Determination $c_{pe,10}$ for curved roofs (Eurocode 1, Fig. 7.11)........123
Figure 109: Open roofs (Eurocode 1, Fig. 7.15)........124
Figure 110: Zoning of vertical sides of buildings (Eurocode 1, Fig. 7.5)........125
Figure 111: Snow load coefficients for cylinder roofs (Eurocode 1, Fig. 5.6)........126
Figure 112: Distribution axial loads among bolts........137
Figure 113: Distribution shear loads among bolts........137
Figure 114: Distribution bending loads among bolts........138
Figure 115: Elastic response spectra, L'Aquila, Italy........141

List of tables

Table 1: Top 3 ... xii
Table 2: Grid size variations ... 37
Table 3: Steel properties ... 41
Table 4: Durability classes of wood and wood-based products (EN 350, 2016) ... 42
Table 5: Properties of strength class D24 (NEN-EN 338) ... 42
Table 6: Properties of strength class D70 (NEN-EN 338) ... 43
Table 7: Load combinations ... 55
Table 8: Environmental impact per kg steel ... 62
Table 9: Environmental impact per kg chestnut ... 63
Table 10: Environmental impact per kg azobé ... 65
Table 11: Results steel structure joints ... 68
Table 12: Results timber structure joints ... 69
Table 13: Environmental impact values for Grasshopper-script ... 71
Table 14: Properties of top-ranking structural variations ... 81
Table 15: Spacing requirements bolts in timber ... 87
Table 16: Eliminations due to model refinement ... 92
Table 17: Final design selection ... 106
Table 18: Maximal stresses per part of the truss ... 110
Table 19: $c_{p,net}$ values for open roof structures (Eurocode 1, Table 7.7) ... 124
Table 20: $c_{p,net}$ values for free-standing walls (Eurocode 1, Table 7.9) ... 125
Table 21: $c_{pe,10}$ values for vertical sides of buildings (Eurocode 1, Table 7.1) ... 125
Table 22: Properties elastic response spectra, L'Aquila, Italy ... 140

Summary

In April, 2018, a graduation project in the field of architecture was concluded. The project entailed the design of a temporary community centre in the earthquake-damaged historic town centre of L'Aquila, Italy. The underlying social concept was focused on participation of the local population – a critical element missing from the present recovery policy. The design – shown in Figure 1 – includes a grid-like timber shell structure, built-up out of a repetition of only two main structural and light-weight elements: the members and the joints.

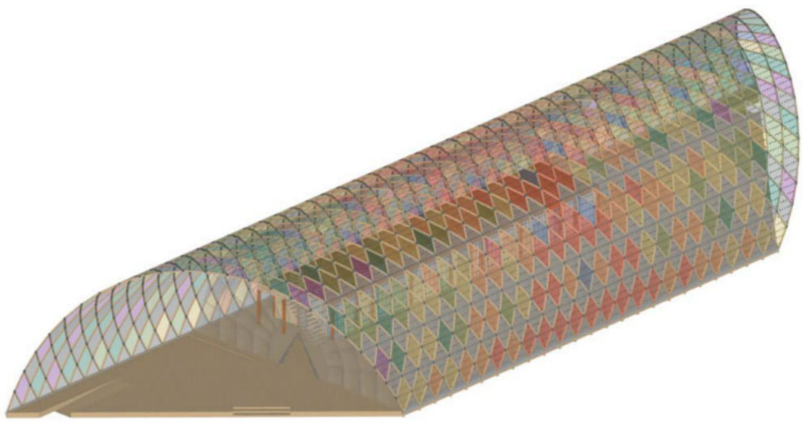

Figure 1: Architectural design

The load-bearing structure of this conceptual design formed the basis for this graduation thesis, which is aimed at its optimisation. The optimisation is carried out focused on many objectives, e.g. its weight, its environmental impact, its structural validity. The goal of this thesis can be summarised in the following research question:

Given the architectural design, how can the main load-bearing structure be optimised for seismic contexts using parametric modelling, considering the following objectives: maximal demountability and structural simplicity, minimal material use, structural weight and environmental impact?

Though automated optimisation tools are available on the market, a method has been chosen combining automated and manual processes, as this gives a high sense of control to the designer. The workflow is shown in Figure 2.

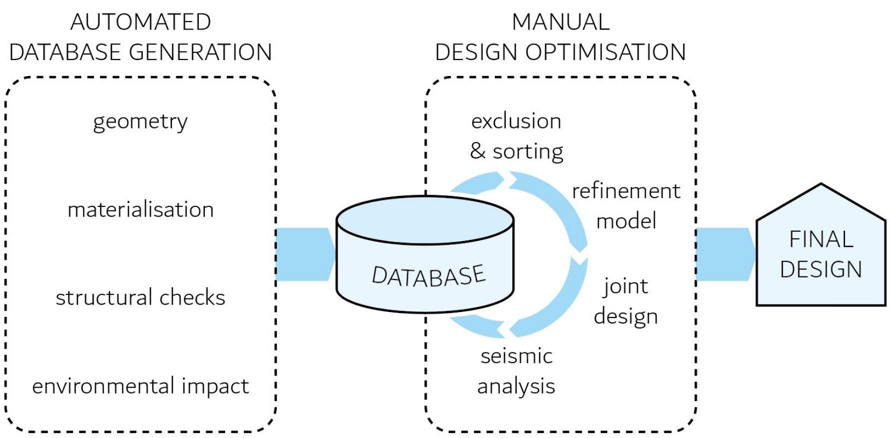

Figure 2: Workflow

Using computational and parametric modelling techniques (Rhino, Grasshopper and Karamba), a database comprising 10 836 different structural configurations has been automatically generated using different geometries and materials, some of which are presented in Figure 3. Loads and load combinations have been defined and applied to each model parametrically.

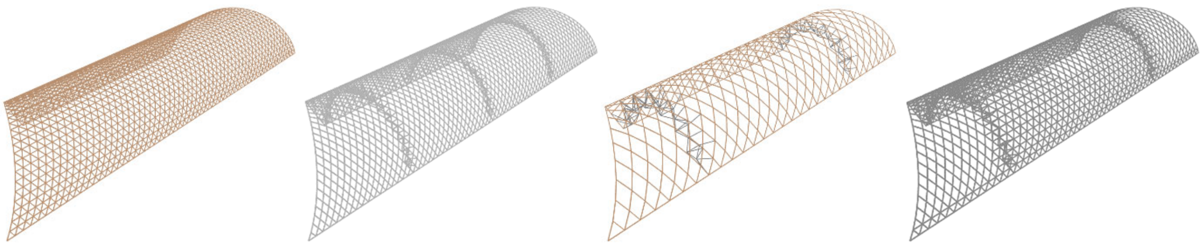

Figure 3: Impression of structural variations

The database contains the generated outcome to structural and environmental analyses for each of the structural configurations. Based on this outcome the database entries has been ranked through exclusion – in case the variation fails structurally – and sorting by its relative environmental impact and compliance with the architectural design and concept. As a result, a top 28 of structural configurations has been defined as presented in Figure 4.

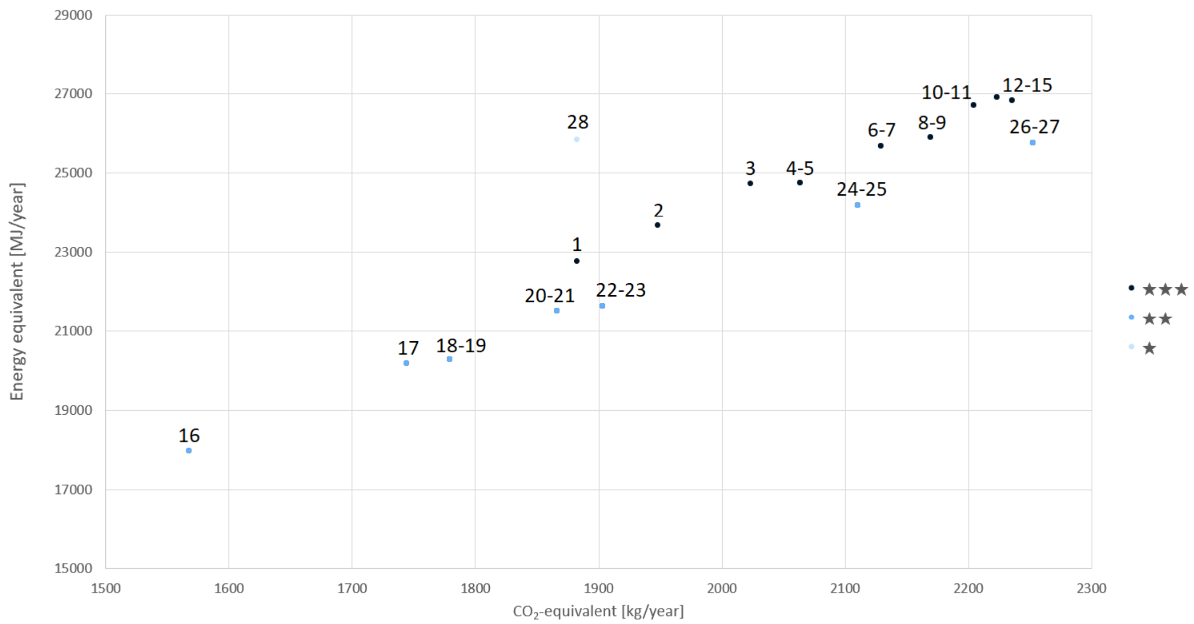

Figure 4: Top-ranking designs

Properties for the three highest-ranking models are shown in Table 1. The Top-1 model consists out of a timber main structure, with three steel trusses underneath, see Figure 5.

Table 1: Top 3

Rank	Basic geometry	In-plane variations	Out-of-plane variations	Cross sections main structure	Cross sections trusses	Element length [m]	Element mass [kg]
1	No hinges	Triangles	3 trusses	D70 150.0 × 150.0 mm²	S355 CHSH 114.3 × 8	1.7	30.5
2	No hinges	Triangles	3 trusses	D70 150.0 × 150.0 mm²	S355 CHSH 139.7 × 8	1.7	30.5
3	No hinges	Triangles	3 trusses	D70 150.0 × 150.0 mm²	S355 CHSH 168.3 × 8	1.7	30.5

Having defined a ranked set of structural configurations, checks and iterations can take place. The first step is to refine the digital model of the structure based on the proposed joint design: hinges are modelled at weak spots and rigid connections are reduced to rotational hinges. This eliminates some of the options in the list of top-ranking designs, as they become unstable.

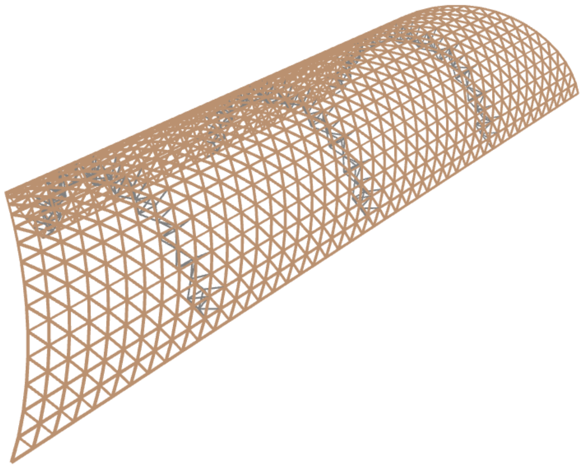

Figure 5: Top-1 design

The next step is to structurally verify the proposed connection detail – see Figure 6. The bolts, the steel plates, the welds and its weight have been checked. It complies with all demands and therefore, no iterations have to take place. The Top-1 design is still in the running.

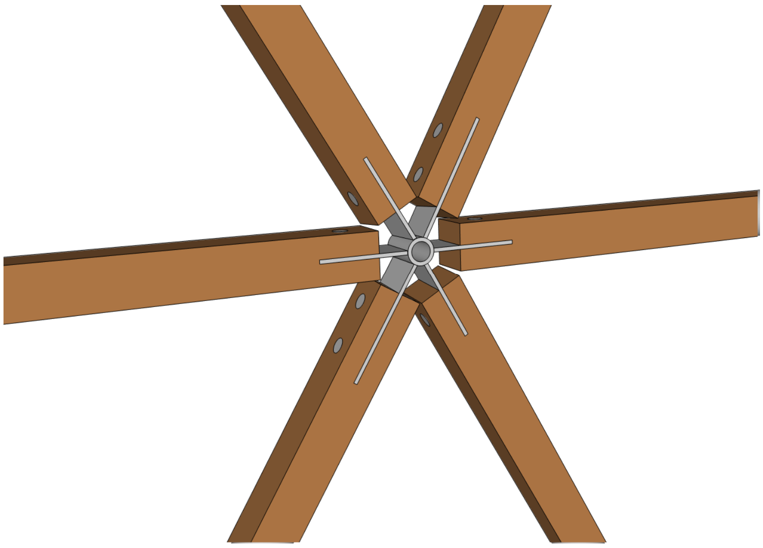

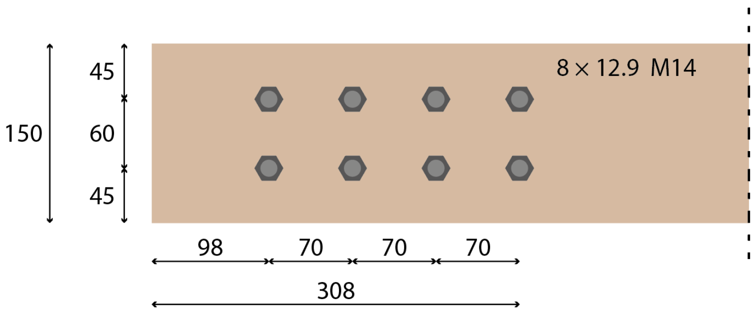

Figure 6: Proposed connection design

The final calculation that needs to be carried is out is with regard to its safety in seismic occurences. The type of analysis carried out is a response spectrum analysis. This analysis is based on the eigenmodes of the structure and the participating mass in both the global X- and Y-direction of the design. Using these masses and the accelerations in the elastic response spectrum of L'Aquila, Italy (see Figure 7), which are directly related to the eigenmodes of the structure, loads have been generated.

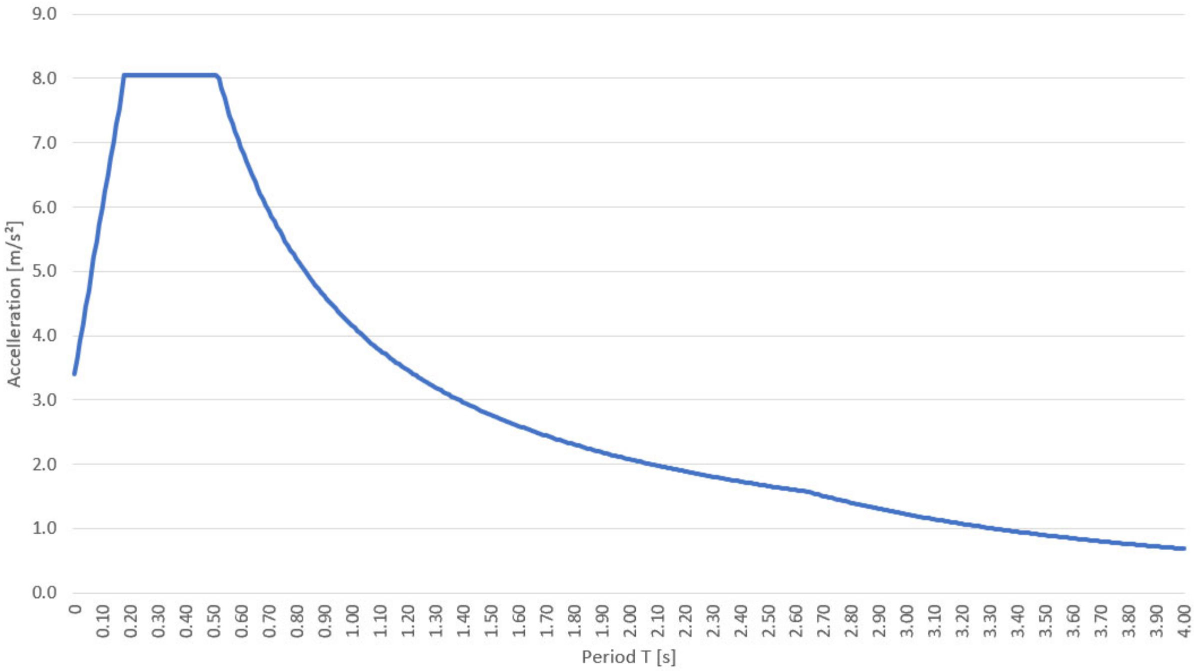

Figure 7: Horizontal elastic response spectrum

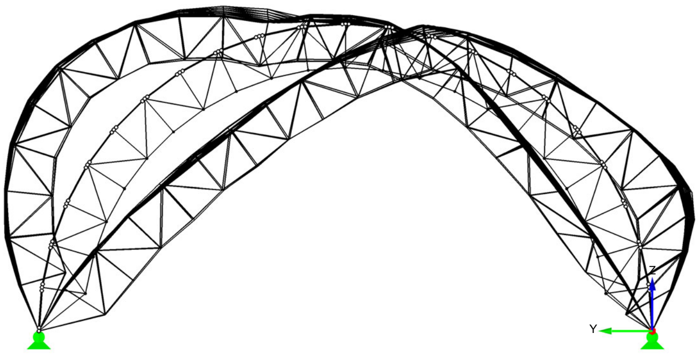

Figure 8: Deflection envelope

The accumulated modes and accompanying loads results in the deflection envelope as presented in Figure 8. The loads that occur as a consequence of this analysis are not governing for the timber structure, but they are governing for the steel trusses underneath the timber structure. However, the steel cross section proposed for the trusses still comply with the structural demands and therefore, the Top-1 design has passed all structural analyses and no iterations were necessary.

In conclusion, with regard to the design, further structural optimisation could take place by reconsidering the shape of the structure. However, the process of automated database generation and manual exclusion, sorting and iterated checks give a great sense of control compared to automated optimisation alternatives. This optimisation process has proven to be very effective in finding a design that balances all objectives well.

Acknowledgements

Having obtained a bachelor's and master's degree in the field of architecture, on April 1, 2019, the time has come to finish my student life at Delft University of Technology when I conclude my second master's at the faculty of civil engineering.

After finishing the architectural bachelor's, I took a gap year doing an internship at WAM architecten, trying to figure out what step to take next. Did I want to continue my career in the beautiful and creative architectural sector, or did I want to transition to civil engineering to be able to apply my love for mathematics in a more technical field? Being torn between my options, I planned a meeting with study counsellor Pascal de Smidt. I am grateful he opened my eyes to the possibility of doing both master programs, which I did not consider an option before. This option would result in at least five more years of studying – including a bridging year to obtain relevant knowledge in the field of civil engineering and twice a two-year master's program, i.e. architecture and structural engineering. I decided to follow up on his advice to do both and though it required time, it has been very rewarding.

While carrying out my final project in the field of architecture, preparation needed to be done for my next graduation thesis. I hoped to be able to carry out a follow-up research that included my own architectural design, but I did not know whether this would be a feasible option. It was not until I had a consultation with Fred Veer regarding my architectural design, that I realised this would indeed be a feasible option. I planned a meeting with Rob Nijsse, who also saw the potential of a follow-up project and who agreed to be the chair of my graduation committee. I want to express my gratitude to him for his guidance during my graduation thesis and, furthermore, his solid advice regarding my follow-up career choices. The committee was joined by three more members from the Delft University of Technology, whom I would like to thank; Fred Veer, for pointing me in the right direction at the beginning of my second graduation and for his interest in following this transition; Henk Jonkers, who introduced me to and guided me through the world of environmental analysis; and lastly, Geert Ravenshorst, who took his time to tutor me with his extensive knowledge in the field of timber engineering.

Originally, I intended to carry out this thesis individually, but an exciting opportunity arose. Beatriz Zapico, who was my advisor during my first graduation project, introduced me to Arup, the company she worked at. I am very grateful to her, as this introduction has not only led to an opportunity to cooperate with this great company and use their vast experience during my thesis, but also to my first job after conclusion of my student life. Through her I got to know Michele Palmieri, who joined my graduation committee on behalf of Arup and whom I would like to thank for his professional guidance in the field of seismic engineering and his enthusiasm about the graduation project from the get-go.

Furthermore, I am grateful to both of my other tutors at Arup, Rick Titulaer and Alex Christodoulou, who have introduced me to the wonderful world of parametric design and engineering, and who have had a significant influence on the path that my graduation has taken. Apart from my assigned tutors, I would like to thank my other colleagues at Arup for their professional advice and for providing me with such a pleasant work environment.

During my last year as a student, I also got the opportunity to gain professional experience as an employee at the marvellous company Octatube. The knowledge I gained there is reflected in the work I have done and I thank my colleagues for granting me advice throughout my project, and for giving me Tuesdays to look forward to.

I would also like to thank my friends, who have supported me and kept me sane throughout the lengthy study path I have chosen – let us have a drink soon to celebrate its conclusion!

And last but not least, I would like to express my gratitude to the ones closest to me. Sis, mom, dad, I would not have been able to reach this milestone without your undying love and support – in every sense of the word.

Conventions

Global coordinate system

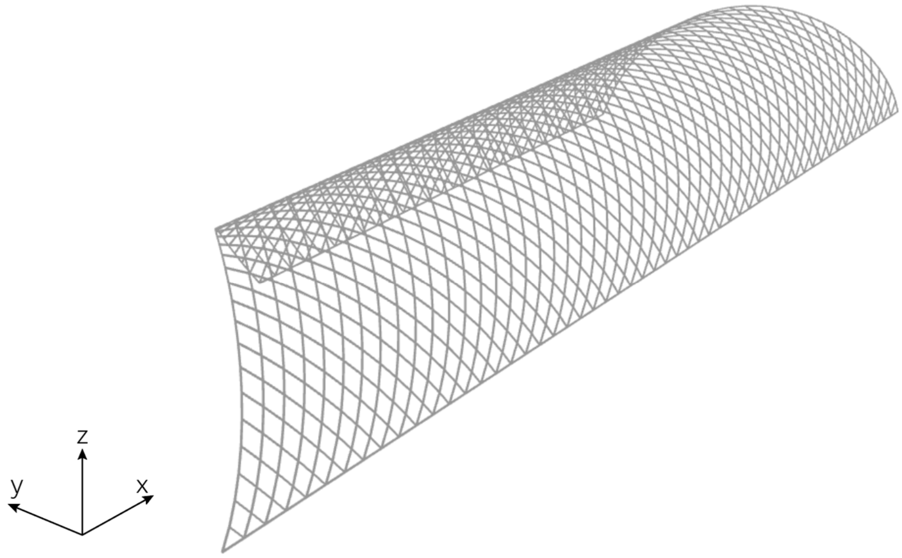

Local coordinate system

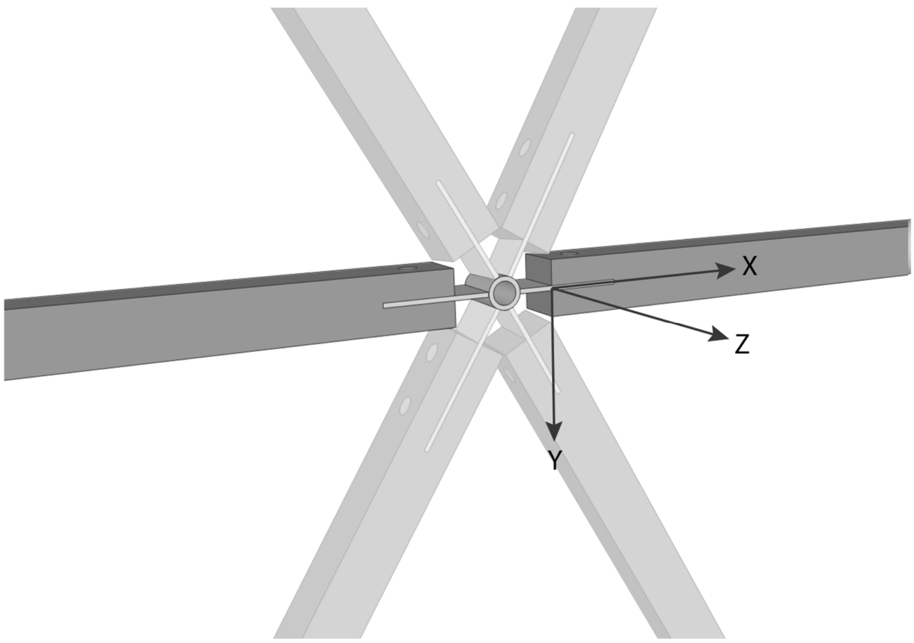

Contents

List of abbreviations ... iii
List of equations ... vi
List of figures ... vii
List of tables ... x
Summary ... xi
Acknowledgements ... xv
Conventions ... xvi
Global coordinate system ... xvi
Local coordinate system ... xvi

Introduction ... 22

I FRAMEWORK ... 23
1 Background ... 24
1.1 Introduction ... 24
1.2 Context ... 24
1.3 Architectural design ... 25
1.3.1 Concept & ideals ... 25
1.3.2 General design ... 27
1.3.3 Structural design ... 29
1.4 Conclusion ... 32
2 Approach ... 33
2.1 Introduction ... 33
2.2 Aim ... 33
2.3 Research question ... 33
2.4 Scope ... 33
2.5 Research method ... 34
2.6 Software ... 34
2.7 Conclusion ... 35

II DATABASE GENERATION ... 36
3 Geometry ... 37
3.1 Introduction ... 37
3.2 Grid size (7 variations) ... 37
3.3 Basic geometry (2 variations) ... 38
3.4 In-plane variations (3 variations) ... 38
3.5 Out-of-plane variations (3 variations) ... 39

3.6 Conclusion 40
4 Materialisation 41
4.1 Introduction 41
4.2 Material properties 41
4.2.1 Steel (Karamba) 41
4.2.2 Timber (Karamba) 41
4.3 Cross sections 43
4.3.1 Steel structure 43
4.3.2 Timber structure 44
4.3.3 Steel & timber structure 44
4.4 Conclusion 44
5 Loads 45
5.1 Introduction 45
5.2 Permanent loads 45
5.2.1 Self-weight 45
5.2.2 Other permanent loads 45
5.3 Wind actions 46
5.3.1 Zoning 46
5.3.2 North wind 47
5.3.3 South wind 47
5.3.4 Side wind 48
5.4 Snow actions 49
5.5 Imposed loads 50
5.5.1 Maintenance: Uniformly distributed load (UDL) 50
5.5.2 Maintenance: Point load (PL) 50
5.6 Seismic actions 51
5.6.1 Seismic actions in X-direction 52
5.6.2 Seismic actions in Y-direction 53
5.7 Load combinations 55
5.8 Conclusion 55
6 Unity Checks 56
6.1 Introduction 56
6.2 Steel 56
6.3 Timber 56
6.3.1 Axial tension 57
6.3.2 Axial compression 57
6.3.3 Bending 57
6.3.4 Shear 58
6.3.5 Combination: bending & axial tension 58
6.3.6 Combination: bending & axial compression 59

6.4 Conclusion 59
7 Environmental impact analysis 60
7.1 Introduction 60
7.1.1 CES EduPack 2018 60
7.2 Main structure 60
7.2.1 Steel 61
7.2.2 Timber: D24 (Chestnut) 62
7.2.3 Timber: D70 (Azobé) 64
7.2.4 Annual environmental burden per kg structure 65
7.3 Structural joints 67
7.3.1 Conceptual joint design 67
7.3.2 Joints steel structure 68
7.3.3 Joints timber structure 68
7.3.4 Annual environmental burden per kg structure 69
7.4 Pre-exclusion 71
7.5 Summary 71
7.6 Conclusion 71
8 Database 72
8.1 Introduction 72
8.2 Database entries 72
8.3 Conclusion 74

III DESIGN OPTIMISATION 75
9 Database ranking 76
9.1 Introduction 76
9.2 Exclusion 76
9.2.1 First step: structural validation 76
9.2.2 Second step: element weight validation 77
9.3 Sorting process 78
9.3.1 First step: environmental impact 78
9.3.2 Second step: architectural value 79
9.4 Conclusion 81
10 Structural validation 82
10.1 Introduction 82
10.2 Factors 83
10.3 Timber check 83
10.4 Steel check 85
10.5 Conclusion 85
11 Connection design 86
11.1 Introduction 86

11.2 Approach ... 86
11.2.1 Spacing between bolts ... 86
11.2.2 Rotational stiffness ... 87
11.2.3 Check: bolts ... 88
11.2.4 Check: steel plates ... 90
11.2.5 Check: welds ... 90
11.3 Model refinement ... 91
11.4 Connection design ... 92
11.4.1 Distances between bolts ... 92
11.4.2 Rotational stiffness ... 93
11.4.3 Check: bolts ... 94
11.4.4 Check: steel plates ... 95
11.4.5 Check: welds ... 97
11.5 Joint weight ... 99
11.6 Conclusion ... 99
12 Seismic analysis ... 100
12.1 Introduction ... 100
12.2 Modal analysis ... 100
12.3 Response spectrum analysis ... 102
12.4 Structural checks ... 103
12.4.1 Steel trusses ... 103
12.4.2 Timber shell ... 104
12.5 Conclusion ... 104

IV CONCLUSION ... 105
13 Final design ... 106
13.1 Recap ... 106
13.2 Structural design ... 107
13.3 Potential refinements ... 108
13.3.1 Joint and element design ... 108
13.3.2 Truss design ... 109
13.3.3 Discussion ... 110
14 Conclusion ... 111
14.1 Introduction ... 111
14.2 Design ... 111
14.3 Method ... 114

REFERENCES & APPENDICES ... 117
References ... 118
Appendix A: Circular Hollow Sections Hot-rolled (CHSH) ... 120

Appendix B: Timber cross sections 121
Appendix C: Wind loads 122
Appendix D: Snow loads 126
Appendix E: Static seismic loads 127
Appendix F: Load combinations 131
Appendix G: Environmental impact analysis 132
Appendix H: Determination of load per bolt 137
Appendix J: Eigenmodes with active masses 139
Appendix K: Elastic spectra of L'Aquila per limit state 140

Introduction

In April 2018, I graduated from the faculty of architecture at the TU Delft with the design of a temporary community centre in Central Italy. This thesis contains the work done during my second follow-up graduation project, in the field of structural engineering, carried out in cooperation with Arup Amsterdam. The main load-bearing structure of the designed community centre will be optimised considering multiple objectives – e.g. environmental impact, demountability, structural weight – using computational modelling techniques and manual iterations. For the optimisation two materials are considered: (1) timber, as prescribed by the architectural design, and (2) steel as an alternative structural material. The thesis is built up out of four main parts, discussed below.

Part I: Framework

The first part of the thesis contains background information. As the topic of this thesis is based on a previous graduation project in the field of architecture, Chapter 0 will present the architectural design. It will cover the context in which the design is situated – the earthquake-damaged historic town centre of L'Aquila Italy – and provide insight the underlying social concept and the architect's ideas with regard to the structural design.

Chapter 0 describes the follow-up to this architectural design, namely this graduation thesis. What is the central research question and the scope of this project, and which approach will be followed to get to the final results? A clear optimisation workflow will be presented, which envelopes the generation of a large database of structural variants and the manual iterations that take place thereafter to find the optimal structural design.

Part II: Database generation

The second part of the thesis concerns the automation script behind the generated database and how the parametric model has been set up. The first step in the computation is the parametric geometry. Chapter 0 starts off with laying out all geometrical variations that will be considered.

Next, Chapter 4 entails the materialisation options that will be modelled with, both the material properties of steel and timber, and the different cross sections that have been applied.

All the load cases and combinations are presented in Chapter 5, while Chapter 0 describes how all models will be structurally analysed for all load combinations.

Sustainability plays a big role in the optimisation process. Chapter 7 covers the environmental impact analyses that have been carried out and linked to the parametric script.

And lastly, the generated database is presented in Chapter 8.

Part III: Design optimisation

The third part of the thesis After the database has been generated, manual exclusion, sorting and iterations will take place to find the optimum structure with regard to the defined objectives. Chapter 0 concerns the exclusion and sorting of the numerous structural variants in the generated database.

After the top-ranking structural variants have been presented, in Chapter 10, extra structural analysis will be carried out to double-check the automated outcomes.

Next, manual iterations will take place among the top-ranking models. The first step in this process is the design and check of the structural joints, which is covered by Chapter 11.

Following the design of the structural joints, seismic analyses will be carried out using the response spectrum of L'Aquila, Italy, to ensure building's safety. These analyses are presented in Chapter 12.

Part IV: Conclusion

The last part of the thesis covers the final design. The optimised design is presented in Chapter 0 including the potentials for further refinement, which is followed by the conclusions and recommendations in Chapter 14, reflecting on the design and the underlying concept, as well as the optimisation method applied.

I

FRAMEWORK

1 Background

1.1 Introduction

The framework of this thesis is the design of a temporary community centre in Italy, which was the result from a previous graduation project at the Delft University of Technology in the field of architecture. This chapter provides the relevant background information to understand the architectural design and specifically the underlying social concept.

1.2 Context

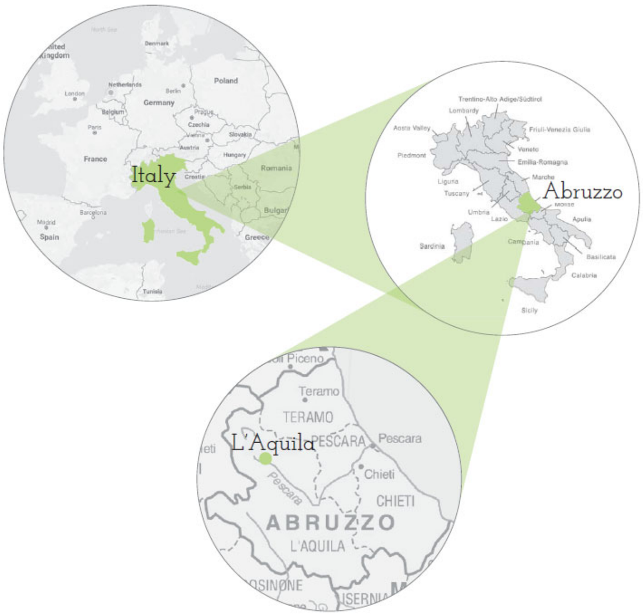

Figure 9: Location | L'Aquila, Italy

April 6, 2009. A heavy earthquake struck Central Italy in the middle of the night. The epicentre was located near the city of L'Aquila, the capital of the province of Abruzzo. The earthquake was felt throughout the whole of Italy, and resulted in more than 300 deaths, over 1 500 people getting injured and an excessive 65 000 + people were rendered homeless in L'Aquila and surrounding areas. The beautiful historic town centre of L'Aquila became an uninhabitable, heavily damaged zone.

Now, ten years later, the situation in L'Aquila has not improved. The town centre remains a ghost town, covered in scaffolding, the damages done by the earthquake still unmistakably present. A solid recovery plan was missing. A lengthy research (Alexander, 2010) draws attention to what was one of the main causes for this: "The missing element in the Italian Government's recovery policy is local participation."

After the earthquake, a lot of focus was directed towards developing decentralised housing solutions. Due to the lack of a coherent redevelopment plan, these temporary solutions have gotten a permanent character. Over time, there have been inquiries into and protests against the policy – or rather, a lack thereof – led by the local populations who have been driven out of their homes, but they have not been heard. To their utmost frustration, their homes have yet to be redeveloped.

Figure 10: Current post-disaster approach

1.3 Architectural design

1.3.1 Concept & ideals

This lack of a coherent redevelopment policy formed the incentive for the architectural design. It proposes a different post-disaster approach, in which all-round participation is triggered and life in the city centre will remain during the recovery period.

Figure 11: Alternative post-disaster approach

Inspiration was found in the developments after the 1991 Oakland fire, in which the construction of a community development centre was said to form an important innovation for two-way communication during the reconstruction period (Olshansky, 2005). Inspired by this precedent, a concept crystallized: the design of a temporary community (recovery) centre in the middle of the damaged town centre of L'Aquila.

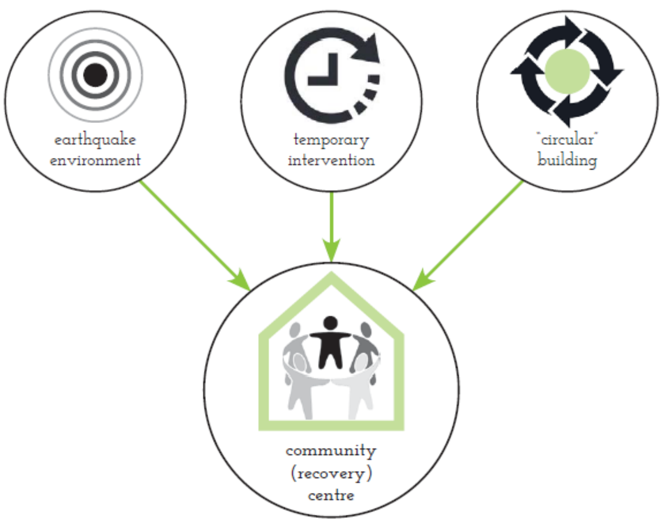

Figure 12: Community (recovery) centre

In the city of L'Aquila, the community centre could be constructed in any of the many *piazzi* – squares – of the town after infrastructure has been cleared up and the area has been declared safe. For the development of the design, the central square of the town was chosen, the Piazza del Duomo. During the recovery period, the centre can host many of the town functions lost during the earthquake, it offers a safe haven and a reason for people to visit the centre and – most importantly – it provides a platform for all-round communication during the reconstruction of the town centre.

Figure 13: Location | Piazza del Duomo, L'Aquila

The Piazza del Duomo is the biggest square of the town centre of L'Aquila, where on a daily basis a market was organised before disaster struck. It is surrounded by a lot of historical palaces, as well as a church and – at the head of the square – the Duomo, or the dome. A free area of 78.0m by 35.0m is available for the design of the community centre.

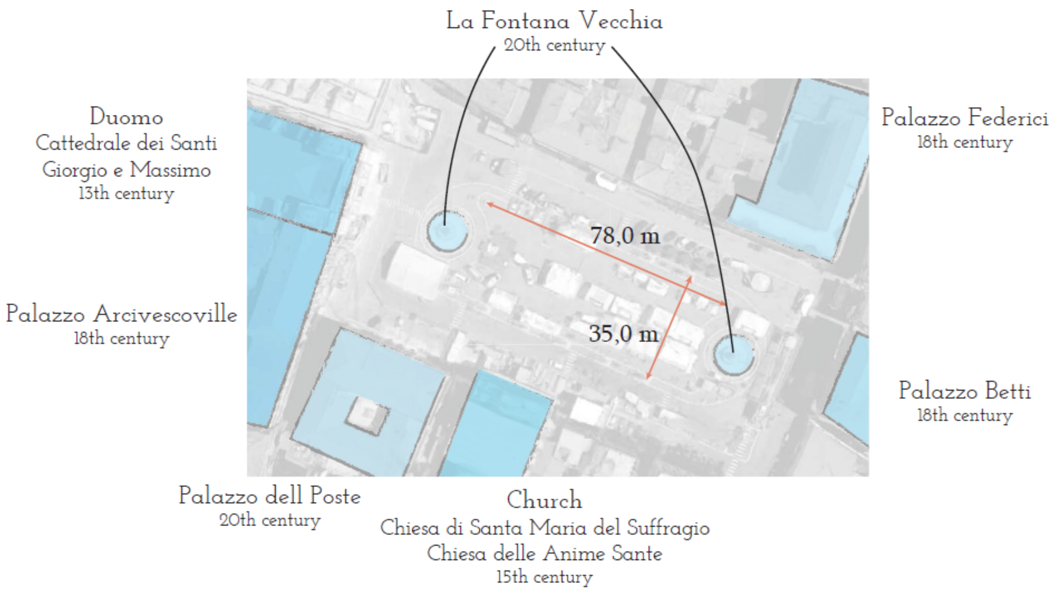

Figure 14: Piazza del Duomo

As local participation was found to be the missing key to successful recovery planning, it has played a leading role both in the conceptual development of the community centre as well as in the detailing of the design.

1.3.2 General design

The main idea behind the design is to make an open and roofed space, which has the flexibility to house many functions – among which public gatherings, cafeteria, church masses and a market. Figure 15 shows the design of the temporary community centre, a colourful roofing structure with an almost completely open floor plan underneath.

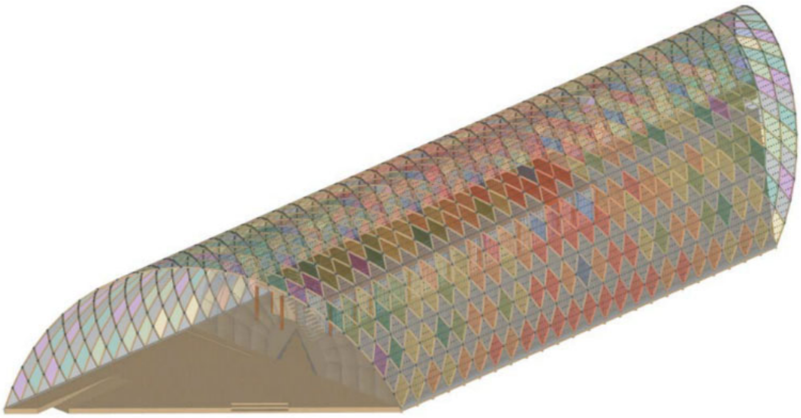

Figure 15: Architectural design

As can be seen in the exploded view of Figure 18, an elevated floor forms the base of the design, while it's roofed by a timber gridstructure. In order to avoid intrusive foundations in the Piazza del Duomo – both to keep the site untouched as well as guarantee higher demountability – the elevated floor must contain enough mass to keep the light-weight structure in place.

The structure is covered by a colourful ETFE-façade, built up out of separate overlapping pieces. This creates a church-like and peaceful experience in the building interior. Underneath the structure hangs a see-through triple-layered ETFE-façade. This part of the façade makes sure the interior climate is pleasant, as the middle layer can be adjusted to either open up to or close off the sun – as shown in Figure 16. Through openings in the roof and Venturi-elements at the top of the structure (see Figure 17), as well as installations integrated in the elevated floor, natural ventilation is provided.

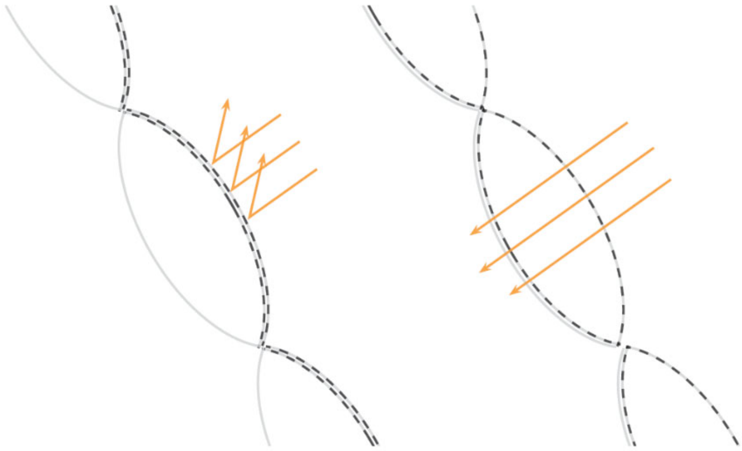

Figure 16: Triple-layered ETFE cushions for climate control

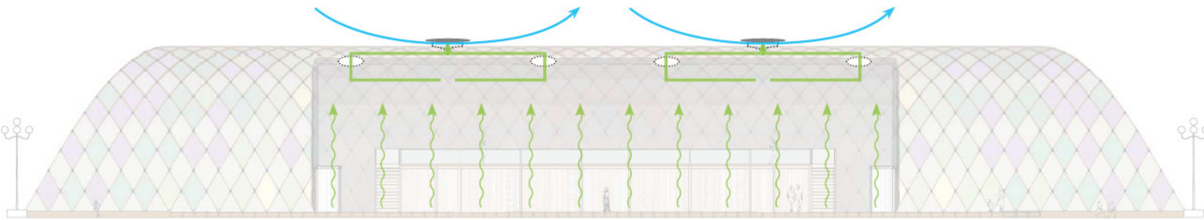

Figure 17: Natural ventilation through Venturi roof elements

The design is completely off-the-grid, as in a post-disaster environment it cannot be assumed electricity and water are up and running. Therefore, rainwater is collected and filtered, the façade contains PV-cells on the south side to generate electricity and light and all installations use a minimum amount of electricity or water.

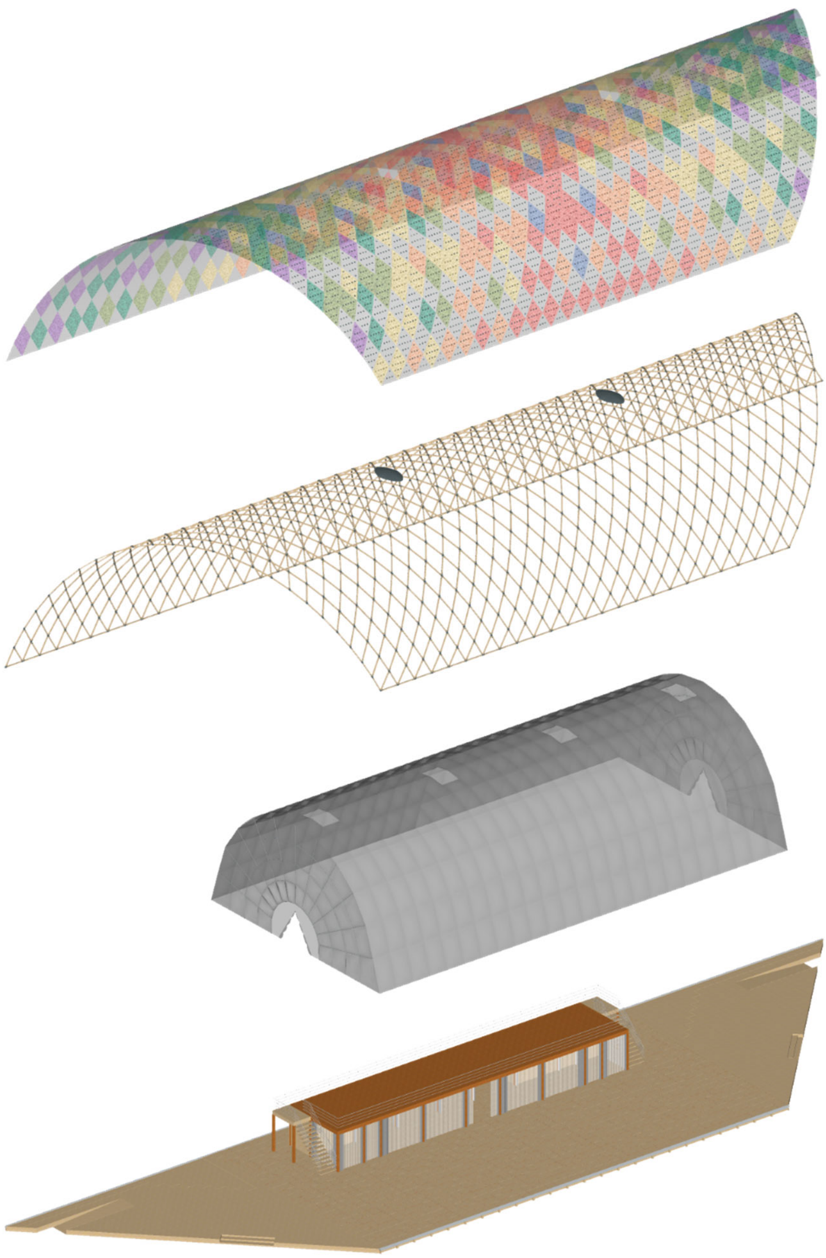

Figure 18: Exploded view

Lastly, by using solid walls only where necessary from a structural and functional point of view and flexible room dividers elsewhere, the floor plan is very easy to adjust to any kind of event. This provides the users of the community center with a lot of flexibility to contribute and organise.

Figure 19: Flexible room dividers

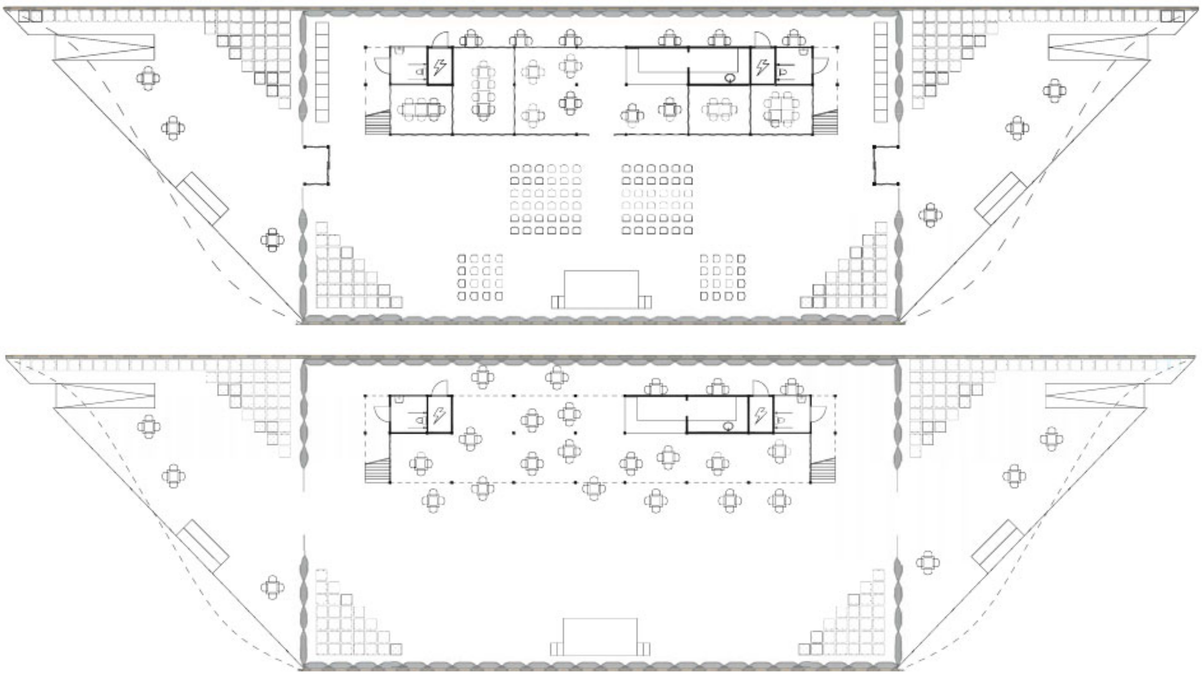

Figure 20: Different possible floor plans | Option A (top) & Option B (bottom)

1.3.3 Structural design

1.3.3.1 Main principles

The primary concept behind the structural design was two-fold:

1. The design should not create any more waste. If anything, the design should have a positive impact by using some of the waste caused by the earthquake.
2. Local participation is one of the key ingredients and therefore the structure should have light-weight elements and an easy-to-assemble design.

The materialisation goals was therefore to apply re-used timber and recycled reinforced plastic. As a secondary material, steel was used at certain positions in the detailing where the slenderness of the steel was required.

1.3.3.2 Overview structural design

Figure 21 shows the main load-bearing structure of the architectural design. It consists out of a diamond-shaped pattern, with angles of 60° at their tops. The timber elements measure 1.5m each, with a cross section of 100×100mm².

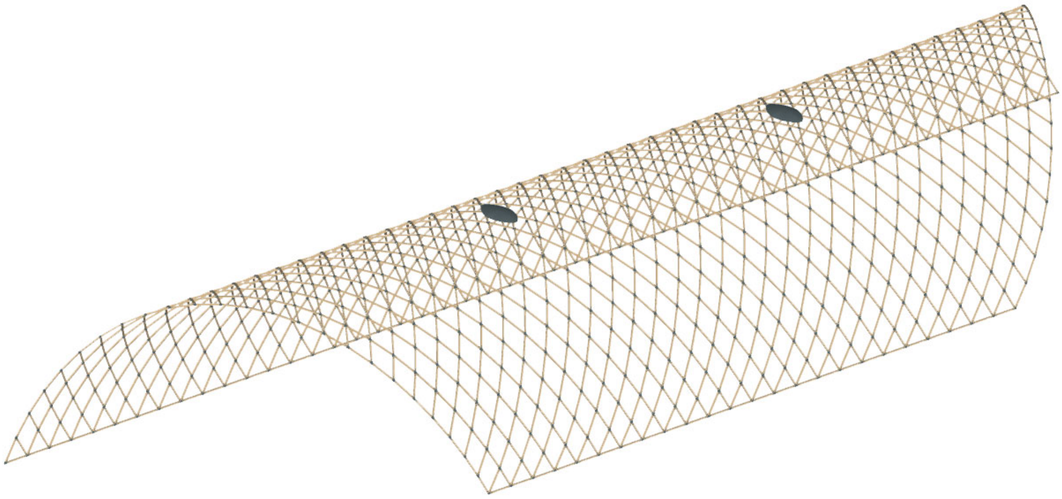

Figure 21: Main load-bearing structure

1.3.3.3 Load distribution

The loads – both from the hanging ETFE-façade on the inside as well as imposed loads from the outside – are transferred through the grid-like structure directly to the ground, while the elevated floor closes the circle. Given the elevated floor can contain sufficient mass, this results in an independent structure for which no intrusive foundations are necessary.

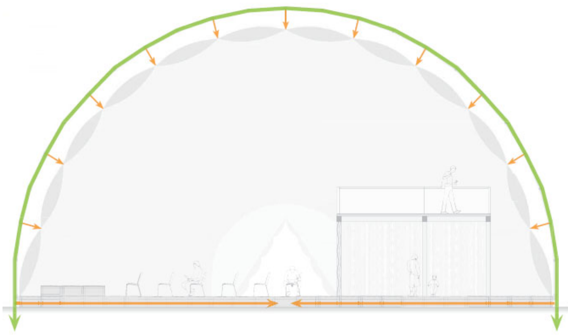

Figure 22: General loads

The structure is open to the sides and the inner ETFE-façade will therefore be exposed to wind loads. These wind loads are distributed radially to the structure by making extra connections around this façade (see Figure 23), the point loads will be more evenly divided over the grid structure, instead of generating excessive peak values.

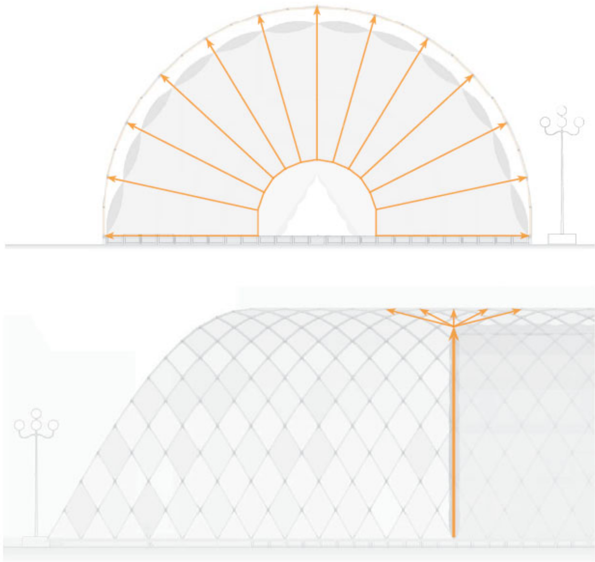

Figure 23: Wind load distribution

1.3.3.4 Connection design

The joints in the architectural design – which have designed to be the same in the entire structure – are made up of 3D-printed reinforced plastic joint elements. This modern technique – which is still under development (Matsuzaki, et al., 2016) – provides a lot of form freedom, so the joint can be designed in the perfect angle. By using a pointy design (see Figure 24) and CNC-milling the timber elements to the perfect shape, only one pin-like connection element necessary to make a rigid connection. A CNC-milled timber screw in chosen to keep everything in place.

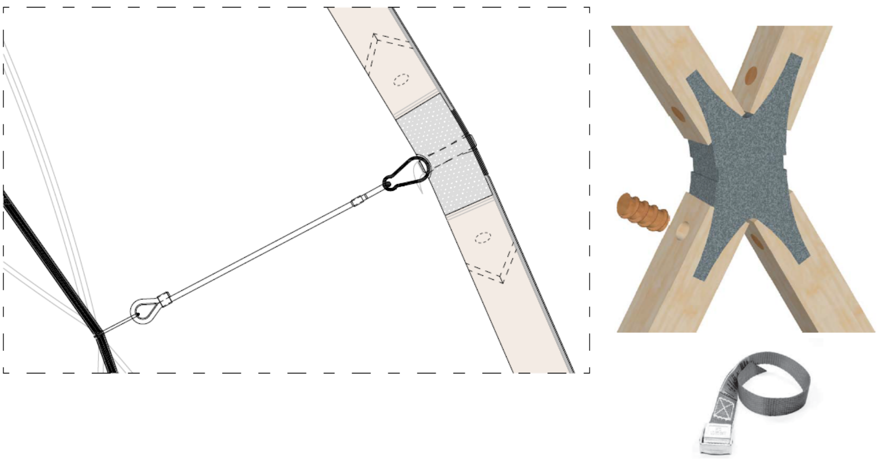

Figure 24: Connection detail

1.3.3.5 Elevated floor design

The floor is built up out of modular timber elements with plastic empty containers, as presented in Figure 25. These containers can be filled with anything that gives the floor enough mass to keep the building in place. One of the options would be to fill these floor elements with rubble from the site; both practical and symbolic.

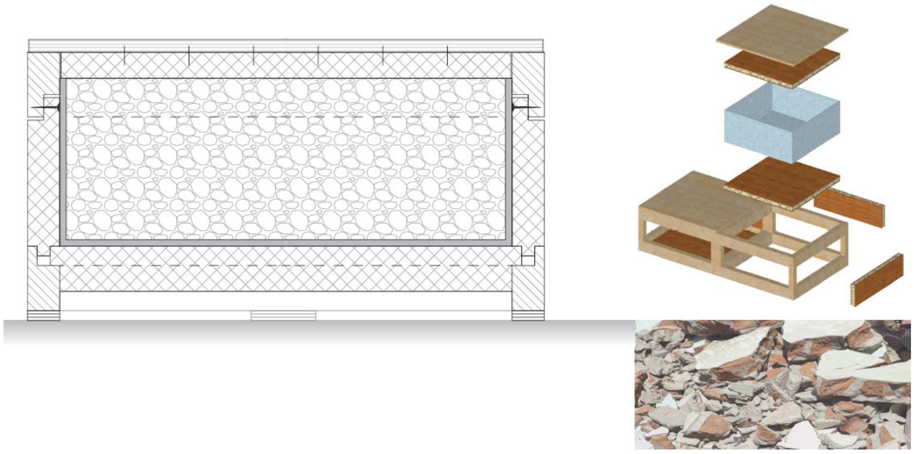

Figure 25: Elevated floor module

The connection of the grid structure with the elevated floor is the only part where steel plays a big role, as shown in Figure 26. The steel U-profile provides a straight-forward base for the structure above, connecting it to the elevated floor. The profile is lifted from the floor by short timber columns, which give room to installations going in through the side of the floor modules (e.g. electricity, ventilation). The columns also ensure a sturdier connection between the structure and the elevated floor.

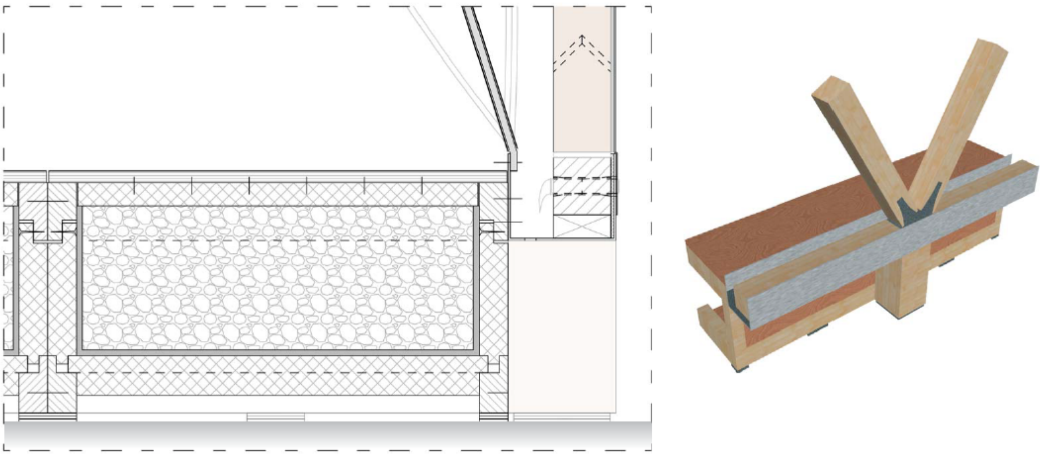

Figure 26: Floor & Structure detail

1.4 Conclusion

The architectural design concerns a temporary community centre in the earthquake-damaged historic town centre of Central Italy. It is based on a solid social concept, as it strives for the participation of the local population in order to reinstate some pride in them after the earthquake has deprived them of many things. This strive for participation manifests itself both in the multi-functional and flexible set-up of the interior, and in the simplicity of the structural design which consists out of light-weight and modular elements.

2 Approach

2.1 Introduction

A context has been provided, after the architectural design of the community centre in L'Aquila, Italy, has been presented in Chapter 0. Based on this design, a new graduation topic can be formulated and carried out. This chapter contains the aim, scope and research methode that have been applied during the graduation project.

2.2 Aim

For this thesis, which is carried out in the field of structural engineering, the focus will lie on the main load-bearing structure of the design. The design has many objectives, such as sustainability, economic circularity, aesthetics and the possibility for the locals to participate in its construction. In order to comply with all these objectives, this project will focus on the multi-objective optimisation of the load-bearing structural design. In the optimisation both quantitative and qualitative aspects need to be considered. The general aim of this thesis is to find the most suitable structural design solution for this context.

2.3 Research question

Based on the general goal of this thesis and comprising all objectives, a central research question has been formulated. It forms the foundation of this graduation project and is stated below.

Given the architectural design, how can the main load-bearing structure be optimised for seismic contexts using parametric modelling, considering the following objectives: maximal demountability and structural simplicity, minimal material use, structural weight and environmental impact?

2.4 Scope

The structural design optimisation will be limited to the load-bearing roof structure, keeping the shape as presented in the architectural design – a single-curved structure, half a cylinder. Thus, what will not be researched during this project are the following: the elevated floor, the interior structure, the façade design and the building physics.

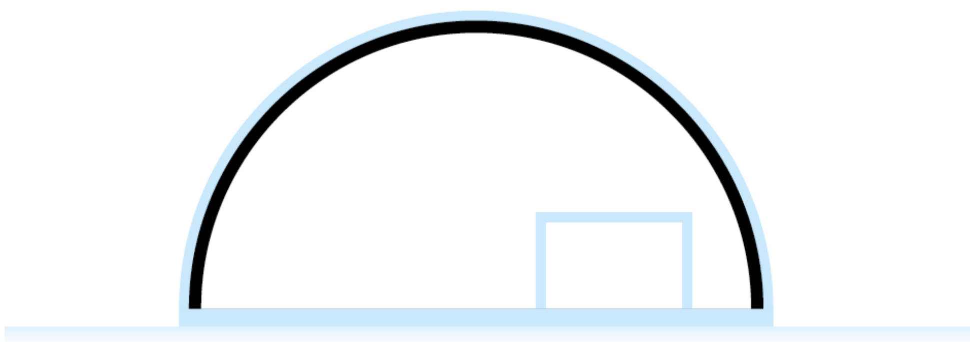

Figure 27: Optimisation scope

2.5 Research method

The general method used during this graduation project is research-by-design; numerous designs will be configured and assessed with respect to the stated objectives. Part of this process will take place by automated modelling, using parametric design methods; part of this process will be carried out manually. The workflow is described in

Figure 28.

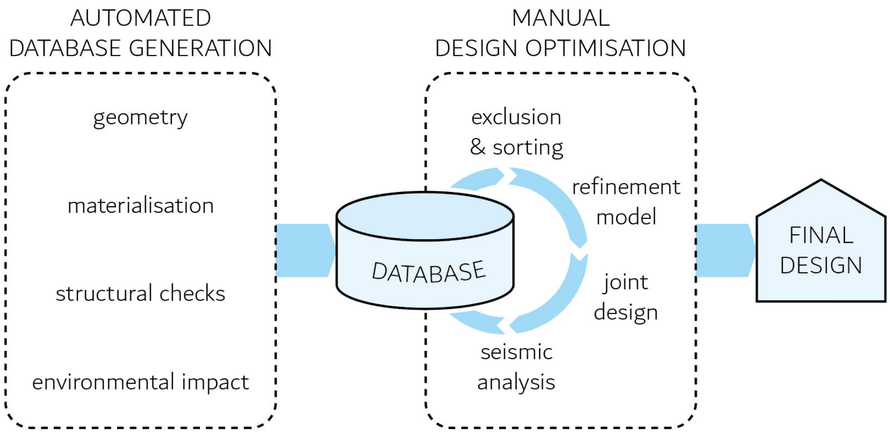

Figure 28: Workflow graduation project

The first step in the workflow is to automatically generate a large set of models with varying geometry and materials using parametric design. Each of these models will be structurally verified through FEM-calculations and environmentally assessed based on environmental impact analyses.

Other relevant quantifiable aspects – such as structural weight – will also be provided as output. A large database is generated, which contains all these models, including their generated output. The next step is to organise this database.

First, exclusion will take place of the models that do not live up to the quantified demands that have been set – the structural demands and the weight of each of the elements.

Secondly, the remaining models will be sorted by comparing their environmental impacts, their aesthetics and to what extent these are in line with the underlying concept.

Lastly, iterations will be carried out among the remainder of the structural models. The start for these iterations will be the highest-ranking design. It will be looked into more in-depth by carrying out checks on the structural joints, after which a seismic analysis will be carried out on the entire structure. If the design does not live up to any of the demands, the next design on the list will be chosen and analysed. This process can be repeated until the most suitable design has been found.

2.6 Software

For this research, multiple kinds of software are used for modelling, FEM-calculations and environmental analysis.

- Rhino 5 — *Platform for 3D-modelling*
- Grasshopper — *Rhino-plugin for parametric design*
- Karamba — *Grasshopper-plugin for FEM-calculations*
- TT Toolbox (Colibri) — *Grasshopper-plugin for automated model generation*
- CES EduPack 2018 — *Material science software with potential Life Cycle Analysis approximations*
- RFEM — *FEM-software, used for double-checking and further analyses*
- RF-DYNAM Pro — *RFEM add-on, used for seismic analysis*

2.7 Conclusion

The goal has been set to optimise the structural design with regard to its many objectives – including a low environmental impact and a low weight per structural element. This optimisation will be carried out by a combination of automated processes resulting in a database of many structural variants and manual exclusion and iterations, based on multiple kinds of analyses.

II

DATABASE GENERATION

3 Geometry

3.1 Introduction

As discussed in Chapter 2, a database will be generated through parametric scripting in Grasshopper, a plug-in to the 3D-modelling software Rhino. The first step in setting up the parametric model is the definition of the different geometrical options. Though the shape of the structure will remain the same, the total amount of geometrical sums up to 126.

3.2 Grid size (7 variations)

The original architectural design had grid elements with a length of 1.5 m, which was just a rough estimate. The grid size could therefore be adjusted, as long as the shape of the structure remains more or less the same. Seven variations will be taken into consideration in the Grasshopper-script.

Table 2: Grid size variations

	Element length [m]	No. of elements [-]	Length [m]	Span [m]
1	2.60	658	78.00	20.11
2	2.05	1062	78.00	20.40
3	1.70	1562	78.00	20.58
4	1.44	2158	78.00	20.72
5	1.26	2850	78.00	20.82
6	1.11	3638	78.00	20.89
7	1.00	4522	78.00	20.96

Keeping the length of the structure at a steady 78.0m and the span between 20.0m and 21.0m, some important values are derived for the different grid sizes, presented in Table 2. The two most extreme grid sizes are shown in Figure 29.

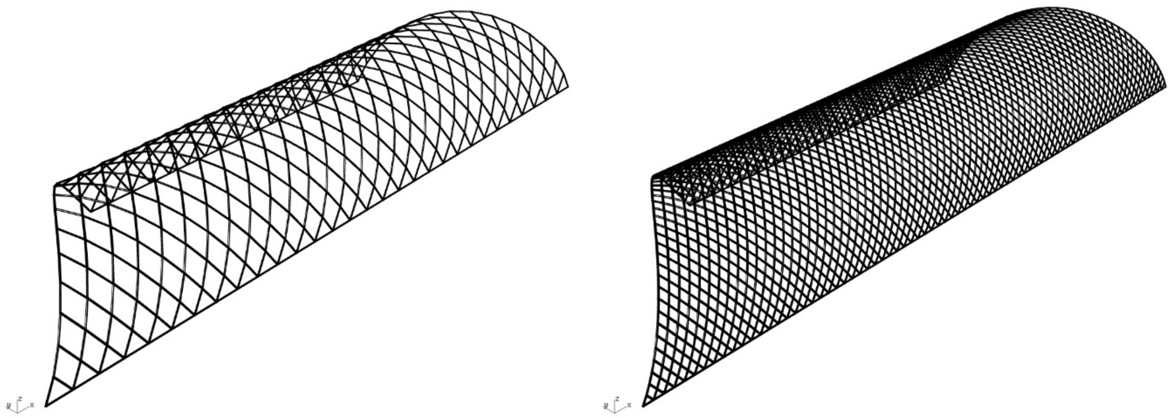

Figure 29: Grid size | Two variations with element size of 2.6m (left) and of 1.0m (right)

3.3 Basic geometry (2 variations)

The assumption in the architectural design was that all joints were rigid. However, as hinges are usually easier to design, several patterns of hinging connections in the structural grid have been considered. Only one came out as a feasible alternative to the original design with all rigid connections. Both variations are presented in Figure 30 – the red lines with dotted ends representing the hinging elements which won't exert any bending moments to the structural joints they are connected with.

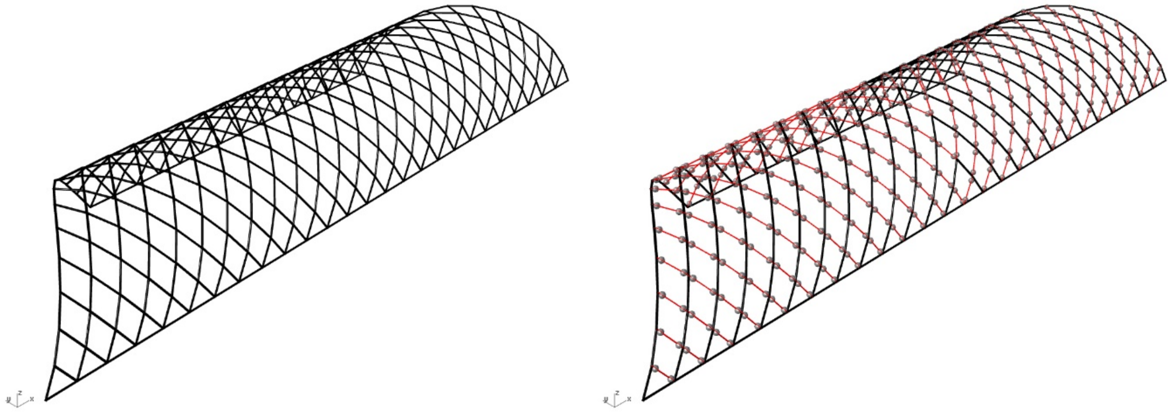

Figure 30: Basic geometry | Rigid connections (L) & Combined connections (R)

3.4 In-plane variations (3 variations)

One of the variations keeps the original diamond-shaped pattern. However, in order to create a potentially stronger design, it is relevant to look at variations in the curved plane.

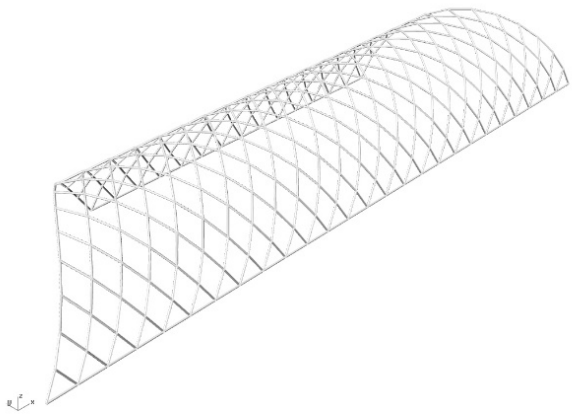

Figure 31: No in-plane additions

Due to the angle of 60° in the original diamond-shaped grid, the possibility arises to apply horizontal elements. These will be applied as bars with hinging connections, as presented in Figure 32.

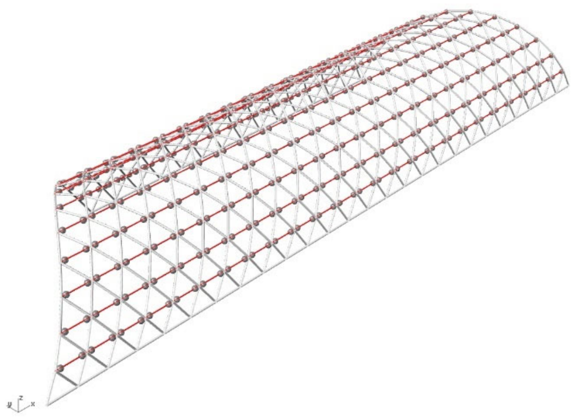

Figure 32: All horizontals

Lastly, a pattern of horizontals has been determined through BESO – Bi-directional Evolutionary Structural Optimisation (Xia, Xia, Huang, & Xie, 2016) – which basically calculates where in the structure the need for mass is highest. The Grasshopper plug-in Karamba, which is used for structural calculations, contains a component that applies BESO calculation. Using the governing load – snow – a pattern of horizontals has been determined as presented in Figure 33. Compared to the variation in Figure 32, only 50% of the horizontals remain. Also, in this case, all additional members will be connected using hinges.

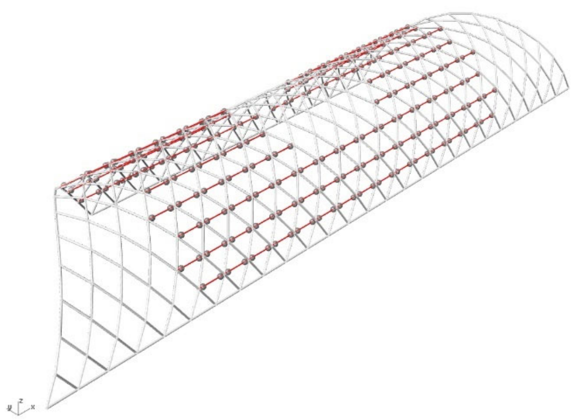

Figure 33: BESO-horizontals

3.5 Out-of-plane variations (3 variations)

As the project progressed, it became noticeable that by making in-plane additions to the structure as shown in paragraph 3.4, very limited stiffness is added in the Y-direction of the building. As shown in Figure 34, the width remains just as thin and can deform relatively easily.

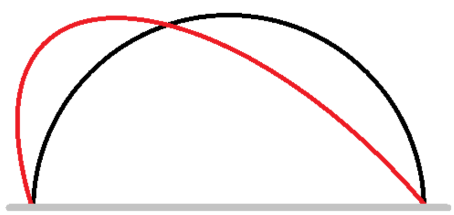

Figure 34: Deformations

Thus, apart from in-plane variations, out-of-plane variations in the form of trusses will also be considered. The variations with either two or three trusses are presented in Figure 36, modelled with all hinging connections.

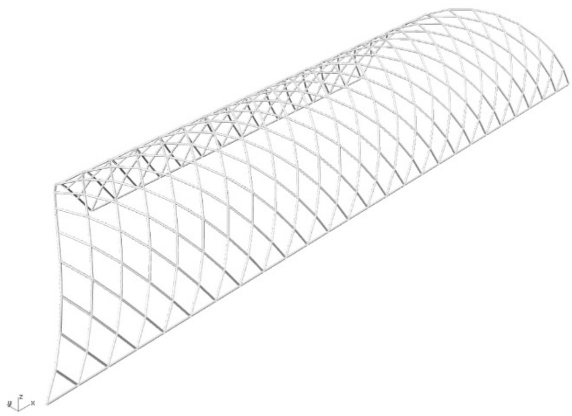

Figure 35: No out-of-plane additions

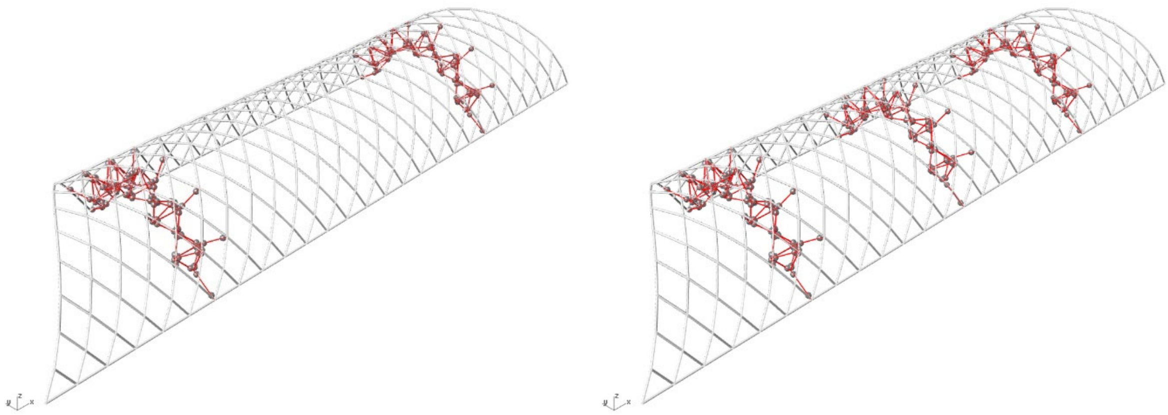

Figure 36: Two trusses (left) & Three trusses (right)

3.6 Conclusion

Having defined 7 different grid sizes, 2 geometrical basis variations, 3 in-plane variations and 3 out-of-plane variations in the parametric Grasshopper-script and cross-referencing all options results in $7 \times 2 \times 3 \times 3 = 126$ different geometrical set-ups. All these geometries will be carried out using different materials and cross sections as will be presented in the Chapter 4.

4 Materialisation

4.1 Introduction

After defining the geometrical variations in Chapter 0 – a total of 126 models – the next step is to define the different materials and cross sections that these different geometries will be built up out of.

The original architectural design of the structure is mainly built up out of timber elements. However, the automated research opens up the possibility to investigate a whole range of materials, as opposed to just timber which was mainly decided upon based on conceptual ideas. For this research, the range of materials will be limited to two steel types of cross sections, and two timber types of cross sections.

4.2 Material properties

4.2.1 Steel (Karamba)

Karamba – the FEM-plugin for Grasshopper and Rhino – has material libraries readily available for steel (Preisinger, 2018). The steel properties that are assigned automatically by the software are presented in Table 3.

Table 3: Steel properties

	E [N/mm²]	G [N/mm²]	γ [kN/m³]	α_T [1/°C]	f_y [N/mm²]
Steel	210 000	80 760	78,5	1,2E-05	235

4.2.2 Timber (Karamba)

At this point in its development, Karamba does not have extensive libraries available for timber as for steel. This means that although steel properties are readily available, timber properties need to be entered manually. Two species of timber will be considered: a local medium-strength timber species and an imported high-strength timber species.

4.2.2.1 Local timber

With regard to reducing the environmental impact, a local species of timber will be selected. In Italy, the following types of timber can be found (Advameg, 2018):

- Sweet chestnut
- Beech
- Oak
- Poplar

As the structure is partially exposed to the elements, the durability class of timber needs to be considered, which is prescribed in the *NEN-EN 350 Durability of wood and wood-based products – Testing and classification of the durability to biological agents of wood and wood-based materials* (2016). The durability classes are presented in Table 4.

Table 4: Durability classes of wood and wood-based products (EN 350, 2016)

Class	Durability
1	Very durable
2	Durable
3	Moderately durable
4	Slightly durable
5	Not durable

Due to the exposed conditions of the structure, a timber species with a high durability class is required. Beech and poplar both have class 5 (EN 350, 2016), and are therefore excluded as possibilities.

According to NEN-EN 350 (2016), sweet chestnut has a durability class of 1-2, while oak is considered to be of class 2-4. Furthermore, sweet chestnut is more readily available in Italy (Advameg, 2018) and is therefore chosen to be one of the timber species to be modelled.

4.2.2.2 Sweet Chestnut

The strength class of sweet chestnut is D24 (Vega, Arriaga, Guaita, & Baño, 2013), as has also been included in the latest update of *NEN-EN 1912 Structural timber – Strength classes – Assignment of visual grades and species* (2012). In Table 5, the properties of strength class D24 are presented in accordance with *NEN-EN 338 Structural timber - Strength classes* (2016).

Table 5: Properties of strength class D24 (NEN-EN 338)

Strength class D24		
Strength properties [N/mm^2]		
Bending	$f_{m,k}$	24
Tension parallel	$f_{t,0,k}$	14
Tension perpendicular	$f_{t,90,k}$	0.6
Compression parallel	$f_{c,0,k}$	21
Compression perpendicular	$f_{c,90,k}$	4.9
Shear	$f_{v,k}$	3.7
Stiffness properties [kN/mm^2]		
Mean modulus of elasticy, parellel bending	$E_{m,0,mean}$	10.0
5^{th}-percentile modulus of elasticity, parellel bending	$E_{m,0,k}$	8.4
Mean modulus of elasticity, perpendicular bending	$E_{m,90,mean}$	0.67
Mean shear modulus	G_{mean}	0.63
Density [kg/m^3]		
5^{th}-percentile density	ρ_k	485
Mean density	ρ_{mean}	580

The material properties that are relevant for the input of parametric model are as follows – in units requested by the plug-in Karamba:

- Elastic modulus E = 10.0 kN/mm^2 = 1000 kN/cm^2
- Shear modulus G = 0.63 kN/mm^2 = 63 kN/cm^2
- Density ρ = 485 kg/m^3 = 4.85 kN/m

4.2.2.3 *Imported timber*

Beside the local timber species chosen, a species of timber from abroad is chosen which has better mechanical properties. Both have advantages and disadvantages with regard to mechanical properties, weight and environmental impact. The selected imported timber is azobé, which has a durability class of 1-2 (EN 350, 2016).

4.2.2.4 *Azobé*

The strength class of azobé is D70, which is significantly stronger than sweet chestnut. In Table 6, the material properties are presented according to *NEN-EN 338 Structural timber - Strength classes* (2016).

Table 6: Properties of strength class D70 (NEN-EN 338)

Strength class D70		
Strength properties [N/mm^2]		
Bending	$f_{m,k}$	70
Tension parallel	$f_{t,0,k}$	42
Tension perpendicular	$f_{t,90,k}$	0.6
Compression parallel	$f_{c,0,k}$	36
Compression perpendicular	$f_{c,90,k}$	12.0
Shear	$f_{v,k}$	5.0
Stiffness properties [kN/mm^2]		
Mean modulus of elasticy, parellel bending	$E_{m,0,mean}$	20.0
5th-percentile modulus of elasticity, parellel bending	$E_{m,0,k}$	16.8
Mean modulus of elasticity, perpendicular bending	$E_{m,90,mean}$	1.33
Mean shear modulus	G_{mean}	1.25
Density [kg/m^3]		
5th-percentile density	ρ_k	800
Mean density	ρ_{mean}	960

The material properties that are relevant for the input of parametric model are as follows – in units requested by the software:

- Elastic modulus E = 20.0 kN/mm² = 2000 kN/cm²
- Shear modulus G = 1.25 kN/mm² = 125 kN/cm²
- Density ρ = 800 kg/m³ = 8.00 kN/m

4.3 Cross sections

4.3.1 *Steel structure*

With regard to the original architectural design and structural efficiency, only one type of cross section is taken into account in this research:

- Circular Hollow Section Hot-rolled (CHSH)

The circular hollow sections that will be considered for the database generation will be limited from a minimal diameter of 100 mm to maximum diameter of 200 mm, with a thickness of 4.0mm/6.0mm/8.0mm/10.0mm/12.0mm. After narrowing down the selection by carrying out some test runs in the Grasshopper-script the following cross sections have been selected: in case of a structure of S235, the smallest section will be CHSH114.3×4.0 and the largest CHSH193.6×10.0; in case of a structure in S355, the smallest section will be CHSH114.3×4.0 and the largest CHSH193.6×10.0.

This brings the total list to 17 and respectively 21 cross sections. (See Appendix A for the full list of circular hollow steel sections.)

4.3.2 Timber structure

The timber elements – both chestnut and azobé – will be sawn. In accordance with the architectural design, square and near-square cross sections are taken into account. The smallest one will be 100×100mm², while the biggest one will be 225×225 mm². The list sums up to a total of 16 timber cross sections. See Appendix B for the full list.

4.3.3 Steel & timber structure

In most of the variations, the trusses are assumed to consist out of the same cross-sections as the rest of the structure. However, some extra variations are added in which the main structure consists out of timber elements, while the trusses are built up out of steel elements. This is done both from an architectural point of view and for the sake of structural clarity for the laymen that the structure is designed for.

To reduce the number of models that needs to be calculated – all steel truss elements need to be cross-referenced with all timber elements – only three cross sections are considered: CHSH114.3×8.0, CHSH139.7×8.0 and CHSH168.3×8.0 (see Appendix A). All are carried out in steel grade S355.

4.4 Conclusion

By cross-referencing all geometrical variations with the cross sections and cross-sectional combinations, 16 884 models are generated. These models include timber structures, steel structures and combinations of both. Chapter 5 will concern the loads and load combinations that are applied to all these models, based on the Eurocode and the Italian national annex.

5 Loads

5.1 Introduction

After having defined 16 884 structural variations, loads and load combinations need to be defined in the Grasshopper-script. For the structural calculations of all models, the FEM-program Karamba is used with 1st-order analysis. The loads are entered into the parametric as mesh loads – loads applied to any kind of divided up surface – or as point loads in some cases. Redistribution to the structure happens automatically. For faster calculation, the mesh loads generate point loads to the nodes of the structure as opposed to line loads to the elements in-between the nodes. However, when double-checking the calculations in Karamba using separate FEM-software, the loads will be applied in a more refined manner.

5.2 Permanent loads

5.2.1 Self-weight

The first permanent load to be considered is the self-weight of the structure. This depends on the kind of elements that are applied in the model, which vary as the script runs. Karamba automatically takes this into account during calculations.

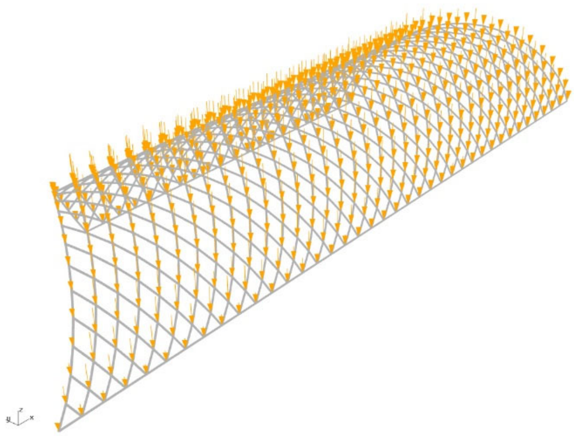

Figure 37: Self-weight

5.2.2 Other permanent loads

The façade in the architectural design consists out of very light-weight ETFE-elements, which would exert a surface load of approximately 0.1 kN/m². However, as the structure is designed to be reusable in different context around the world, and as the exact façade design is not defined at this stage, a higher load of 1.0 kN/m² has been taken into account instead to provide the possibility for different kinds of façades.

The tent-like interior façade – consisting of triple-layered ETFE as discussed in paragraph 1.3.2 – hangs from the central part of the structure. For this permanent load a value of 1.0 kN/m² is assumed as well.

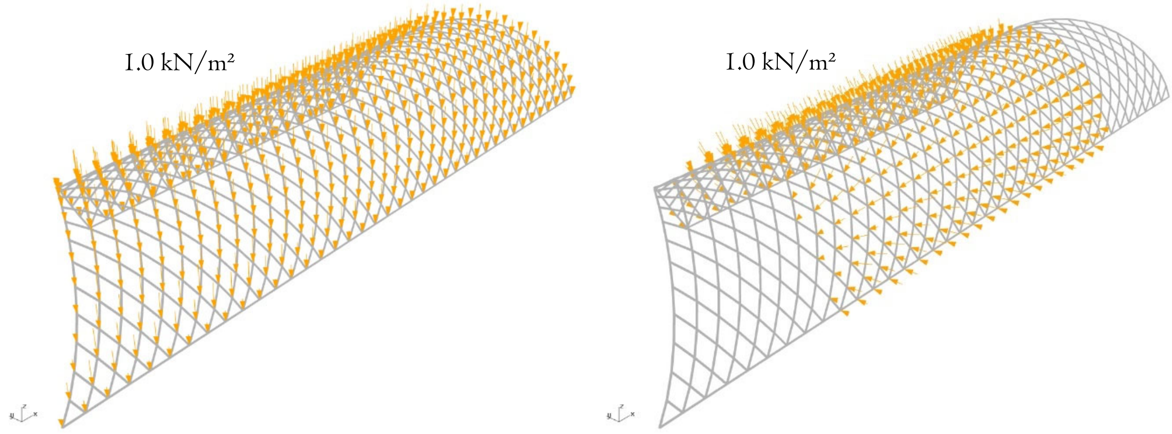

Figure 38: Exterior façade loads (left) & interior façade loads (right)

5.3 Wind actions

The wind actions are not very easy to determine. The values presented in this paragraph have been assumed based on several different design situation – e.g. a curved roof, a free-standing wall and a free-standing roof – as described in the Eurocode (EN 1991-1-4, 2011), taking into account the general wind pressure as prescribed in the Italian national annex (UNI-EN 1991-1-4, 2007):

$$q_p(z) = 0.724\ kN/m^2$$

See Appendix C for elaboration on this part.

5.3.1 Zoning

The first important thing to note is the zoning that have been applied to the building, in order to define the wind loads comprehensively. The middle zone is more or less treated like a closed cylindrically shaped building, but the open east and west zones add a little bit of complexity to the wind action determination.

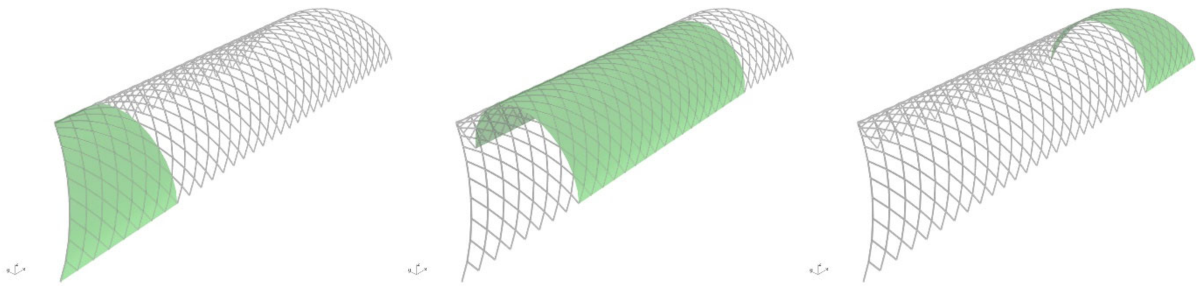

Figure 39: East zone, middle zone & West zone

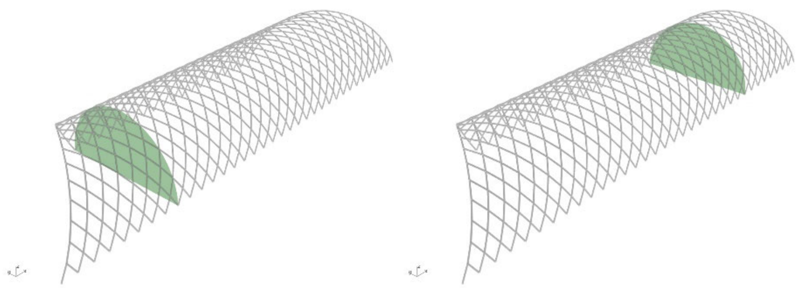

Figure 40: East side & west side

5.3.2 North wind

The middle zone is treated like a closed building with a cylindrical roof, and the loads have been elaborated upon in in Appendix C.

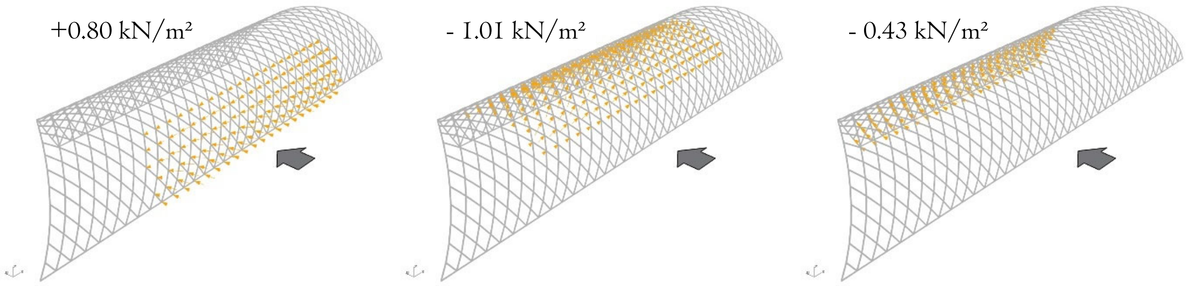

Figure 41: Wind load 1, North | Middle zone

As the East and West zone are open, the loads there are estimated to increase by 10%. They are comparable to free-standing walls, which can have increased suction on the backside (see Appendix C).

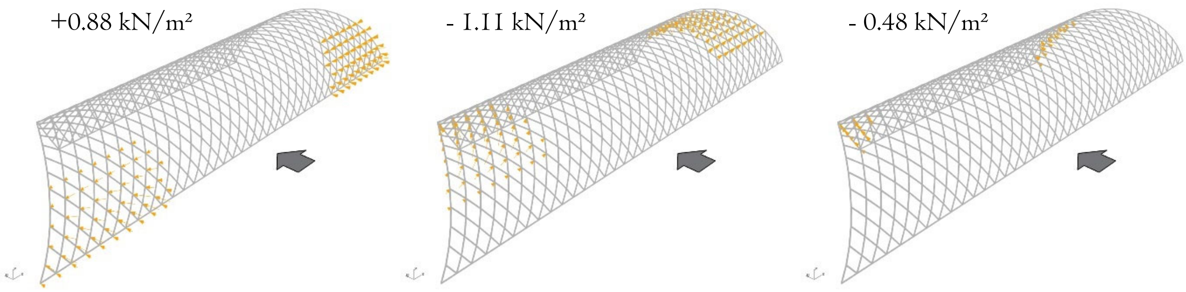

Figure 42: Wind load 1, North | East & West zone

5.3.3 South wind

As with north wind, the middle zone has been treated as a closed building with a cylindrical roof (see Appendix C).

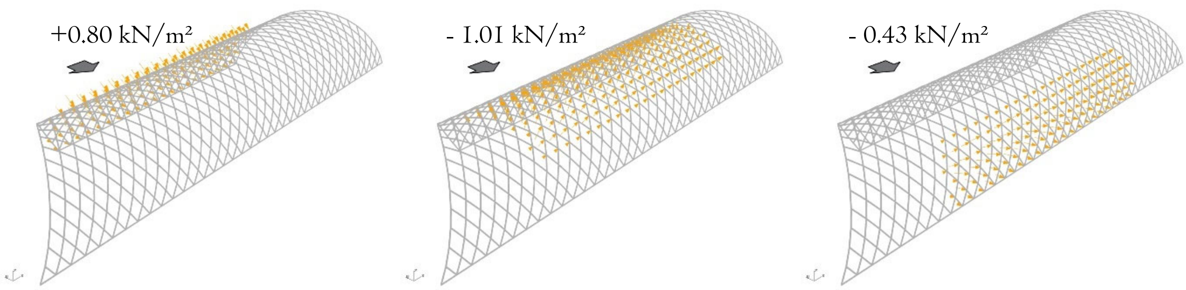

Figure 43: Wind load 2, South | Middle zone

The front side of the east and west zone has been treated as with the north wind, with an increase of 10%. The roof and the back side, however, have an even higher rise in wind pressure as the wind load can build up quite a lot as it is "trapped". They've been compared to an open roof with a big blockade and the free-standing wall (see Appendix C). A $c_{p,net}$ of respectively -2.1 and -1.8 has been assumed.

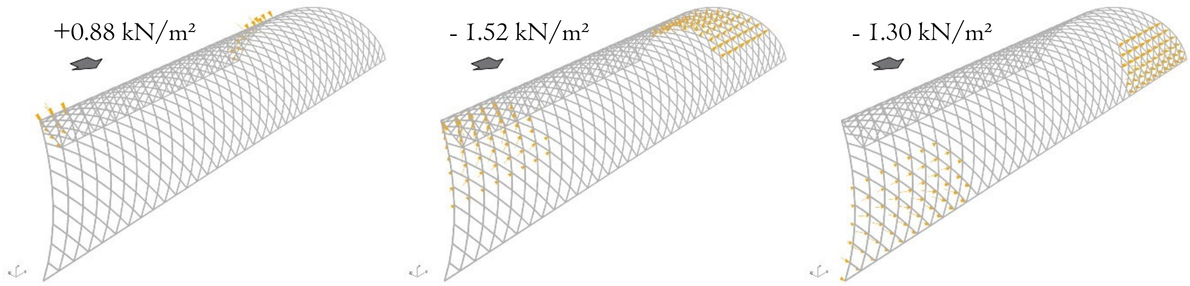

Figure 44: Wind load 2, South | East & West zone

For the sides of the building, a $c_{p,net}$ of +0.80 has been assumed over the whole façade. The loads are transferred from these facades as point loads to the load-bearing structure.

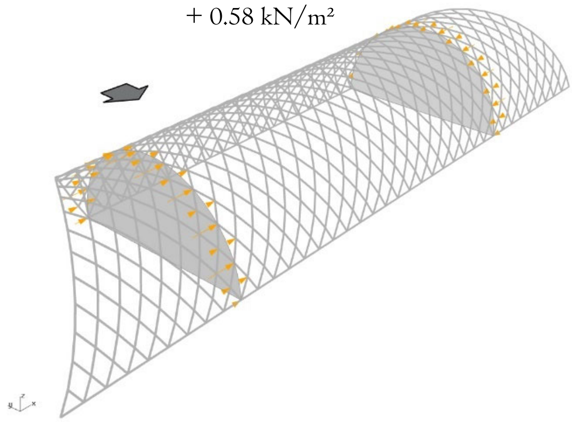

Figure 45: Wind load 2, South | East & West side

5.3.4 Side wind

With both east and west wind, the whole roofing structure is treated as a vertical façade of a building (see Appendix C), resulting in suction in the entire zone. The general suction, in de middle zone, is -1.01 kN/m². On the side the wind approaches, an increase is assumed due to pressure building up underneath the structure, while on the other side a decrease is assumed due to suction underneath the structure.

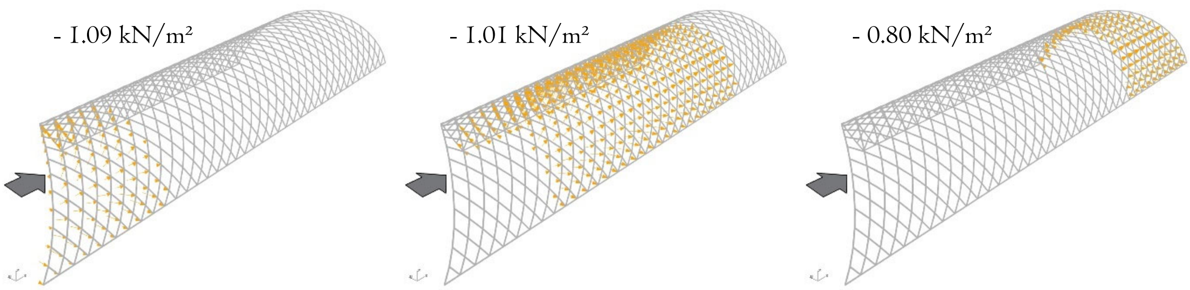

Figure 46: Wind load 3, Side | East, Middle & West zone

In straight-forward buildings, the $c_{pe,10}$ on the front façade would be +0.8. However, as pressure can build up underneath this structure, it is assumed to be +1.1. Combining this with an internal pressure coefficient of -0.3, the cp,net results in +1.1 – –0.3 = +1.4.

The other side of the building has been treated as the backside of a normal building, with a cpe,10 of -0.3. Combined with an internal pressure coefficient of +0.2, this becomes –0.3 –+0.2 = –0.5. These factors result in the forces shown in Figure 47.

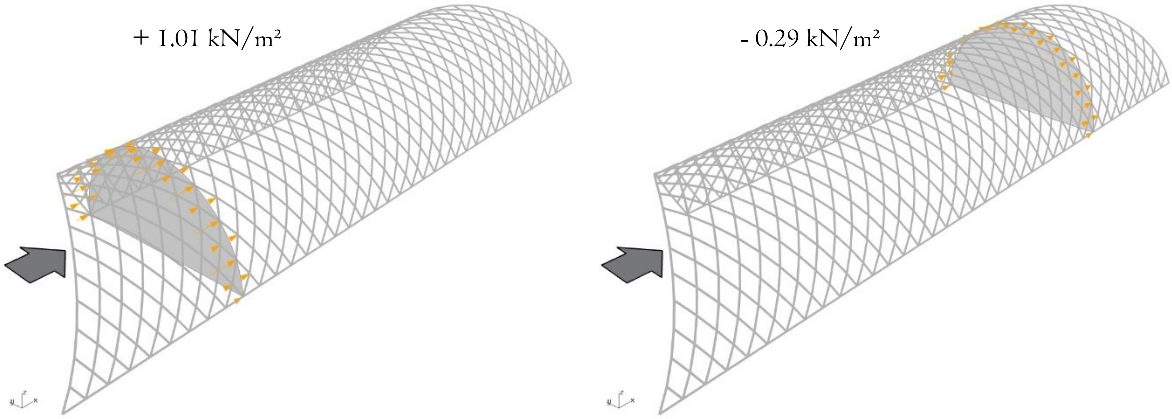

Figure 47: Wind load 3, Side | East & West side

5.4 Snow actions

The city of L'Aquila is located around 700m above sea level in a region that is well-known for winter holidays. Thus, snow plays a big role as well. The exact calculation of the snow load is presented in Appendix D, based on the Eurocode (EN 1991-1-3, 2011) and the Italian national annex (UNI-EN 1991-1-3, 2007). For snow, three different load cases need to be taken into account. The original one, where snow is divided evenly over the top of the cylinder, generates a uniformly distributed load of 2.28 kN/m², as shown in Figure 48. However, EN 1991-1-3 (2011) prescribes a redistribution of snow also needs to be taken into account. As the structure is not completely symmetrical, this is done on both sides of the central axis, as is presented in Figure 49.

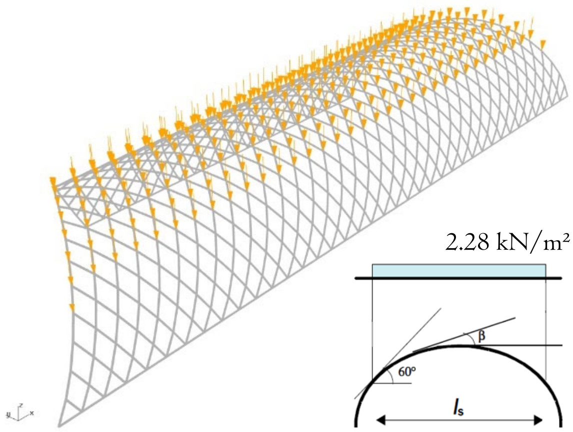

Figure 48: Snow load 1 | Before redistribution

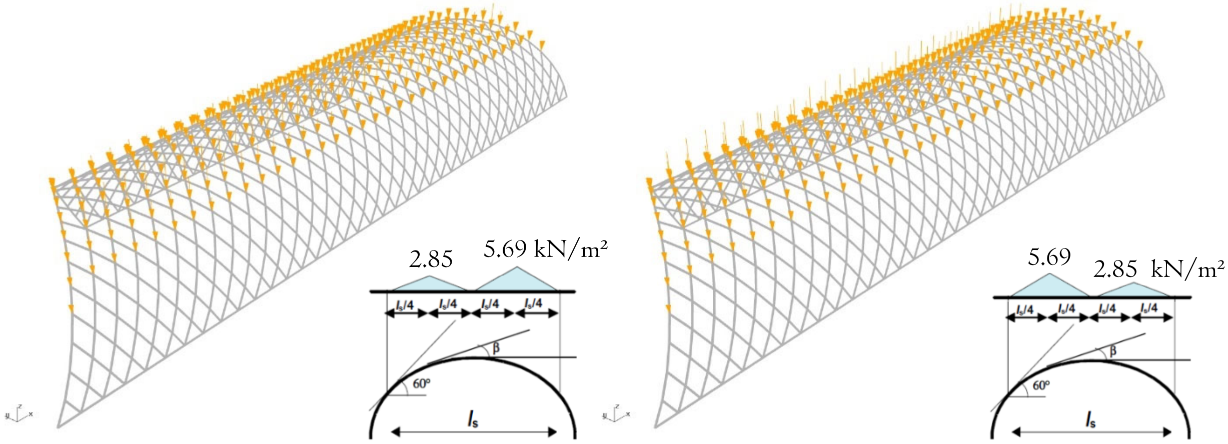

Figure 49: Snow load 2 & 3 | After redistribution

5.5 Imposed loads

The imposed loads on the structure also needs to be taken into account. As the roof is not meant to be accessible, apart from for maintenance activities, only limited imposed loads need to be considered.

5.5.1 Maintenance: Uniformly distributed load (UDL)

For the maintenance of the building a uniformly distributed load of 0.5 kN/m² is considered over a 25 m² area. There are two uniformly distributed maintenance loads to be looked at: one placed at the middle of the structure, and one placed asymmetrically, close to the edge of the roof. See Figure 50.

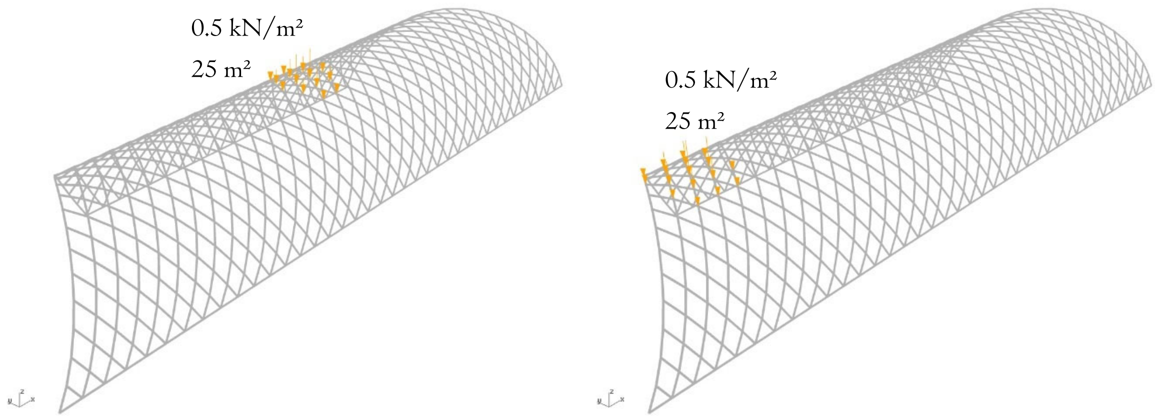

Figure 50: Maintenance UDL | Middle & Side

5.5.2 Maintenance: Point load (PL)

The maintenance point load is assumed to be quite high – 5.0 kN – to account for unexpected usage of the structure as safety plays a big role, especially in a post-disaster context. The point load has been placed on two locations on the structure, similar to the uniformly distributed load, as shown in Figure 51.

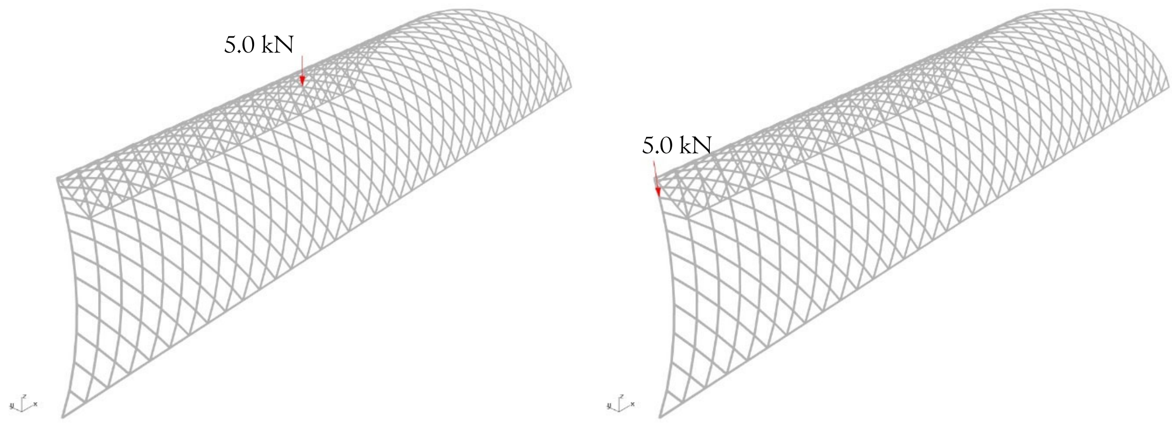

Figure 51: Maintenance point load | Middle & Side

5.6 Seismic actions

After generating and sorting the database, the structures will be iteratively researched seismically through modal analysis using the software RFEM. However, to prevent having to carry out excessive iterations, the structures will be analysed using a horizontal static load case during the computational modelling and FEM-analysis, to account for horizontal loading that might occur during a seismic event.

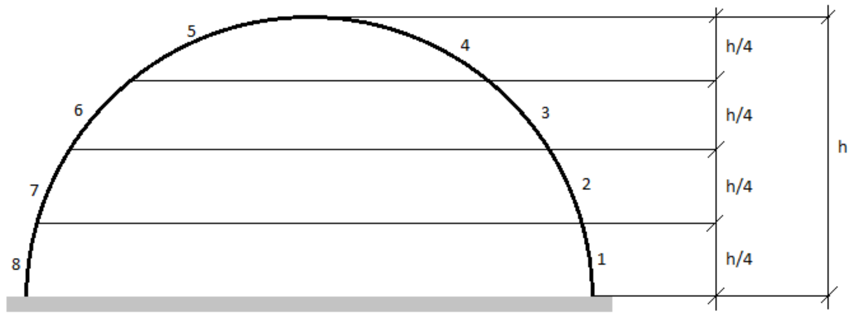

Figure 52: Zoning seismic loading

For the definition of the horizontal earthquake loads, the building has been divided into 8 zones. Each of these zones will get a different uniformly distibuted load depending on:

- the total mass;
- the fraction of the mass that lies in each zone;
- the height of the mass centre of each zone;
- the eigenperiod of the structure in both horizontal directions and;
- the peak ground accelleration at the building site in L'Aquila.

The most unfavourable structural option has been used for the calculation of these loads, which will be applied in all of the structural variations to limit the calculation time of the Grasshopper-script. For more extensive calculations, please refer to Appendix E.

5.6.1 Seismic actions in X-direction

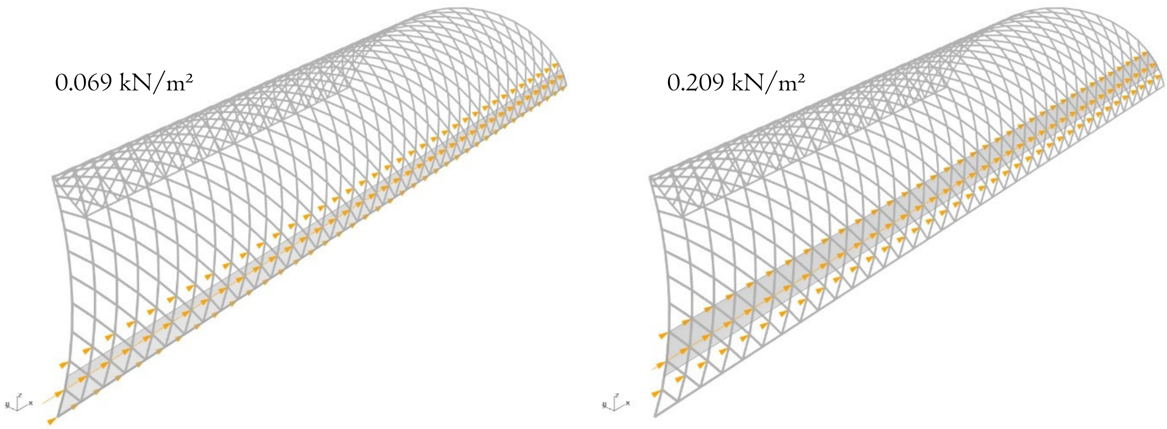

Figure 53: Seismic actions X-direction | Zone 1 (L) & Zone 2 (R)

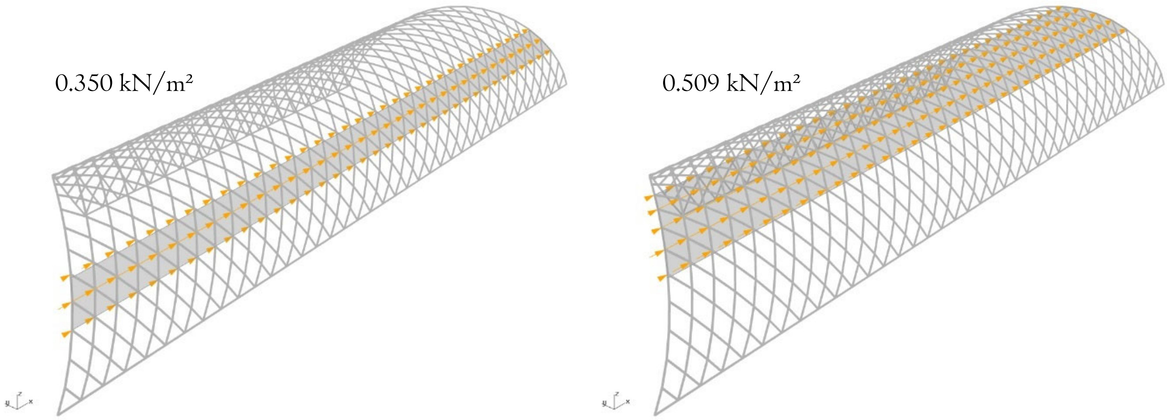

Figure 54: Seismic actions X-direction | Zone 3 (L) & Zone 4 (R)

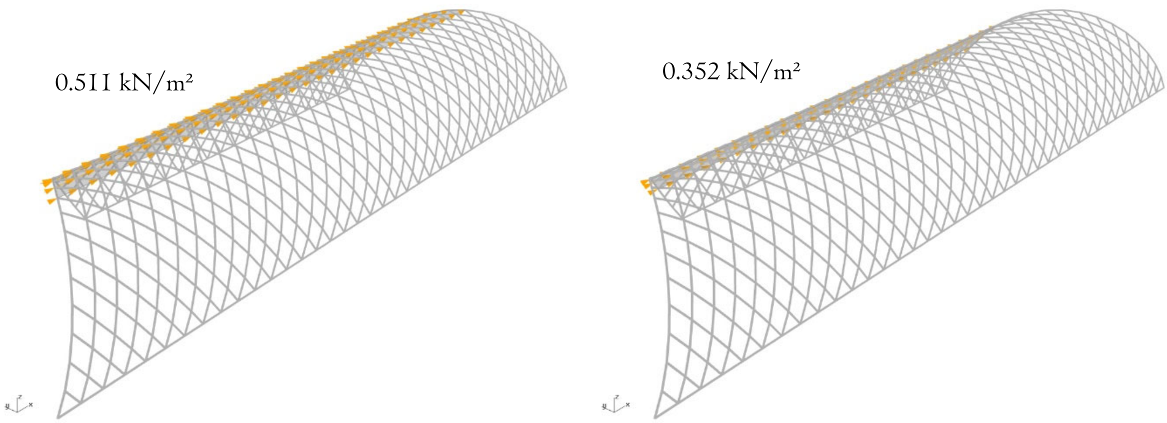

Figure 55: Seismic actions X-direction | Zone 5 (L) & Zone 6 (R)

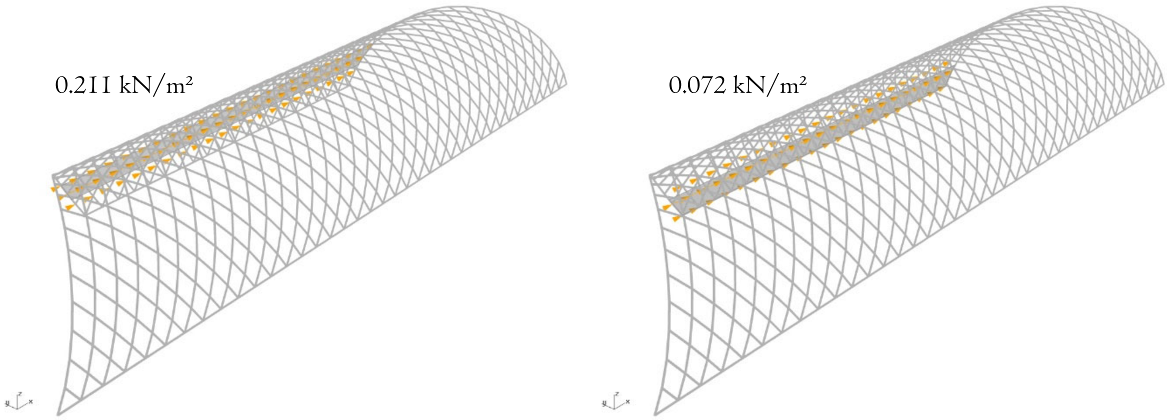

Figure 56: Seismic actions X-direction | Zone 7 (L) & Zone 8 (R)

5.6.2 Seismic actions in Y-direction

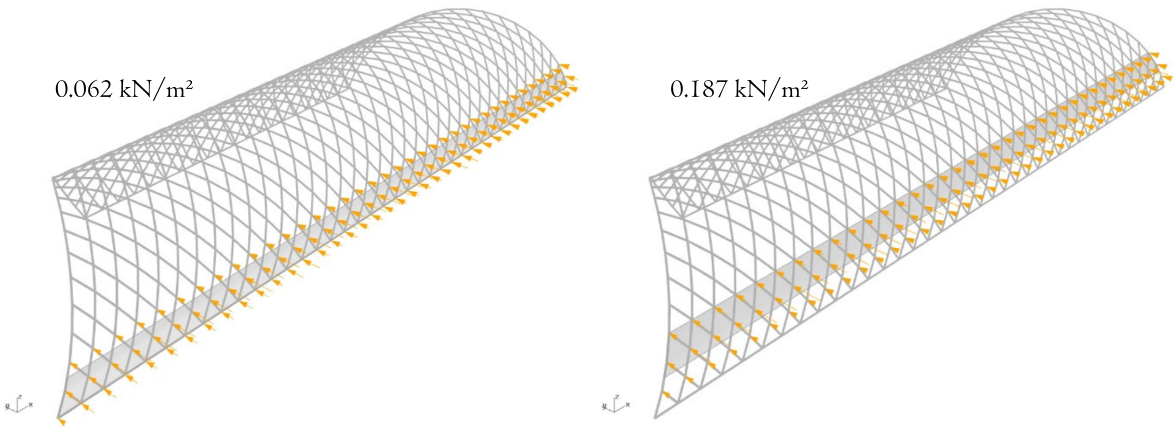

Figure 57: Seismic actions Y-direction | Zone 1 (L) & Zone 2 (R)

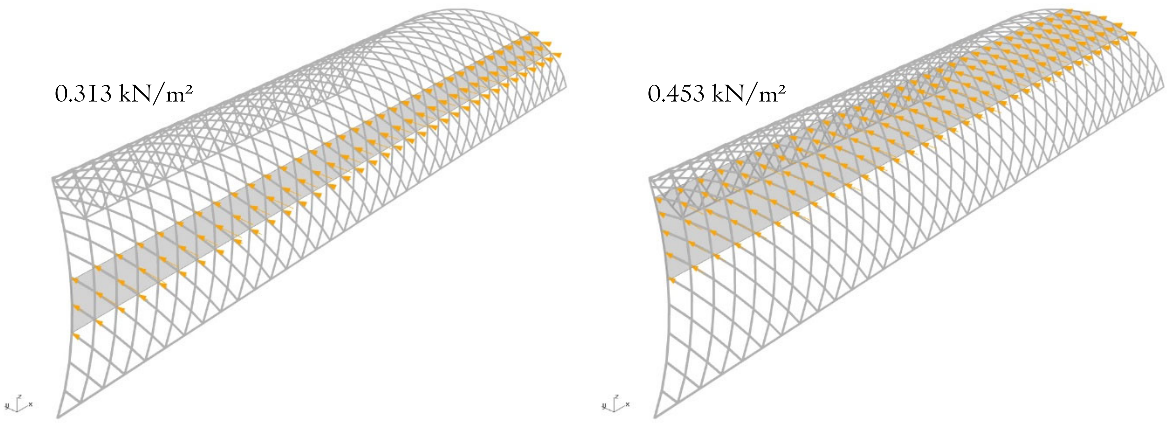

Figure 58: Seismic actions Y-direction | Zone 3 (L) & Zone 4 (R)

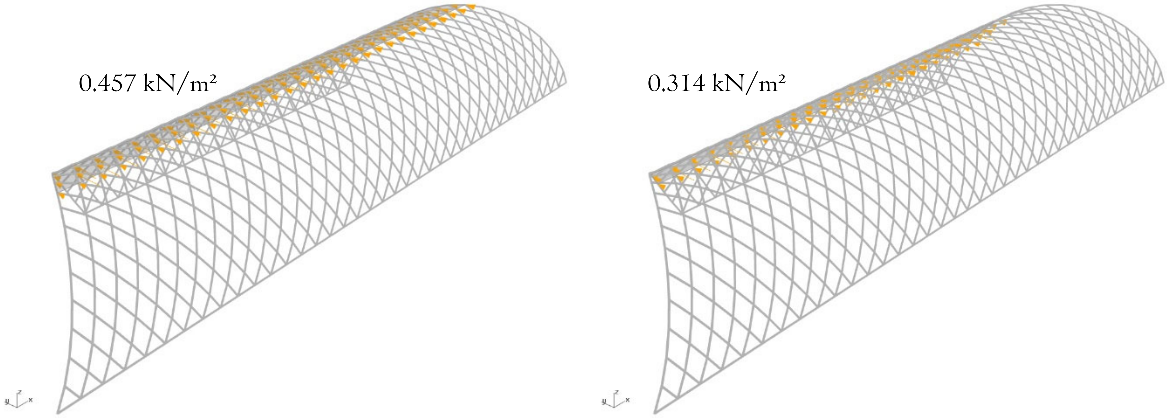

Figure 59: Seismic actions Y-direction | Zone 5 (L) & Zone 6 (R)

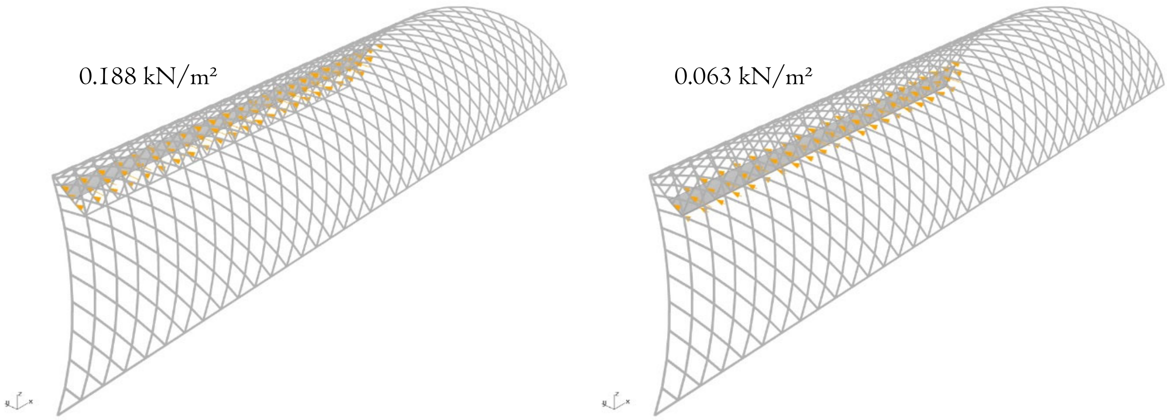

Figure 60: Seismic actions Y-direction | Zone 7 (L) & Zone 8 (R)

5.7 Load combinations

In accordance with the Eurocode (EN 1990, 2011) and the Italian national annex (UNI-EN 1990, 2007), 40 load combinations have been defined, which are presented in Table 7. For the origin of these load combinations, please refer to Appendix F.

Table 7: Load combinations

			A | Self-weight	B | Exterior loads	C | Interior loads	D | Wind 1 (North)	E | Wind 2 (South)	F | Wind 3 (East/West)	G | Snow 1	H | Snow 2	J | Snow 3	K | Maintenance UDL 1	L | Maintenance UDL 2	M | Maintenance PL 1	N | Maintenance PL 2	O | Seismic loads X	P | Seismic loads Y
SLS	101	**PERMANENT**		1.0													
SLS	102	permanent + **WIND 1**		1.0		1.0											
SLS	103	permanent + **WIND 2**		1.0			1.0										
SLS	104	permanent + **WIND 3**		1.0				1.0									
SLS	105	permanent + **SNOW 1**		1.0					1.0								
SLS	106	permanent + **SNOW 2**		1.0						1.0							
SLS	107	permanent + **SNOW 3**		1.0							1.0						
SLS	108	permanent + snow 1 + **MAINTENANCE UDL 1**		1.0					0.2			1.0					
SLS	109	permanent + snow 2 + **MAINTENANCE UDL 1**		1.0						0.2		1.0					
SLS	110	permanent + snow 3 + **MAINTENANCE UDL 1**		1.0							0.2	1.0					
SLS	111	permanent + snow 1 + **MAINTENANCE UDL 2**		1.0					0.2				1.0				
SLS	112	permanent + snow 2 + **MAINTENANCE UDL 2**		1.0						0.2			1.0				
SLS	113	permanent + snow 3 + **MAINTENANCE UDL 2**		1.0							0.2		1.0				
SLS	114	permanent + snow 1 + **MAINTENANCE PL 1**		1.0					0.2					1.0			
SLS	115	permanent + snow 2 + **MAINTENANCE PL 1**		1.0						0.2				1.0			
SLS	116	permanent + snow 3 + **MAINTENANCE PL 1**		1.0							0.2			1.0			
SLS	117	permanent + snow 1 + **MAINTENANCE PL 2**		1.0					0.2						1.0		
SLS	118	permanent + snow 2 + **MAINTENANCE PL 2**		1.0						0.2					1.0		
SLS	119	permanent + snow 3 + **MAINTENANCE PL 2**		1.0							0.2				1.0		
ULS	201	**PERMANENT**		1.3													
ULS	202	permanent + **WIND 1**		1.0		1.5											
ULS	203	permanent + **WIND 2**		1.0			1.5										
ULS	204	permanent + **WIND 3**		1.0				1.5									
ULS	205	permanent + **SNOW 1**		1.3					1.5								
ULS	206	permanent + **SNOW 2**		1.3						1.5							
ULS	207	permanent + **SNOW 3**		1.3							1.5						
ULS	208	permanent + snow 1 + **MAINTENANCE UDL 1**		1.3					0.3			1.5					
ULS	209	permanent + snow 2 + **MAINTENANCE UDL 1**		1.3						0.3		1.5					
ULS	210	permanent + snow 3 + **MAINTENANCE UDL 1**		1.3							0.3	1.5					
ULS	211	permanent + snow 1 + **MAINTENANCE UDL 2**		1.3					0.3				1.5				
ULS	212	permanent + snow 2 + **MAINTENANCE UDL 2**		1.3						0.3			1.5				
ULS	213	permanent + snow 3 + **MAINTENANCE UDL 2**		1.3							0.3		1.5				
ULS	214	permanent + snow 1 + **MAINTENANCE PL 1**		1.3					0.3					1.5			
ULS	215	permanent + snow 2 + **MAINTENANCE PL 1**		1.3						0.3				1.5			
ULS	216	permanent + snow 3 + **MAINTENANCE PL 1**		1.3							0.3			1.5			
ULS	217	permanent + snow 1 + **MAINTENANCE PL 2**		1.3					0.3						1.5		
ULS	218	permanent + snow 2 + **MAINTENANCE PL 2**		1.3						0.3					1.5		
ULS	219	permanent + snow 3 + **MAINTENANCE PL 2**		1.3							0.3				1.5		
SLV	301	permanent + **SEISMIC X** + seismic y		1.0												1	0.3
SLV	302	permanent + seismic x + **SEISMIC Y**		1.0												0.3	1

5.8 Conclusion

In total, 40 load combinations have been defined and applied to the parametric models, including loads resulting from wind, snow, earthquakes, maintenance and permanent elements. The next step is to define the structural checks that need to be carried out for all the models, which will be described in Chapter 0.

6 Unity Checks

6.1 Introduction

As the loads and load combinations have been defined in Chapter 5, the structural verifications that are to be carried out need to be defined. Two different materials have been used for the parametric models – steel and timber – and both of these need to be checked differently.

6.2 Steel

For steel, all unity checks are integrated in Karamba based on the Eurocode for steel (EN 1993-1-1, 2016), as described by the program's manual (Preisinger, 2018). The calculations the program carries out are assumed to be correct. The software provides some flexibility with regard to the national differences, so that the partial material factor used for structural steel in the Italian national annex (UNI-EN 1993-1-1, 2007) can be applied:

$$\gamma_M = 1.05$$

However, though the calculations are assumed to be correct, the final design chosen will be double-checked using the alternative calculation software RFEM.

6.3 Timber

As mentioned, the unity checks for timber have to be integrated in the Grasshopper-script manually using Python-scripting. The following results for each of the timber element will be extracted from the parametric models, at two locations in every beam – at the start and end point:

- Axial load N [kN]
- Shear load V_y [kN]
- Shear load V_z [kN]
- Bending moment M_y [kNm]
- Bending moment M_z [kNm]

The members will be structurally verified at each of the aforementioned locations. The design value of a strength property needs to be calculated as follows (EN 1995-1-1, 2011):

$$X_d = k_{mod} \cdot \frac{X_k}{\gamma_M} \tag{1}$$

In which:

X_d	Design value of any strength property of timber
X_k	Characteristic value of any strength property of timber
k_{mod}	Modification factor taking into account load duration and moisture content
γ_M	Partial factor for material properties

The Italian national annex (UNI-EN 1995-1-1, 2007) prescribes the following value for the partial factor in case of sawn timber:

$$\gamma_M = 1.5$$

As the timber in the structure is partially exposed to the elements, the least favourable climate class will be assumed (class 3) in which the moisture content of the timber can be high. This combined with the fact solid sawn timber is applied, results in the following modification factors according to the Italian national annex (UNI-EN 1995-1-1, 2007):

$k_{mod} = 0.50$ in case of permanent loads, i.e. self-weight

$k_{mod} = 0.55$ in case of long-term loads, i.e. storage

$k_{mod} = 0.65$ in case of medium-term loads, i.e. imposed loads

$k_{mod} = 0.70$ in case of short-term loads, i.e. snow

$k_{mod} = 0.90$ in case of instantaneous loads, i.e. wind

The checks that have to be carried out are in accordance with the Eurocode for timber structures (EN 1995-1-1, 2011) and the Italian national annex (UNI-EN 1995-1-1, 2007), and will be described in the following paragraphs.

6.3.1 Axial tension

If a member is loaded by axial tension without bending, the unity check needs to be carried out as prescribed in the equation below:

$$\frac{\sigma_{t,0,d}}{f_{t,0,d}} \leq 1 \tag{2}$$

In which:

$\sigma_{t,0,d}$ Design value of the stresses due to tension parallel to the grain

$f_{t,0,d}$ Design value of the tensile strength parallel to the grain

6.3.2 Axial compression

If a member is loaded by axial compression without bending, the following unity check needs to be carried out:

$$\frac{\sigma_{c,0,d}}{f_{c,0,d}} \leq 1 \tag{3}$$

In which:

$\sigma_{c,0,d}$ Design value of the stresses due to compression parallel to the grain

$f_{c,0,d}$ Design value of the compressive strength parallel to the grain

6.3.3 Bending

If pure bending occurs, the following two unity checks need to be carried out:

$$\frac{\sigma_{m,y,d}}{f_{m,y,d}} + k_m \cdot \frac{\sigma_{m,z,d}}{f_{m,z,d}} \leq 1 \tag{4}$$

$$k_m \cdot \frac{\sigma_{m,y,d}}{f_{m,y,d}} + \frac{\sigma_{m,z,d}}{f_{m,z,d}} \leq 1 \tag{5}$$

In which:

$\sigma_{m,y,d}$	Design value of stresses due to bending around the y-axis
$\sigma_{m,z,d}$	Design value of stresses due to bending around the z-axis
$f_{m,y,d}$	Design value of the bending strength around the y-axis
$f_{m,z,d}$	Design value of the bending strength around the z-axis
k_m	Factor taking into account the stress redistribution and the heterogeneity of the material in its cross section

For rectangular cross sections – which are the only cross sections considered in the parametric model – the following factor applies:

$$k_m = 0.7$$

6.3.4 Shear

The shear that occurs in the member, needs to be checked using the following unity check:

$$\frac{\tau_d}{f_{v,d}} \leq 1 \tag{6}$$

In which:

τ_d	Design value of the stresses due to shear
$f_{v,d}$	Design value of the shear strength

6.3.5 Combination: bending & axial tension

When members are loaded by both bending and axial tension, the following combined unity checks need to be carreid out:

$$\frac{\sigma_{t,0,d}}{f_{t,0,d}} + \frac{\sigma_{m,y,d}}{f_{m,y,d}} + k_m \cdot \frac{\sigma_{m,z,d}}{f_{m,z,d}} \leq 1 \tag{7}$$

$$\frac{\sigma_{t,0,d}}{f_{t,0,d}} + k_m \cdot \frac{\sigma_{m,y,d}}{f_{m,y,d}} + \frac{\sigma_{m,z,d}}{f_{m,z,d}} \leq 1 \tag{8}$$

In which:

$\sigma_{t,0,d}$	Design value of the stresses due to tension parallel to the grain
$f_{t,0,d}$	Design value of the tensile strength parallel to the grain
$\sigma_{m,y,d}$	Design value of stresses due to bending around the y-axis
$\sigma_{m,z,d}$	Design value of stresses due to bending around the z-axis
$f_{m,y,d}$	Design value of the bending strength around the y-axis
$f_{m,z,d}$	Design value of the bending strength around the z-axis
k_m	Factor taking into account the stress redistribution and the heterogeneity of the material in its cross section (see paragraph 6.3.3)

6.3.6 Combination: bending & axial compression

Lastly, members that are loaded by both bending and axial compression, need to be structurally verified using the following unity checks:

$$\left(\frac{\sigma_{c,0,d}}{f_{c,0,d}}\right)^2 + \frac{\sigma_{m,y,d}}{f_{m,y,d}} + k_m \cdot \frac{\sigma_{m,z,d}}{f_{m,z,d}} \leq 1 \tag{9}$$

$$\left(\frac{\sigma_{c,0,d}}{f_{c,0,d}}\right)^2 + k_m \cdot \frac{\sigma_{m,y,d}}{f_{m,y,d}} + \frac{\sigma_{m,z,d}}{f_{m,z,d}} \leq 1 \tag{10}$$

In which:

$\sigma_{c,0,d}$	Design value of the stresses due to compression parallel to the grain
$f_{c,0,d}$	Design value of the compressive strength parallel to the grain
$\sigma_{m,y,d}$	Design value of stresses due to bending around the y-axis
$\sigma_{m,z,d}$	Design value of stresses due to bending around the z-axis
$f_{m,y,d}$	Design value of the bending strength around the y-axis
$f_{m,z,d}$	Design value of the bending strength around the z-axis
k_m	Factor taking into account the stress redistribution and the heterogeneity of the material in its cross section (see paragraph 6.3.3)

6.4 Conclusion

The members in each of the models will be checked using the relevant structural checks. The verifications for steel members are integrated in the Karamba software and will be carried out automatically. The timber checks as described in this chapter have been added to the script manually using Python, based on a script previously defined during a graduation project at the TU Delft concerning the optimisation of a timber bridge (Koning, 2018). The final step in the definition of the Grasshopper-script is the determination of environmental values, which will be covered in Chapter 7.

7 Environmental impact analysis

7.1 Introduction

After having defined all structural input for the Grasshopper-script in the previous chapters, a final step needs to be taken to finish up: the determination of the environmental impact. Designing for an after-disaster setting requires some special attention due to the sensitivity of the situation. The goal of the architectural design was not to add extra waste to what is already there and even to try and have a positive impact by using the surrounding rubble as foundational weight. The envisioned demountability also plays a big part in this regard, by making it entirely reusable for multiple cycles of up to 10 years. The envisioned life time would be around 50 years.

Keeping this goal in mind during the structural design, the environmental impact of each of the models should be taken into consideration as well. The first idea was to carry out a Life Cycle Assessment (LCA) and to link the outcoming values to variables in the script (e.g. structural weight). However, an LCA usually gets performed on a finished product. It is also very extensive and there are set demands for the amount of impact fields that need to be expressed. Carrying out such an extensive analysis on a conceptual design would require a lot of work while simultaneously basing all that work on assumptions.

Therefore, a simplified version of the LCA is carried out, an environmental impact analysis using the softwere CES EduPack 2018. The environmental impact will be expressed in a CO_2-equivalent (in kg per year) and an energy-equivalent (in MJ per year). The goal of this analysis is two-fold:

1. Finding the environmental impacts per kg of each structural material in the global structure (the less weight, the better);
2. Finding the environmental impacts per joint, which are relatively labour-intensive to produce (the fewer joints, the better).

These values will be linked to the total structural weight as well as the number of nodes that represent the number of joints that are necessary. For these values, the end-of-life potential will also be taken into account.

7.1.1 CES EduPack 2018

CES EduPack 2018 is a set of teaching resources that support materials education across engineering, design, science and sustainable development (CES EduPack, 2018). The software contains a tool called Eco Audit, which calculates the equivalent annual environmental burden with regard to CO_2-footprint and energy consumption.

The calculation of the impacts during the lifetime of a product is very well-founded, using averaged values based on the outcome of several databases, scholarly papers and reports. The references include the online database Ecoinvent (Ecoinvent v2.2, 2010), an environmental inventory produced by the University of Bath (Hammond & Jones, 2008) and a study performed to support the Dutch environmental policy of dematerialisation (Voet, Oers, & Nikolic, 2008).

CES EduPack also provides an estimate for the end-of-life potential for both the CO_2-footprint and the energy-equivalent. However, only little insight is provided into the calculations carried out by the software. Therefore, the end-of-life potential will be based on self-defined assumptions.

7.2 Main structure

This paragraph gathers the main information with regard to the CES calculation, please refer to Appendix G for more detail. Both steel strengths have a very similar background, and therefore will be covered together in one paragraph. Both timber species have a very different origin, and will therefore be treated seperately.

7.2.1 Steel

7.2.1.1 Lifetime assumptions

The exposure category of a steel structure in L'Aquila is C3 (EN-ISO 12944-2, 2018), which is the case for urban and industrial atmospheres with moderate pollution. It means there is a medium level of corrosivity of the steel due to atmospheric exposure.

Untreated steel in this atmosphere loses about 0.025 to 0.030 mm of thickness in one year. Making the conservative assumption that this the thickness decreases linearly, this would meen that the steel loses about 1.25 to 2.50 mm thickness in its intended lifetime of 50 years. In order to account for this thickness loss, much thicker profiles would be needed for the structure to function properly throughout its lifetime. For example, a steel profile with a thickness of 6.3mm would be needed instead of a 4.0mm, meaning the material increases by more than 50%. This means the total structural mass increases by a very significant amount. On top of that, the elements are not as easily reusable at the end of their lifetime due to heavy corrosion.

Therefore, a hot-dip galvanised coating will be applied to the steel. This surface treatment provides the best durability results in the exposed setting of the design. In a C3 exposure category, the treated steel elements will be intact for more than 50 years, while the coating remains unaffected for more than 40 years. It is assumed that during the initial lifetime of 50 years no maintenance is necessary. However, in order to reuse the elements, the steel would need to be treated again and thus the necessary surface treatment is assumed to be 200% to be able to reuse the material after its initial lifetime of 50 years.

The assumptions relevant for CES EduPack 2018 are as follows:

- Lifetime — the lifetime taken into account is 50 years;
- Material — 1 kg of structure needs 1 kg of steel (there are no losses throughout the lifetime); the database of CES does not contain S235 and S355 and for this analysis they have been replaced by AISI1020 and AISI1040 respectively;
- Manufacturing — the primary process of the steel is roll-forming;
- Finishing — the database of CES does not provide the option of hot-dip galvanisation in the Eco Audit tool, and it has therefore been replaced by electroplating;
- Transport — the steel is transported by an 8-axle truck over a distance of 600 km from production in Milan to L'Aquila.

7.2.1.2 End-of-life assumptions

For the end-of-life potential, it is assumed that due to the surface retreatment, the steel can be reused for a second lifetime. However, after this lifetime, the steel will have degraded and will therefore be remanufactured by melting it down. It is assumed that by melting down the steel 33.3% of the initial material and manufacturing input (both CO_2 and energy) can be saved for future appliances compared to the production using virgin materials.

Thus, there will be a total loss of 66.7% at the end of the two lifetimes. Divided over the two lifetimes, this gives a loss of 33.3% per lifetime and thus and end-of-life potential of (-) 66.7% of the material and manufacturing input.

7.2.1.3 Results S235 & S355

Table 8: Environmental impact per kg steel

	S235				S355			
	Energy [MJ]		CO_2-footprint [kg]		Energy [MJ]		CO_2-footprint [kg]	
	Absolute	Relative	Absolute	Relative	Absolute	Relative	Absolute	Relative
Material	32.30	83.6%	2.370	84.6%	32.30	82.53%	2.370	84.08%
Manufacture	5.73	14.8%	0.386	13.8%	6.21	15.87%	0.404	14.33%
Transport	0.43	1.1%	0.031	1.1%	0.43	1.09%	0.031	1.09%
Disposal	0.20	0.5%	0.014	0.5%	0.20	0.51%	0.014	0.50%
SUBTOTAL	38.66	100.0%	2.801	100.0%	39.14	100.00%	2.819	100.00%
EoL potential	-25.35	-65.6%	-1.84	-65.6%	-25.67	-65.6%	-1.85	-65.6%
TOTAL	13.30	34.4%	0.96	34.4%	13.46	34.4%	0.97	34.4%
TOTAL per year	**0.266**		**0.0193**		**0.269**		**0.0194**	

Gathering all assumptions and information in CES as well as applying the self-defined end-of-life assumptions, the environmental burden is expressed in Table 8 for both S235 and S355. Note that the end-of-life potential percentages are a little different than the aforementioned 66.7%. The 66.7% end-of-life potential was compared to only the material an manufacturing equivalents, while the table percentages are relative to all four inputs.

S355 is slightly more labour-intensive to produce, but apart from that the environmental impact of the two steels is very comparable.

7.2.2 Timber: D24 (Chestnut)

7.2.2.1 Lifetime assumptions

The durability class of chestnut is Class 2 (EN 1912, 2012). This means that structures of chestnut can live for more than 50 years when protected properly and up to 40 years when exposed to the elements above ground (Durability Class, 2018). About a third of the total structure is exposed to the elements, as shown in Figure 61. It is assumed that the chestnut in this part of the structure – say 30% – needs replacing in order to be able to reach the envisioned lifetime of 50 years.

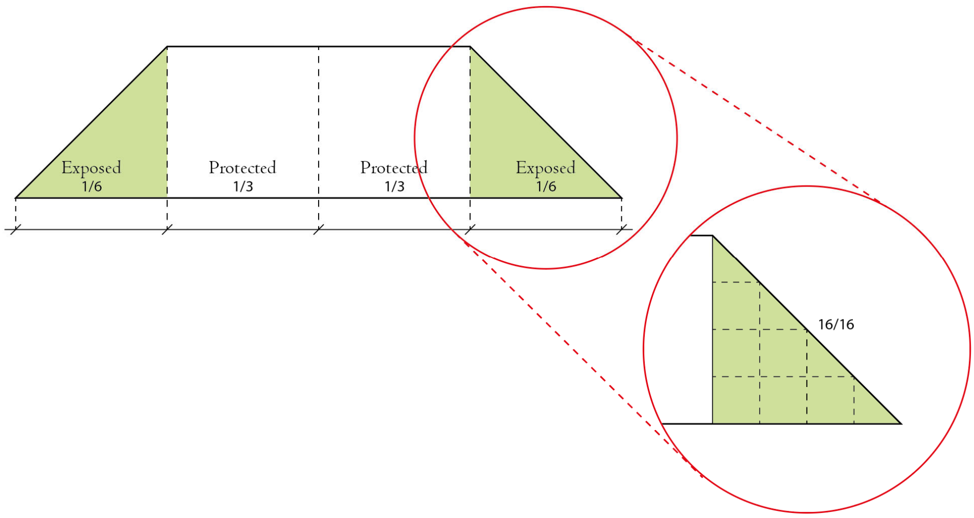

Figure 61: Fraction of D24 to be replaced

The assumptions relevant for CES EduPack 2018 are as follows:

- Lifetime — the lifetime taken into account is 50 years;
- Material — 1 kg of structure needs 1.3 kg of timber (30% needs replacing throughout the lifetime);
- Manufacturing — the environmental burden of the primary process of timber is integrated in the material burden; the secondary process is cutting and trimming of the elements through which 10% of the material gets removed;
- Finishing — the timber does not require any further finishing;
- Transport — the sweet chetsnut is transported by an 8-axle truck over a distance of 700 km from production in Mezzocorona, Italy, to L'Aquila.

7.2.2.2 End-of-life assumptions

Considering the life expectancy and taking into account the partial replacement of the structure, it is assumed that 25% of the chestnut structure can be reused after its initial lifetime of 50 years. Timber that cannot be reused will be combusted. That means that after the first lifetime 75% will be combusted, while the other 25% will be combusted after the second lifetime.

It is assumed that the CO_2-release during combustion is evened out by the absorbed CO_2 during the growth stage of the timber, and therefore no additional CO_2-footprint is assigned due to combustion. As there is no extra release, nor a positive impact on the CO_2-footprint, the end-of-life potential is set to 0%.

During combustion, energy will be generated, and it is assumed that only 50% of input energy will be lost. These means the following, for the timber in the structure:

- When conbusted after the first lifetime, there is 50% end-of-life potential with regard to energy, while there is 0% end-of-life potential with regards to CO_2-footprint;
- When combusted after the second lifetime, the total losses need to be divided over the two lifetimes. This means that there is 100-(50/2)= 75% end-of-life potential with regard to energy, and 100-(100/2)= 50% end-of-life potential with regard to CO_2-footprint.

Taking these values into account as well as the assumed percentages of the structure that will have one respectively two lifetimes, the following values for the end-of-life potential are produced:

- Energy end-of-life potential: $0.75 \times 50 + 0.25 \times 75 = 56.25\%$
- CO_2-footprint end-of-life potential: $0.75 \times 0 + 0.25 \times 50 = 12.50\%$

Note that these percentages regard the the environmental burdens of the material and manufacturing, so without considering the transport and disposal values.

7.2.2.3 Results D24 (Chestnut)

Gathering all assumptions and information in CES as well as applying the self-defined end-of-life assumptions, the environmental burden is expressed in Table 9 for chestnut.

Table 9: Environmental impact per kg chestnut

	Chestnut			
	Energy [MJ]		CO_2-footprint [kg]	
	Absolute	Relative	Absolute	Relative
Material	17.60	93.41%	0.872	90.78%
Manufacture	0.04	0.23%	0.003	0.35%
Transport	0.65	3.43%	0.047	4.84%
Disposal	0.55	2.93%	0.039	4.03%
SUBTOTAL	18.84	100.00%	0.961	100.00%
EoL potential	-9.92	-52.7%	-0.11	-11.4%
TOTAL	8.92	47.3%	0.85	88.6%
TOTAL per year	**0.178**		**0.0170**	

7.2.3 Timber: D70 (Azobé)

7.2.3.1 Lifetime assumptions

The durability class of azobé is Class 1-2 (EN 1912, 2012). This means that a structure of azobé can live for more than 50 years when protected properly, and more than 40 years when exposed to the elements above ground. About a third of the total structure is exposed to the elemtens, as shown in Figure 61. However, some parts of the structure are more exposed than others. As azobé is slightly more durable than chestnut, only the more exposed part is assumed to need replacement – say 15% – in order to reach the envisioned lifetime of 50 years.

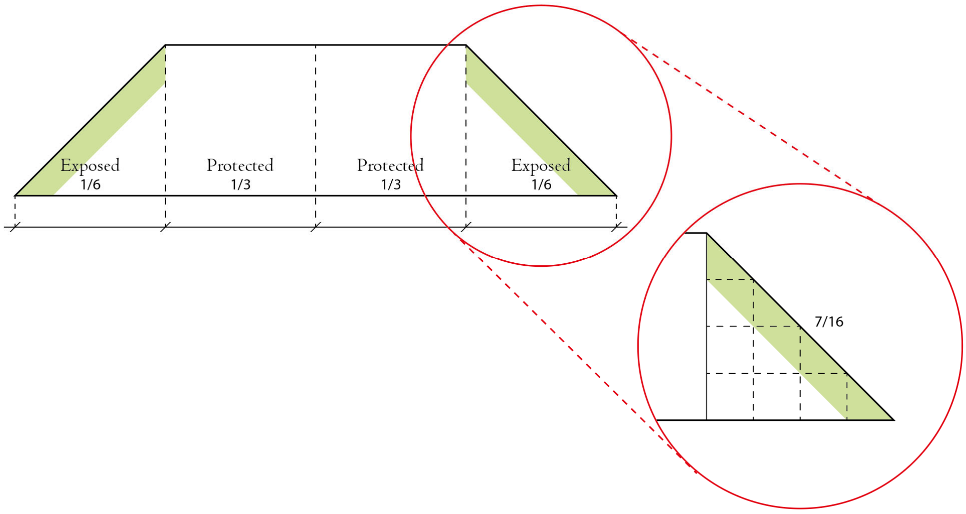

Figure 62: Fraction of D70 to be replaced

The assumptions relevant for CES EduPack 2018 are as follows:

- Lifetime — the lifetime taken into account is 50 years;
- Material — 1 kg of structure needs 1.15 kg of timber (15% needs replacing throughout the lifetime);
- Manufacturing — the environmental burden of the primary process of timber is integrated in the material burden; the secondary process is cutting and trimming of the elements through which 10% of the material gets removed;
- Finishing — the timber does not require any further finishing;
- Transport — the azobé is transported by an 8-axle truck over a distance of 350 km from production in Akure, Nigeria, to the harbour of Lagos, Nigeria; it is then transported by ocean freight over a distance of 7400 km from Lagos, Nigeria to the harbour of Fiumicino, Italy; lastly, it is transported by an 8-axle truck over a distance of 200 km from Fuimicino to L'Aquila.

7.2.3.2 End-of-life assumptions

Considering the life expectancy and taking into account the partial replacement of the structure, it is assumed that 50% of the azobé structure can be reused after its first lifetime of 50 years. Timber that cannot be reused will be combusted. That means that after the first lifetime 50% will be combusted, while the other 50% will be combusted after the second lifetime.

As was described for chestnut (see paragraph 7.2.2), the following assumptions are made for the end-of-life:

- When conbusted after the first lifetime, there is 50% end-of-life potential with regard to energy, while there is 0% end-of-life potential with regards to CO_2-footprint;
- When combusted after the second lifetime, the total losses need to be divided over the two lifetimes. This means that there is 100-(50/2)= 75% end-of-life potential with regard to Energy, and 100-(100/2)= 50% end-of-life potential with regard to CO_2-footprint.

Taking into account the assumed percentages of the structure that will have one and two lifetimes, this gives the following values for the end-of-life potential:

- Energy end-of-life potential: $0.50 \times 50 + 0.50 \times 75 = 62.50\%$
- CO_2-footprint end-of-life potential: $0.50 \times 0 + 0.50 \times 50 = 25.00\%$

Note that these percentages regard the the environmental burdens of the material and manufacturing, so without considering the transport and disposal values.

7.2.3.3 Results D70 (Azobé)

Table 10: Environmental impact per kg azobé

	Azobé			
	Energy [MJ]		CO_2-footprint [kg]	
	Absolute	Relative	Absolute	Relative
Material	15.60	86.56%	0.771	81.58%
Manufacture	0.04	0.21%	0.003	0.31%
Transport	1.98	10.99%	0.143	15.13%
Disposal	0.40	2.24%	0.028	2.98%
SUBTOTAL	18.02	100.00%	0.945	100.00%
EoL potential	-9.77	-54.2%	-0.19	-20.5%
TOTAL	8.25	45.8%	0.75	79.5%
TOTAL per year	**0.165**		**0.0150**	

Gathering all assumptions and information in CES as well as applying the self-defined end-of-life assumptions, the environmental burden is expressed in Table 10 for azobé.

7.2.4 Annual environmental burden per kg structure

Figure 63 shows the annual environmental burden per kg structure. These values will be integrated in the parametric script by linking the values to the total mass of the structure. Figure 64 gathers all values presented in the previous paragraphs summing up to a total environmental burden to grant overview.

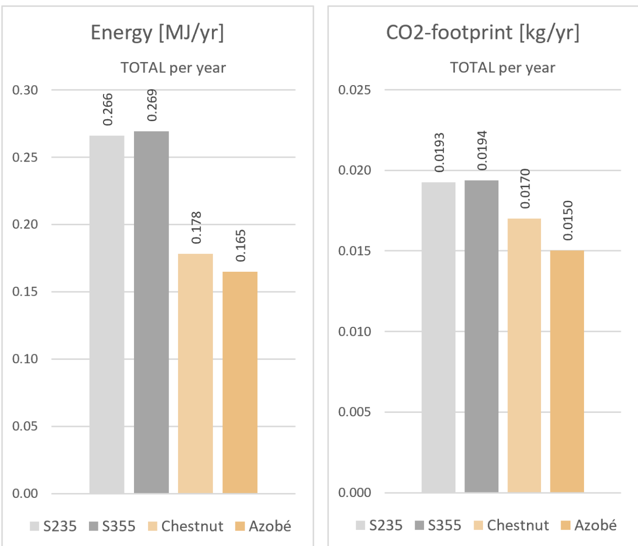

Figure 63: Annual environmental burden per kg structure

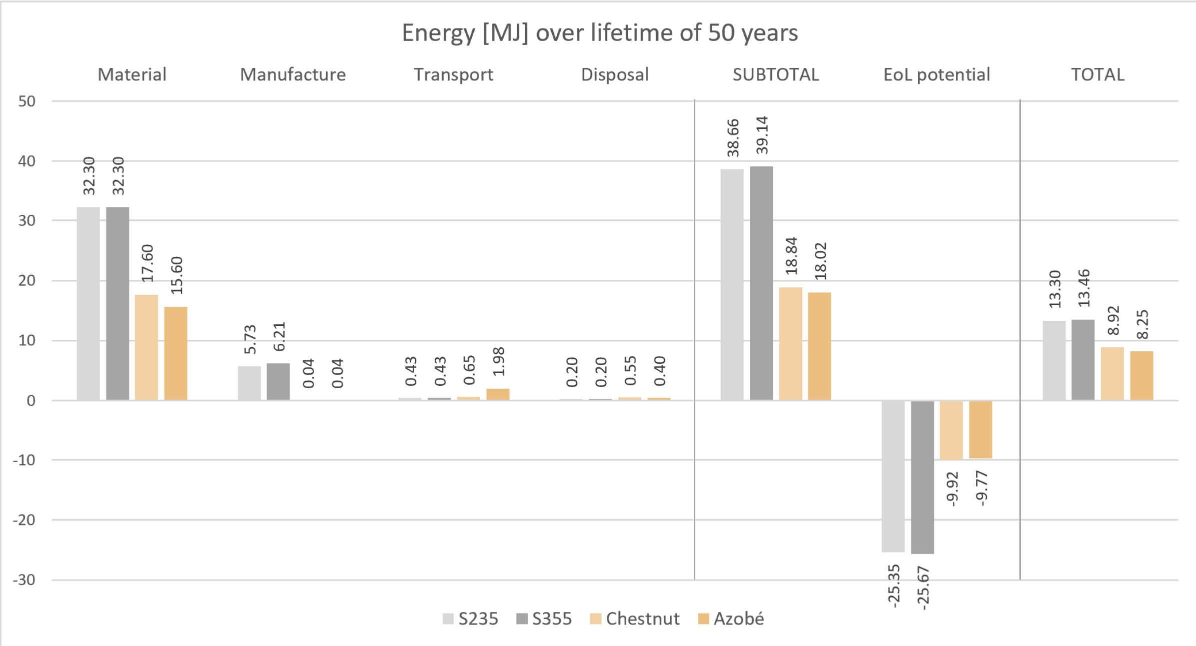

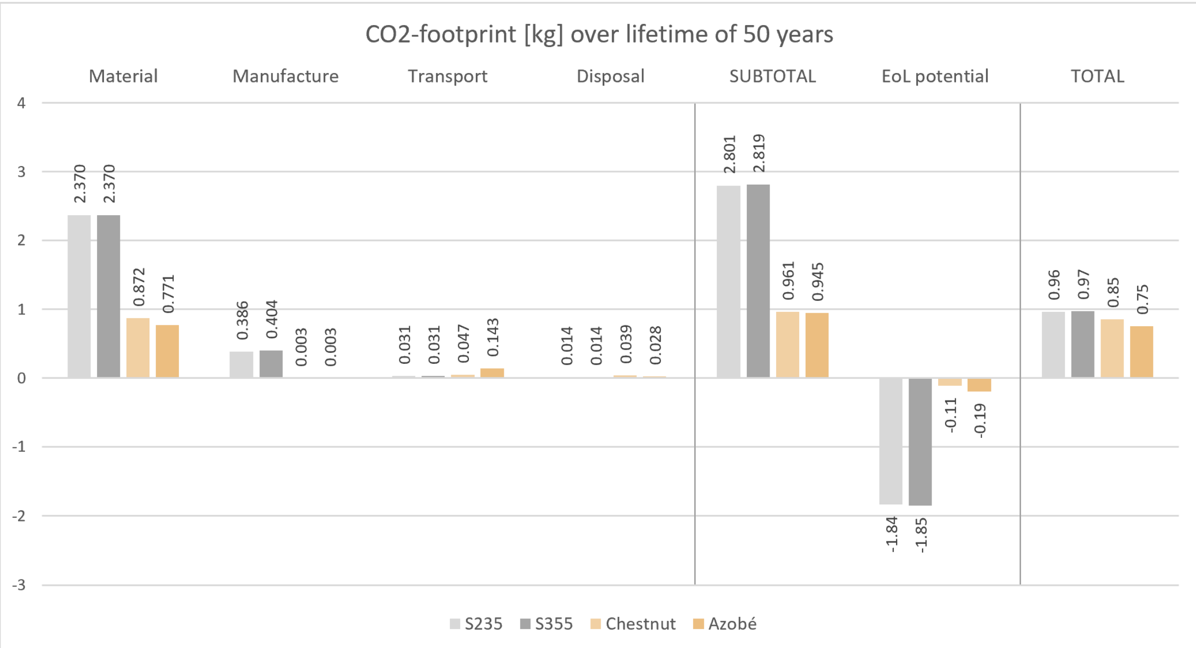

Figure 64: Environmental burden over lifetime of 50 years per kg of structure

7.3 Structural joints

Apart from the structural weight, the joints also have a significant influence on the environmental impact of each of the structural configurations.

7.3.1 Conceptual joint design

A conceptual joint design for both the steel variations and the timber variations is shown in Figure 65.

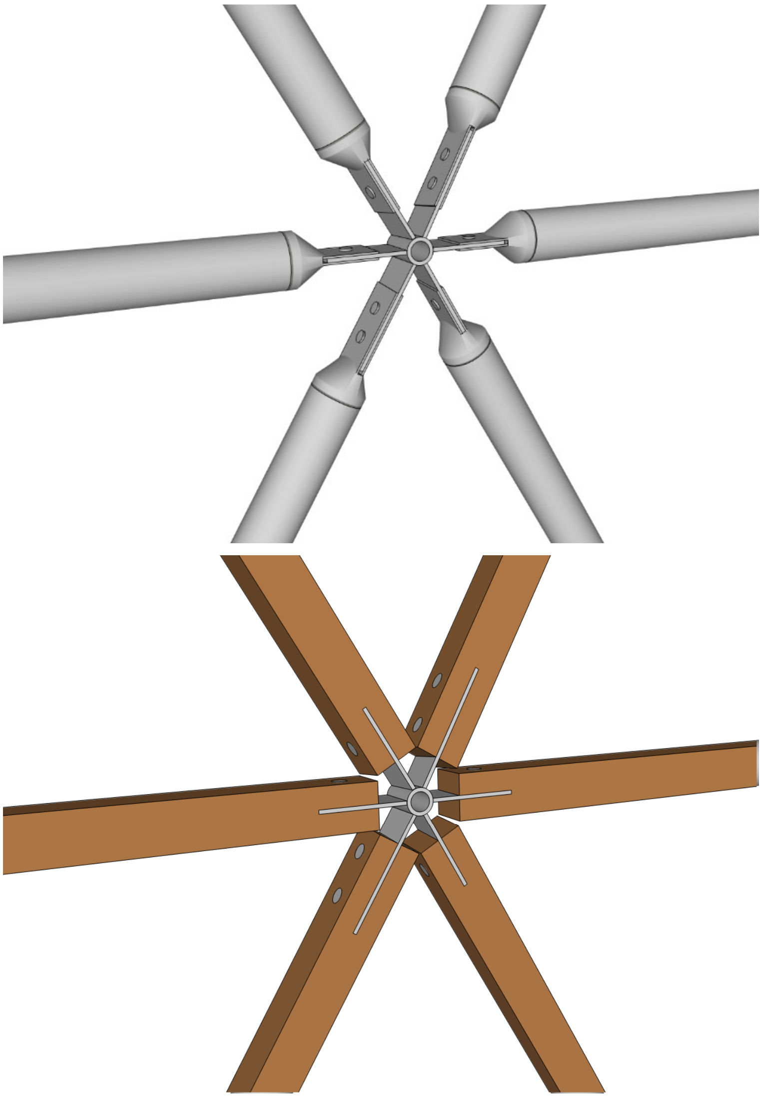

Figure 65: Conceptual joint design steel structure (top) and timber structure (bottom)

The main goal during the design was to make sure that structural elements can be replaced individually in case damage occurs during the lifetime. In the timber design this was relatively simple to achieve. However, to ensure the same structural flexibility in the steel design, cast connectors have been welded to the structural elements.

7.3.2 Joints steel structure

7.3.2.1 Lifetime assumptions

The assumptions relevant for CES EduPack 2018 are as follows (see Appendix G for derivation):

- Lifetime: the lifetime taken into account is 50 years;
- Material & manufacturing: 1 joint needs 16.8 kg of roll-formed plates and 30 kg of casted connectors of steel grade AISI 1040 (≈S355);
- Finishing & joining: no finishing, 8 large fasteners and 5.19 m of welds are taken into account;
- Transport: the steel is transported by an 8-axle truck over a distance of 600 km from production in Milan to L'Aquila.

7.3.2.2 End-of-life potential

As with the steel structure (see paragraph 7.2.1.2), the end-of-life potential of the steel connectors is assumed to be 66.7% of the material and manufacturing input.

7.3.2.3 Results steel structure joints

The results for both the energy-equivalent and the CO_2-equivalent per year are presented in Table 11.

Table 11: Results steel structure joints

	Joint steel structure - S355			
	Energy [MJ]		CO_2-footprint [kg]	
	Absolute	Relative	Absolute	Relative
Material	1510.00	77.3%	111.000	77.1%
Manufacture	413.00	21.2%	30.900	21.5%
Transport	19.90	1.0%	1.440	1.0%
Disposal	9.36	0.5%	0.655	0.5%
SUBTOTAL	1952.26	100.0%	143.995	100.0%
EoL potential	-1282.06	-65.7%	-94.60	-65.7%
TOTAL	670.20	34.3%	49.39	34.3%
TOTAL per year	**13.404**		**0.9878**	

7.3.3 Joints timber structure

7.3.3.1 Lifetime assumptions

The assumptions relevant for CES EduPack 2018 are as follows (see Appendix G for derivation):

- Lifetime: the lifetime taken into account is 50 years;
- Material & manufacturing: 1 joint needs 17.4 kg of roll-formed plates of steel grade AISI 1040 (≈S355);
- Finishing & joining: no finishing, 8 large fasteners and 2.1 m of welds are taken into account;
- Transport: the steel is transported by an 8-axle truck over a distance of 600 km from production in Milan to L'Aquila.

7.3.3.2 End-of-life potential

As with the steel structure (see paragraph 7.2.1.2), the end-of-life potential of the steel connectors is 66.7% of the material and manufacturing input.

7.3.3.3 Results timber structure joints

The results for both the energy-equivalent and the CO_2-equivalent per year are presented in Table 12.

Table 12: Results timber structure joints

	Joint timber structure - S355			
	Energy [MJ]		CO_2-footprint [kg]	
	Absolute	Relative	Absolute	Relative
Material	562.00	88.44%	41.300	88.35%
Manufacture	62.60	9.85%	4.670	9.99%
Transport	7.41	1.17%	0.534	1.14%
Disposal	3.48	0.55%	0.244	0.52%
SUBTOTAL	635.49	100.0%	46.748	100.0%
EoL potential	-416.42	-65.5%	-30.65	-65.6%
TOTAL	219.07	34.5%	16.10	34.4%
TOTAL per year	**4.381**		**0.3220**	

7.3.4 Annual environmental burden per kg structure

Figure 66 shows the annual environmental burden per joint for the two material variations. These values will be integrated in the parametric script. Figure 67 gathers all values presented in the previous paragraphs summing up to a total environmental burden per joint to grant overview.

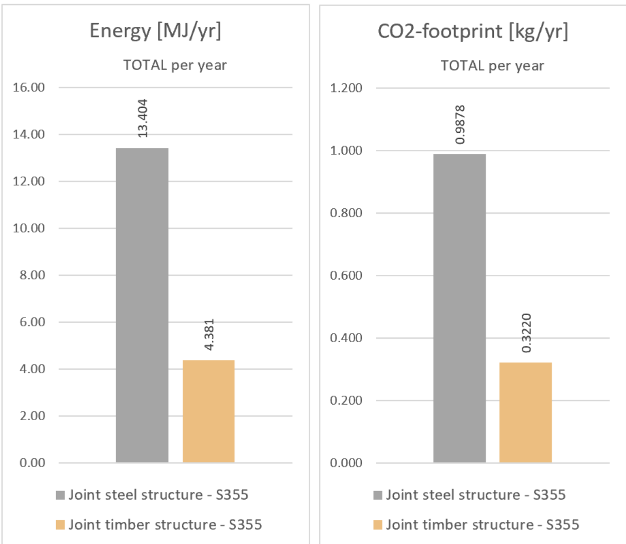

Figure 66: Annual environmental burden per joint

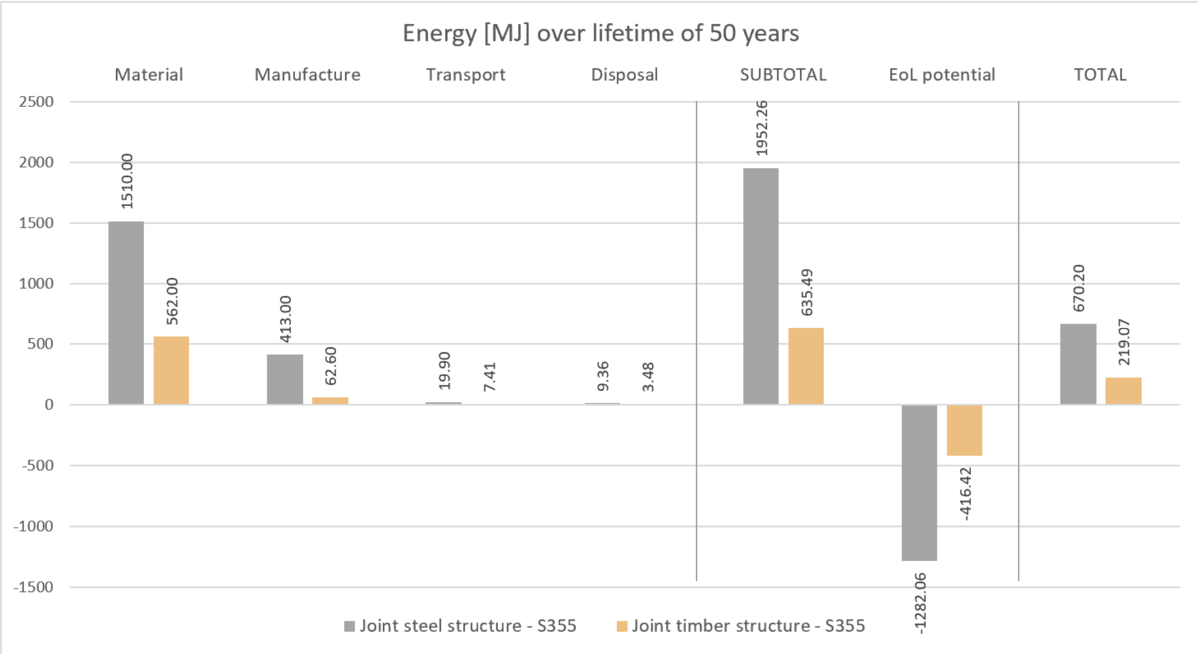

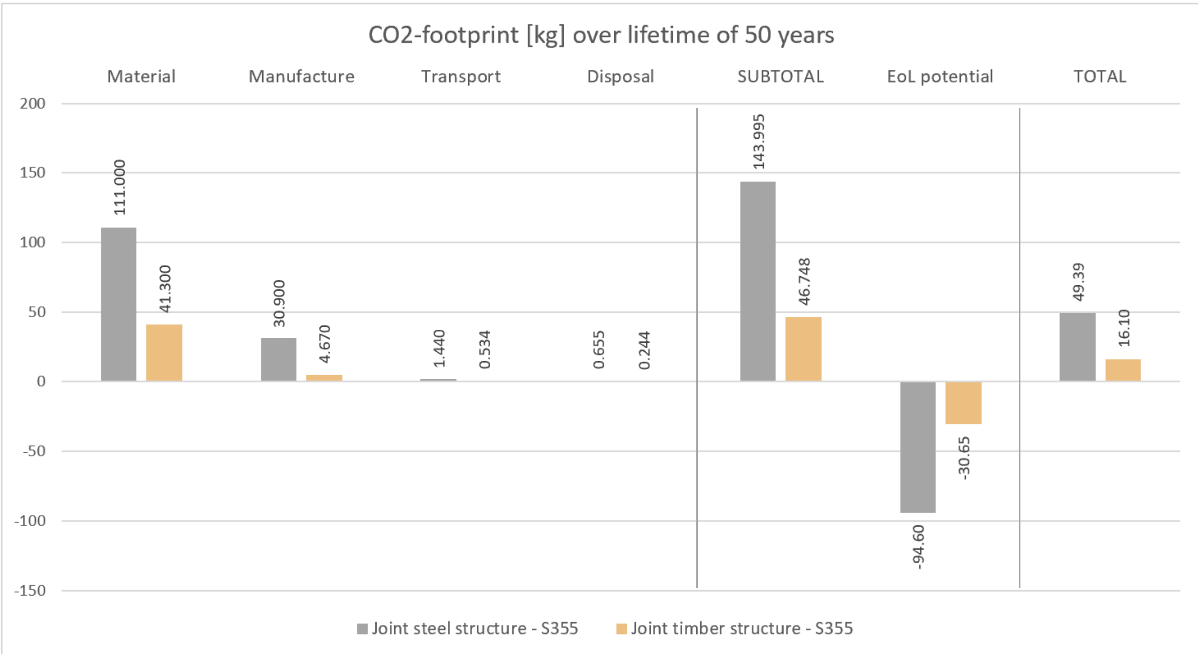

Figure 67: Environmental burden over lifetime of 50 years per joint

7.4 Pre-exclusion

An interesting fact has arisen, concerning the environmental impact score of local sweet chestnut (D24) compared to azobé (D70). Though the choice for sweet chestnut was made from an environmental point of view – it is a local material and therefore does not need as much transport – it turns out that it scores lower in the environmental department than the azobé that needs to be imported from Africa. This is due to fact that azobé is a more durable material and is therefore assumed to need less replacement during its lifetime as well as to have a higher end-of-life potential. As azobé is environmentally better than chestnut based on previous assumptions, as well as significantly stronger, chestnut is taken out of the equation.

Therefore, the remaining materials that will be investigated from here on out are: steel grades S235 and S355, and timber grade D70 – and for the latter one some exta combinations are considered in which the trusses are made out of steel grade S355, as was presented in paragraph 4.3.3. This reduces the total amount of models to be generated from 16 884 (see paragraph 4.4) to 10 836.

7.5 Summary

The environmental impact values that have been applied in the Grasshopper script and linked to both the total structural weight as well as the amount of joints is presented in Table 13. Note that in the case of a combined structure – with a timber shell and steel trusses – the number of joints on the timber shell and the steel trusses have been counted seperately and linked to their respective values.

Table 13: Environmental impact values for Grasshopper-script

	Energy consumption [MJ/year]	CO_2-footprint [kg/year]
Per kg structure		
S235 structure	0.266	0.0193
S355 structure	0.269	0.0194
~~D24 structure (chestnut)~~	~~0.178~~	~~0.0170~~
D70 structure (azobé)	0.167	0.0150
Per joint		
Steel structure	13.404	0.9878
Timber structure	4.381	0.3220

7.6 Conclusion

Using the software CES EduPack 2018, an environmental analysis has been carried out resulting in an annual energy-equivalent and CO_2-equivalent. The outcomes – per kilogram of structure and per joint – can be linked to the parametric models in the Grasshopper-script. Having defined the geometry, the materialisation, the load and load combinations, the structural verifications and the environmental impact, the database can be generated. The database is presented in Chapter 8.

8 Database

8.1 Introduction

In the previous chapters all relevant input for the Grasshopper-script has been defined: geometry, materialisation, loads and load combinations, structural verifications and the environmental impact. The Grasshopper-script has been run and 10 836 structural variations have been structurally analysed and a database concerning the relevant output for each variation has been generated. The generated database will be presented in this chapter.

8.2 Database entries

In the database, the following output of the Grasshopper-script has been saved:

- Geometry (basic, in-plane and out-of-plane variations)
- Cross sections
- Exact span [m]
- Element length [m]
- Element mass [kg]
- Total mass [kg]
- Max. displacement [mm]
- Max. unity check
- CO_2-equivalent [kg/year]
- Energy-equivalent [MJ/year]

The full database can be viewed online following this link:
https://1drv.ms/x/s!AotyXV-yBJ2wiIlQUIoU95mk_kT_2w

Figure 68 shows a scatter plot including all 10 836 models, sorted by the two generated environmental impact components: the CO_2-equivalent and the energy-equivalent.

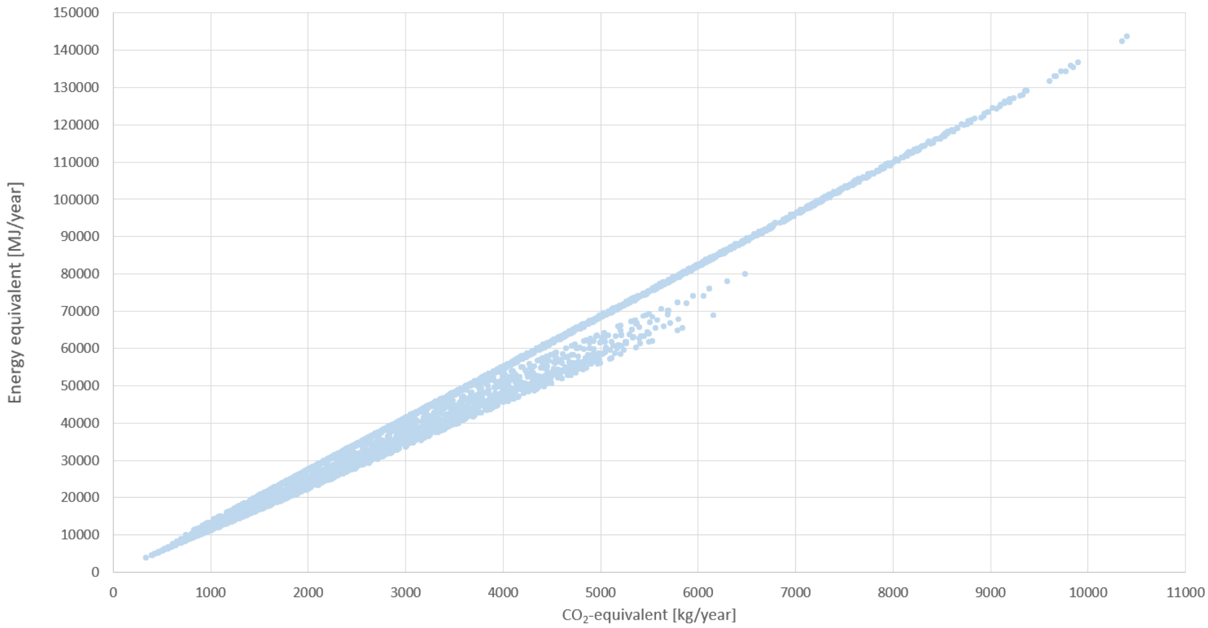

Figure 68: Scatter plot of the full database (10 836 models)

Figure 69 to Figure 72 shows the outcomes per materialisation and how they relate to the other models. The CO_2-equivalent and the energy-equivalent are as good as linearly related. The scatter plot of the combined structure – in which the shell is constructed in timber and the trusses are in steel, Figure 72 – is more scattered as these depend on more input variables: not just one, but two cross sections come into play. Both of the cross sections as well as their connections are linked to different environmental values and therefore the outcome is more varied.

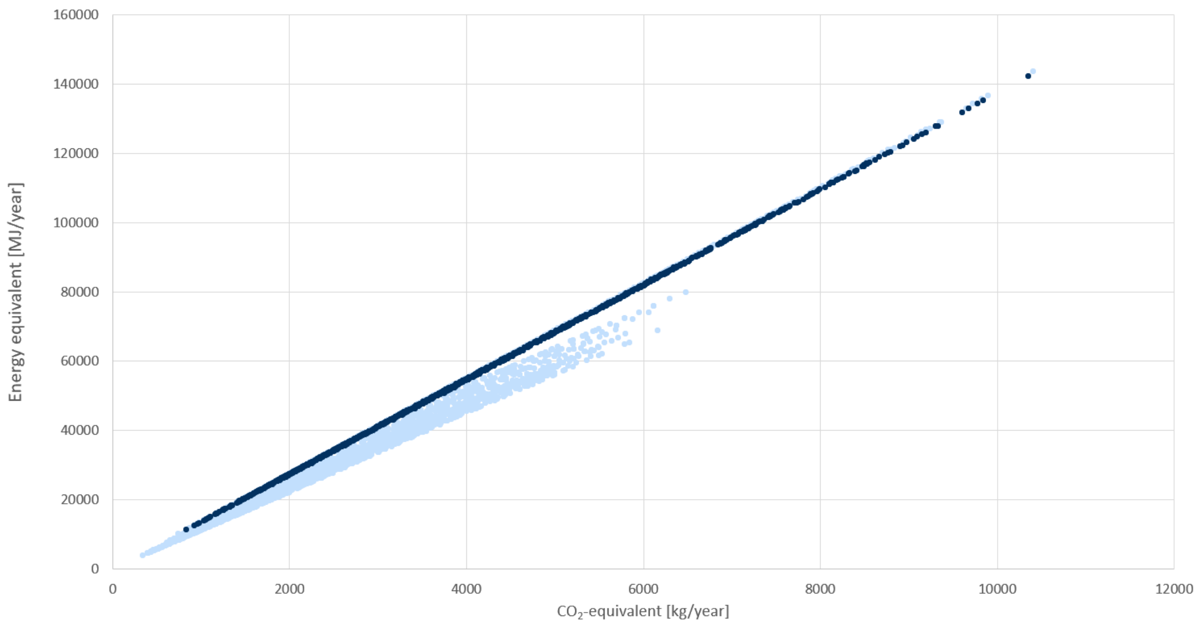

Figure 69: Scatter plot | Steel configurations (S235)

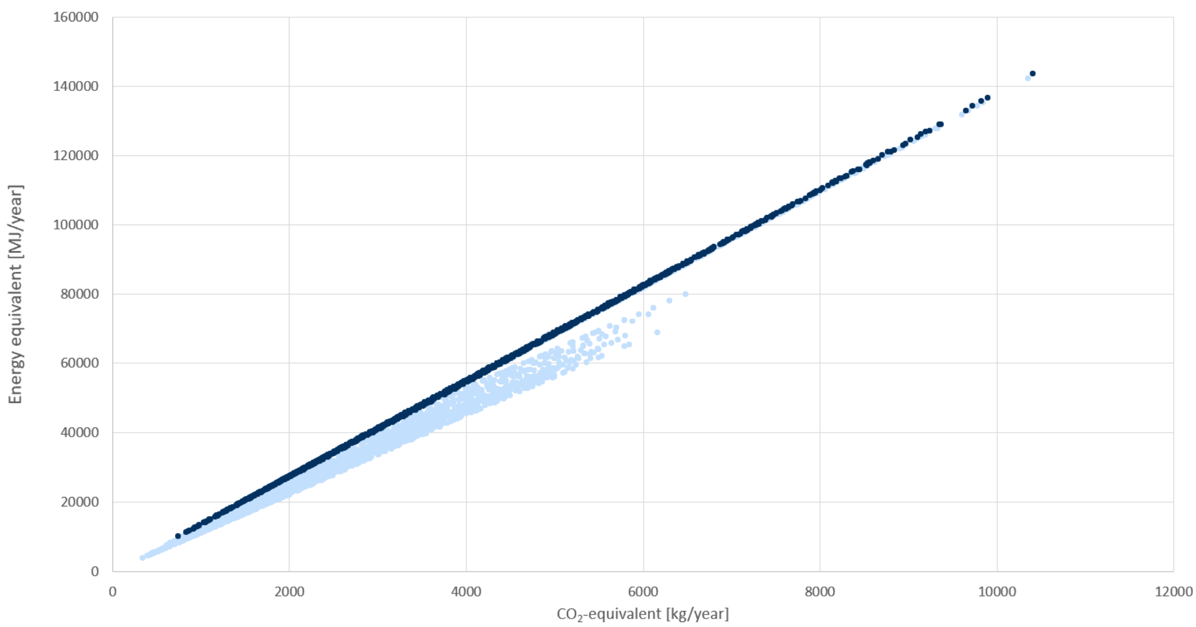

Figure 70: Scatter plot | Steel configurations (S355)

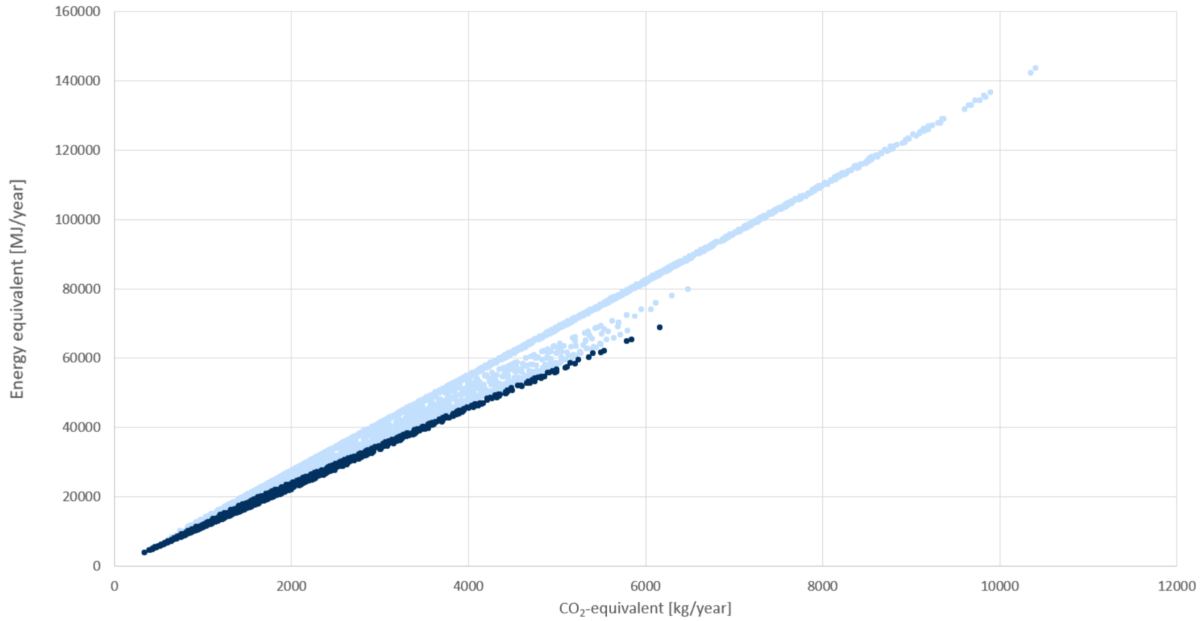

Figure 71: Scatter plot | Timber configurations (D70)

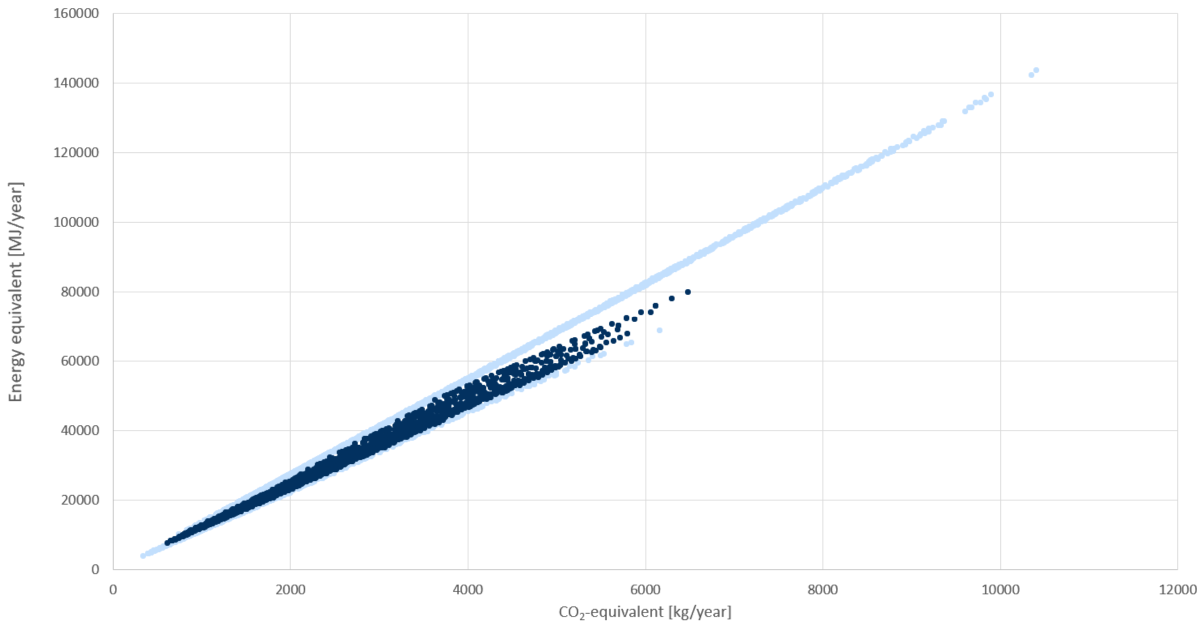

Figure 72: Scatter plot | Combined configurations (D70 & S355)

8.3 Conclusion

A database has been generated, which comprises the generated outputs of all 10 836 models that have been included in the parametric Grasshopper-script. The most important of which are the unity checks, the weight per structural element and the environmental equivalents. This will be explained more clearly in the next part of this thesis, in which the design optimisation will be carried out.

III

DESIGN OPTIMISATION

9 Database ranking

9.1 Introduction

As the database has been generated, comprising a total of 10 836 analysed structural variations, the next step is to rank them. The first step will be exclusion of the configurations that are not viable due to clearly quantified demands: do they comply with the structural demands, and are the elements light-weight enough to ensure the possibility for locals to partake in the construction? Next, the remainder of the database entries will be sorted with regard to their relative environmental impacts. Among the environmental top-scorers a ranking will be further defined based on their aesthetical value and its compliance with the architect's original design.

9.2 Exclusion

The exclusion of models will be based on two outputs:

- Element mass [kg]
- Max. unity check

9.2.1 *First step: structural validation*

The maximum unity check needs to remain below 1.0 for the structure to live up to the ULS- and SLV-checks that have been carried out. A big chunk of all models are excluded this way: 9 335 models are crossed off (marked red in the online database), while 1501 models remain as is shown in Figure 73 and Figure 74 respectively.

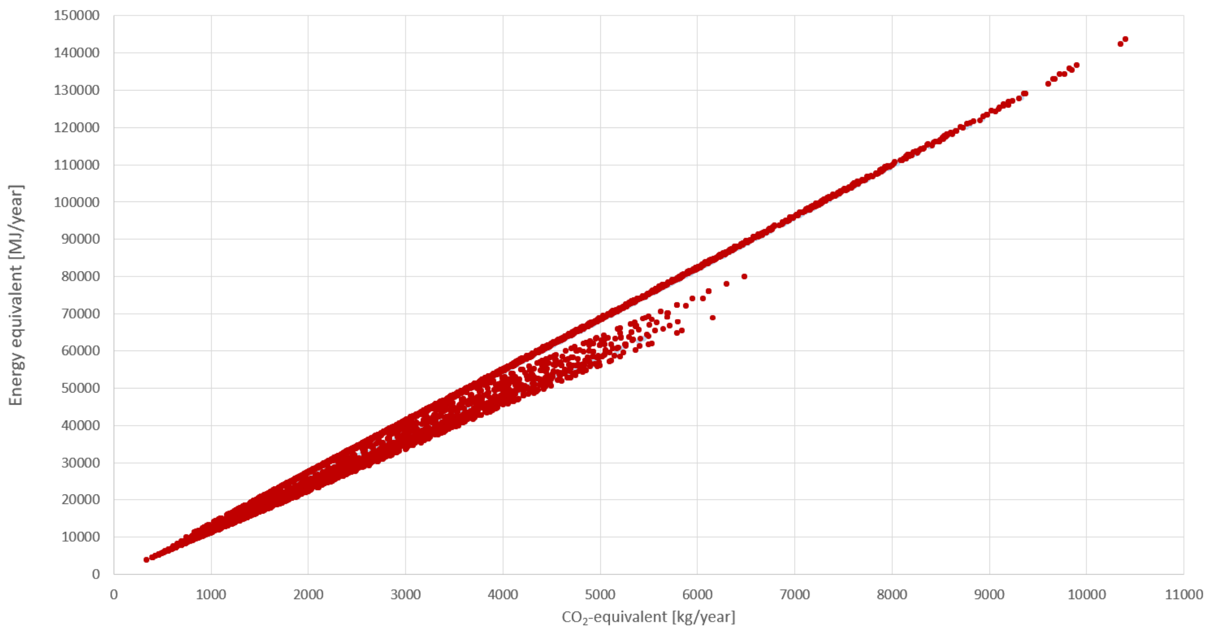

Figure 73: First round of exclusion / Unity check > 1.0

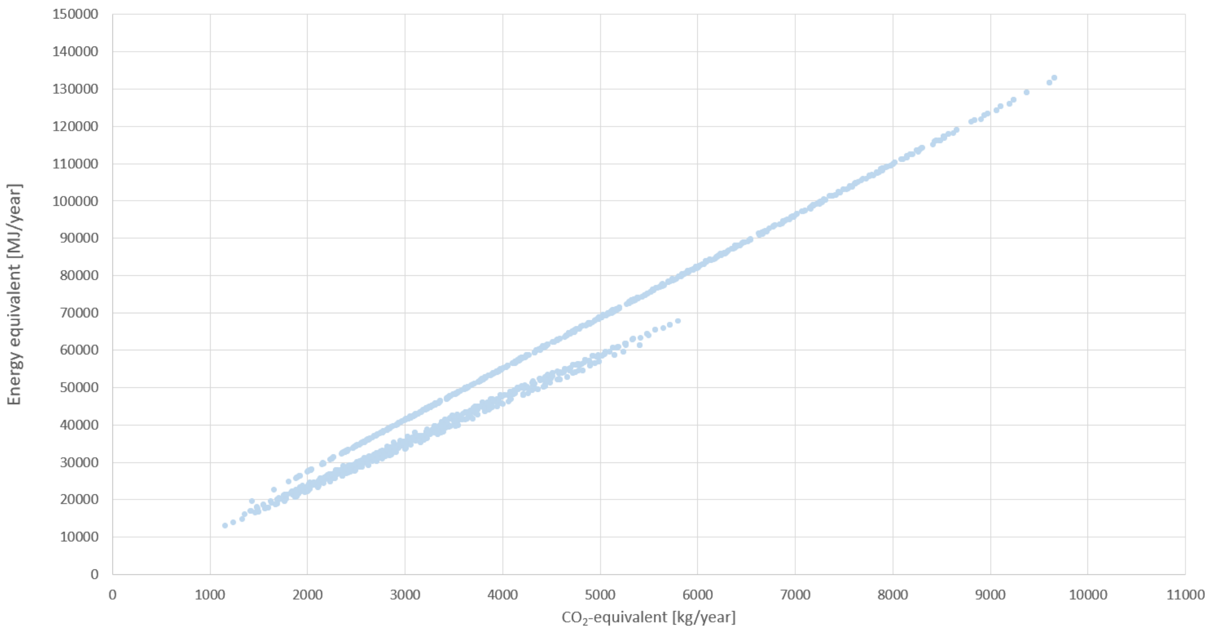

Figure 74: Remainder of models after first round of exclusion

9.2.2 Second step: element weight validation

There is another clearly defined demand, derived from a different point of view. The underlying social concept, which requires the structural design to incorporate local participation in its construction, results in the demand to keep the weight of all individual structural elements below 40 kg. This way, the elements can be carried with two people with relative ease. Applying this demand, another 1124 models are excluded and thus, only 377 models remain that live up to these demands – see Figure 75 and Figure 76.

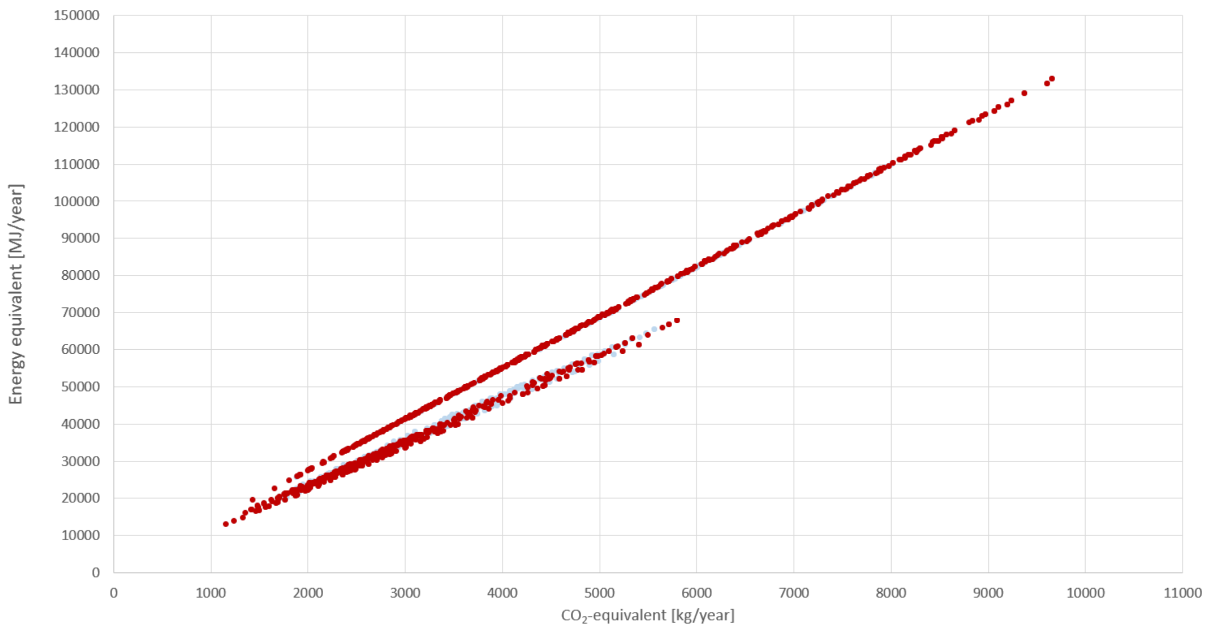

Figure 75: Second round of exclusion | Element weight > 40kg

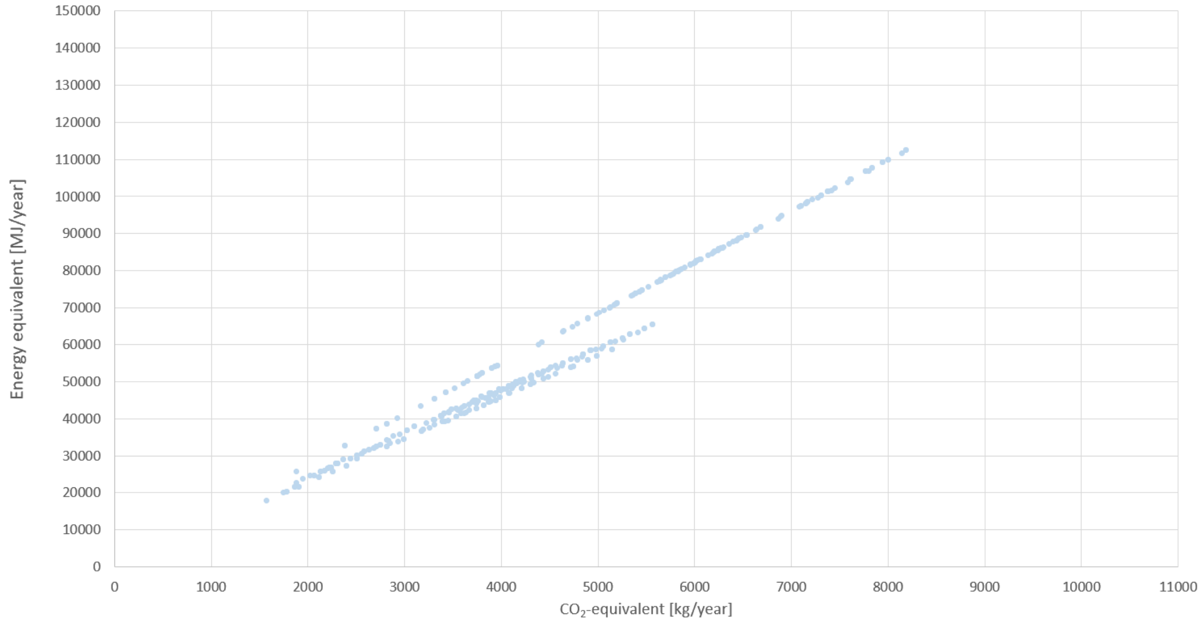

Figure 76: Remainder of models after second round of exclusion

9.3 Sorting process

Now that the models that have not passed the hard demands have been excluded, the remainder needs to be sorted for iterations. The sorting process is a bit less black-and-white. This is where relative values come into play, as well as qualitative aspects that have not been generated as part of the database.

9.3.1 First step: environmental impact

The environmental impact – expressed in CO_2- and energy-equivalent – needs to be taken into account as sustainabiltiy plays a big role, especially in such damaged surroundings. Therefore the list is sorted by CO_2- and energy-equivalent and a number of 28 models – approximately 7.4% of the total remainder – is extracted which scores best in both of these fields.

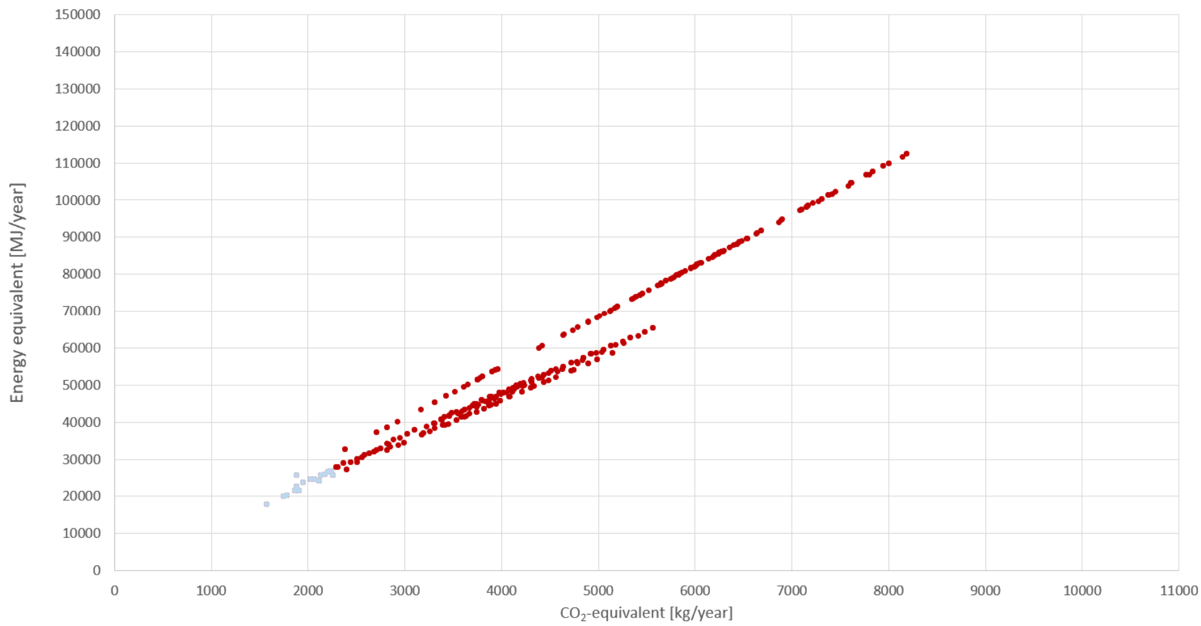

Figure 77: Extracting the environmental top-scorers

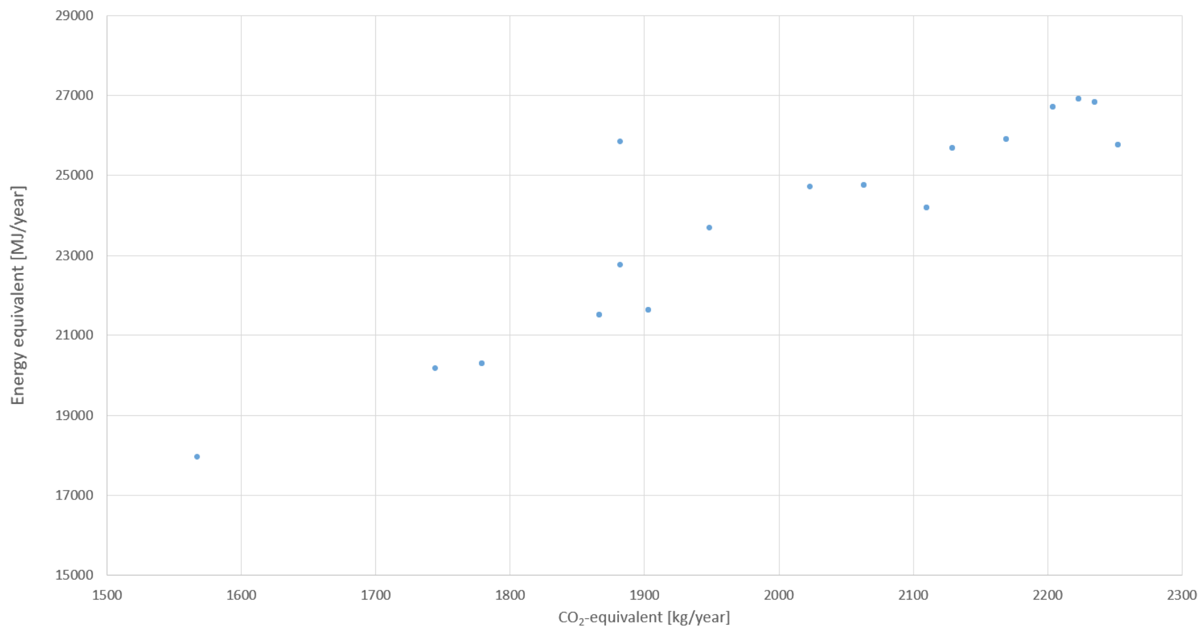

Figure 78: Most environmentally friendly models

9.3.2 Second step: architectural value

Next, the initial architectural design and underlying aesthetical concept need to be taken into consideration. The original design consisted out of one slim timber layer of load-bearing structure with one type of joint and one type of member. This provides both a very elegant design from an aesthetical point of view – as if folding a single layer of paper – as well as a very comprehensive structure for non-experts.

The structural design development has introduced some variations that differ from this initial design. Therefore, a ranking is introduced to sort the list of 28 models further.

- No trusses: timber ★★★★★
- No trusses: steel ★★★★
- Trusses: timber & steel ★★★
- Trusses: timber ★★
- Trusses: steel ★

The options without trusses have not passed the exclusion and sorting by environmental impact. The preferred design options among the environmentally highest-ranking designs are therefore the 3-star structures (15 options), followed by the 2-star structures (12 options) and the 1-star structures (1 option). Based on that, a Top 28 has been defined, as shown in Figure 79.

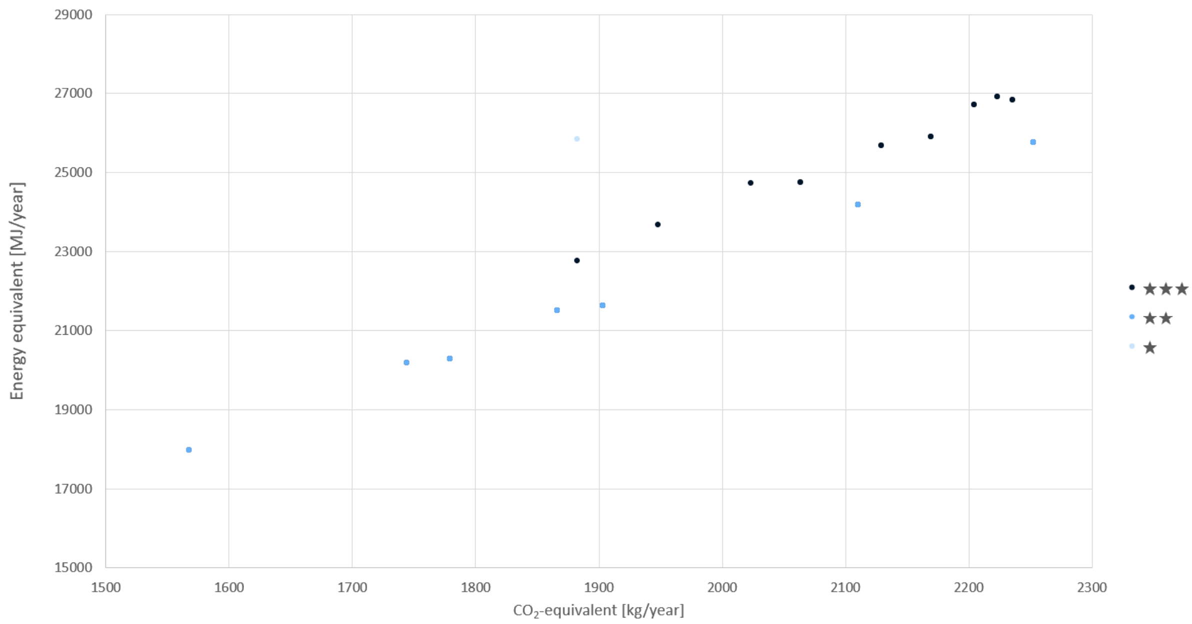

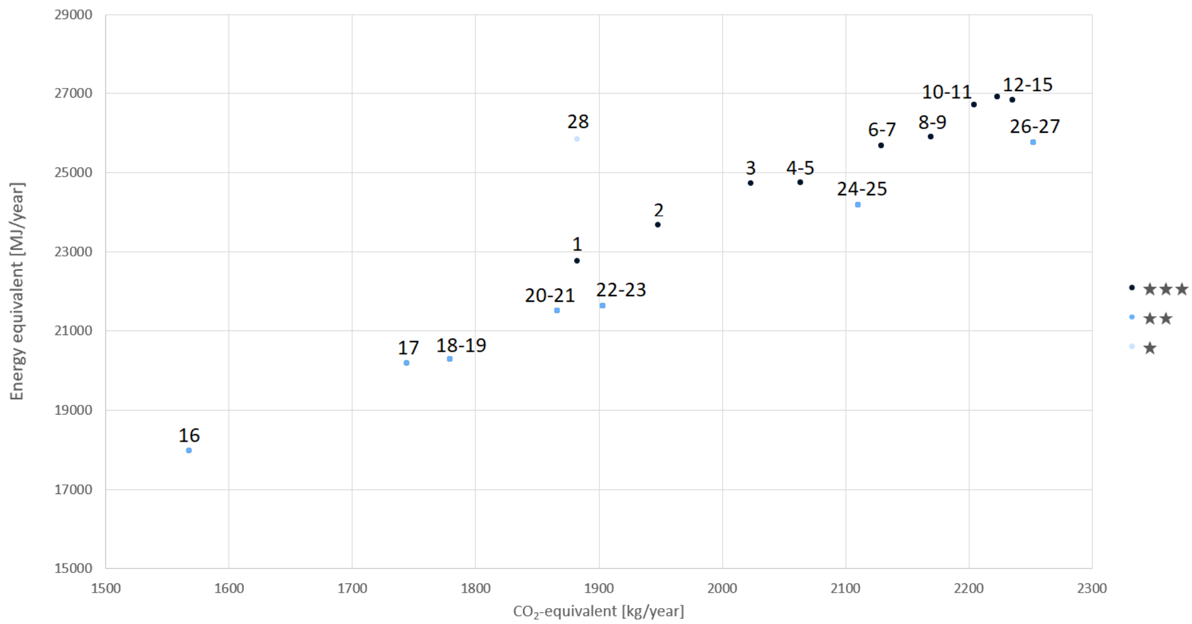

Figure 79: Top 28 designs

Note that some of the options are overlapping in Figure 25, so the visible points on the graph do not add up to 28. It should be noted as well that some of the options do not have a clear ranking as some of them score better with regard to energy-equivalent, while the others score better with regard to CO_2-equivalent. The main properties of the resulting top-28 models have been gathered in Table 14.

Table 14: Properties of top-ranking structural variations

Rank	Basic geometry	In-plane variations	Out-of-plane variations	Cross sections main structure	Cross sections trusses	Element length [m]	Element mass [kg]
1	No hinges	Triangles	3 trusses	D70 150.0 × 150.0 mm²	S355 CHSH 114.3 × 8	1.7	30.5
2	No hinges	Triangles	3 trusses	D70 150.0 × 150.0 mm²	S355 CHSH 139.7 × 8	1.7	30.5
3	No hinges	Triangles	3 trusses	D70 150.0 × 150.0 mm²	S355 CHSH 168.3 × 8	1.7	30.5
4	Hinges	Triangles	3 trusses	D70 175.0 × 150.0 mm²	S355 CHSH 114.3 × 8	1.7	35.6
5	No hinges	Triangles	3 trusses	D70 175.0 × 150.0 mm²	S355 CHSH 114.3 × 8	1.7	35.6
6	Hinges	Triangles	3 trusses	D70 175.0 × 150.0 mm²	S355 CHSH 139.7 × 8	1.7	35.6
7	No hinges	Triangles	3 trusses	D70 175.0 × 150.0 mm²	S355 CHSH 139.7 × 8	1.7	35.6
8	Hinges	Triangles	3 trusses	D70 175.0 × 162.5 mm²	S355 CHSH 114.3 × 8	1.7	38.6
9	No hinges	Triangles	3 trusses	D70 175.0 × 162.5 mm²	S355 CHSH 114.3 × 8	1.7	38.6
10	Hinges	Triangles	3 trusses	D70 175.0 × 150.0 mm²	S355 CHSH 168.3 × 8	1.7	35.6
11	No hinges	Triangles	3 trusses	D70 175.0 × 150.0 mm²	S355 CHSH 168.3 × 8	1.7	35.6
12/14	Hinges	Triangles	3 trusses	D70 150.0 × 150.0 mm²	S355 CHSH 114.3 × 8	1.44	26
13/15	No hinges	Triangles	3 trusses	D70 150.0 × 150.0 mm²	S355 CHSH 114.3 × 8	1.44	26
12/14	Hinges	Triangles	3 trusses	D70 175.0 × 162.5 mm²	S355 CHSH 139.7 × 8	1.7	38.6
13/15	No hinges	Triangles	3 trusses	D70 175.0 × 162.5 mm²	S355 CHSH 139.7 × 8	1.7	38.6
16	No hinges	Triangles	3 trusses	D70 150.0 × 150.0 mm²	*Same as main structure*	1.7	30.5
17	No hinges	Triangles	3 trusses	D70 150.0 × 137.5 mm²	*Same as main structure*	1.44	23.8
18	Hinges	Triangles	3 trusses	D70 175.0 × 150.0 mm²	*Same as main structure*	1.7	35.6
19	No hinges	Triangles	3 trusses	D70 175.0 × 150.0 mm²	*Same as main structure*	1.7	35.6
20	Hinges	Triangles	3 trusses	D70 150.0 × 150.0 mm²	*Same as main structure*	1.44	26
21	No hinges	Triangles	3 trusses	D70 150.0 × 150.0 mm²	*Same as main structure*	1.44	26
22	Hinges	Triangles	3 trusses	D70 175.0 × 162.5 mm²	*Same as main structure*	1.7	38.6
23	No hinges	Triangles	3 trusses	D70 175.0 × 162.5 mm²	*Same as main structure*	1.7	38.6
24	Hinges	Triangles	3 trusses	D70 175.0 × 150.0 mm²	*Same as main structure*	1.44	30.3
25	No hinges	Triangles	3 trusses	D70 175.0 × 150.0 mm²	*Same as main structure*	1.44	30.3
26	Hinges	Triangles	3 trusses	D70 175.0 × 162.5 mm²	*Same as main structure*	1.44	32.9
27	No hinges	Triangles	3 trusses	D70 175.0 × 162.5 mm²	*Same as main structure*	1.44	32.9
28	No hinges	Triangles	3 trusses	S355 CHSH 168.3 × 4	*Same as main structure*	2.05	33.2

9.4 Conclusion

After exclusion and sorting, taking into account environmental and aesthetical aspects, the 28 highest-ranking models have been selected. This set of models will be used for further iterations. If all of them fail during the analyses that will following during the next chapters, the list can be expanded as the database comprised 377 passing models.

10 Structural validation

10.1 Introduction

In Chapter 0 the entries in the database have been narrowed down to a Top 28. The top-ranking design consists out of 1.7 m long elements with a 150×150mm² timber cross section of timber class D70, with no hinges in the basic geometry, and horizontal elements applied everywhere. There are three trusses underneath the structure, which consist out of steel trusses of CHSH114.3×8.0 elements of grade S355. The design is presented in Figure 80.

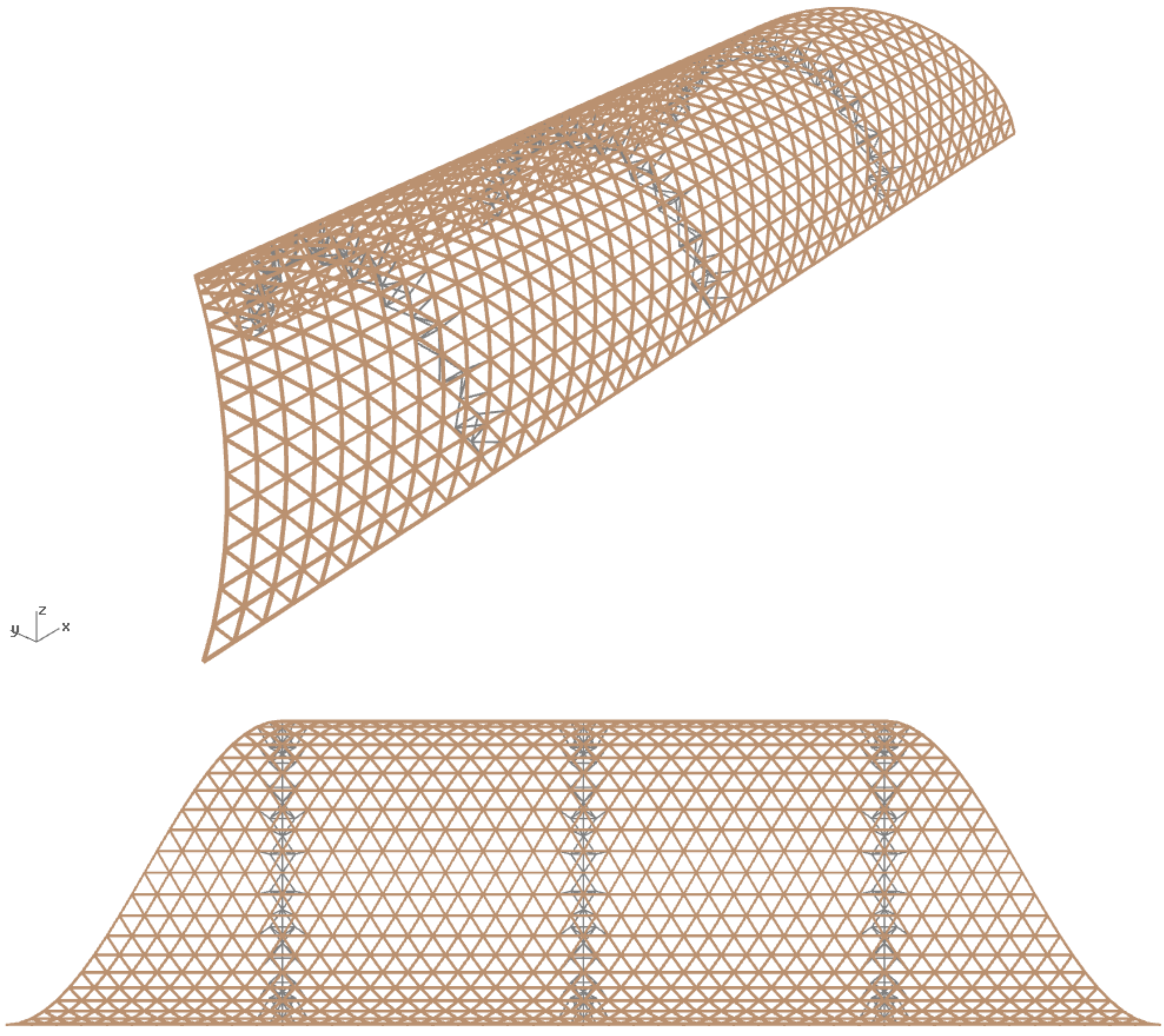

Figure 80: Structural design (Rank 1 out of 28)

To double-check the calculations carried out by Karamba, an extra structural validation will be carried out by the program RFEM. This software provides more insightful graphics than Karamba in each of the individual structural elements.

10.2 Factors

For the calculation, material and load factors need to be considered. To refer back to Equation I (paragraph 6.3), the calculation of the design strength properties of timber is as follows:

$$X_d = k_{mod} \cdot \frac{X_k}{\gamma_M} \tag{1}$$

In which:

X_d	Design value of any strength property of timber
X_k	Characteristic value of any strength property of timber
k_{mod}	Modification factor taking into account load duration and moisture content
γ_M	Partial factor for material properties

The Italian national annex (UNI-EN 1995-1-1, 2007) prescribes the following partial factor for the material properties:

$$\gamma_M = 1.5$$

While the modification factor k_{mod} has been determined to be as follows (see paragraph 6.3), depending on the load duration:

$k_{mod} = 0.50$	in case of permanent loads, i.e. self-weight
$k_{mod} = 0.55$	in case of long-term loads, i.e. storage
$k_{mod} = 0.65$	in case of medium-term loads, i.e. imposed loads
$k_{mod} = 0.70$	in case of short-term loads, i.e. snow
$k_{mod} = 0.90$	in case of instantaneous loads, i.e. wind

10.3 Timber check

The top-ranking structure has been modelled in RFEM including all loads and load combinations. The governing combination is ULS 206 (see paragraph 5.7), the combination in which the snow has been redistributed with the highest load on the wider back side of the building. The factors applicable for this load case are:

$$\gamma_M = 1.5$$
$$k_{mod} = 0.7$$

The relevant characteristic properties – tensile strength and bending strength – of D70 timber are:

$$f_{t,0,k} = 40.0\ N/mm^2$$
$$f_{m,y,k} = 70.0\ N/mm^2$$
$$f_{m,z,k} = 70.0\ N/mm^2$$

This bring the design value of the strength properties of the D70 timber to:

$$f_{t,0,d} = 19.6\ N/mm^2$$
$$f_{m,y,d} = 32.7\ N/mm^2$$
$$f_{m,z,d} = 32.7\ N/mm^2$$

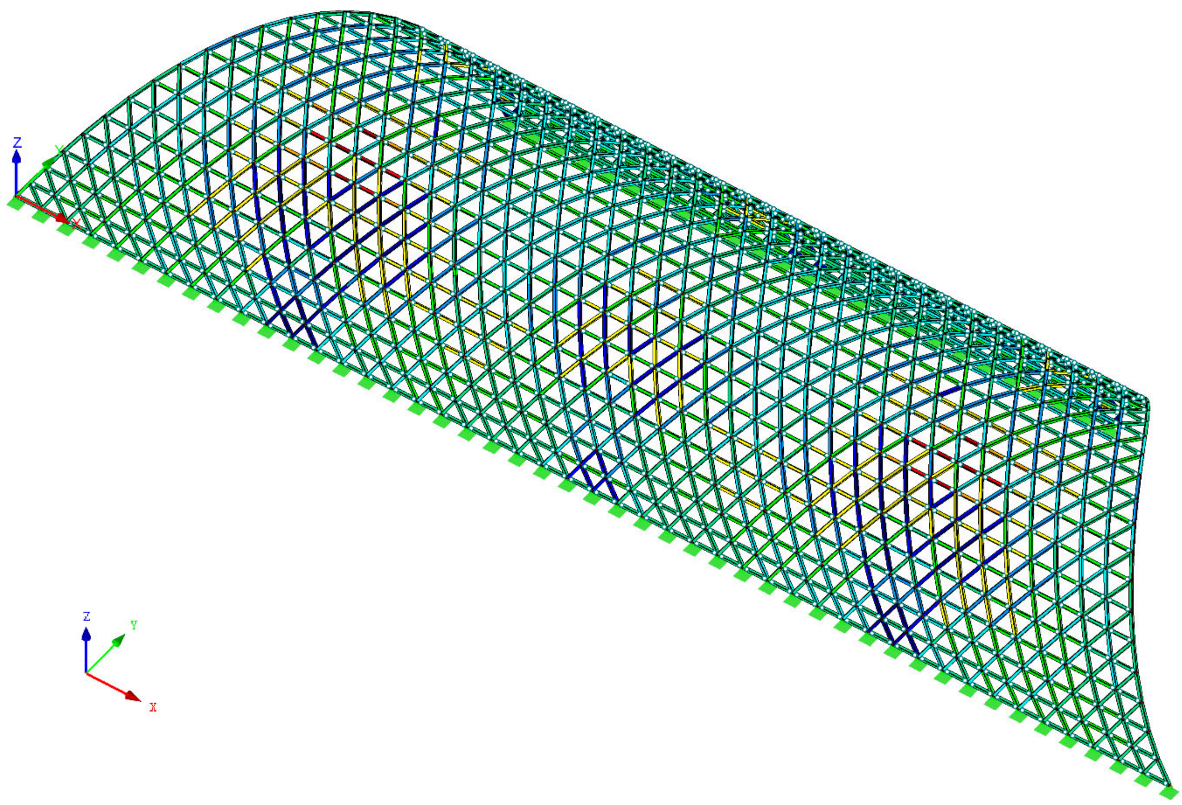

Figure 81: Stresses in the timber structure (the steel trusses are hidden)

The highest stresses in the design occur where the trusses are located, as a consequence of acting as part of that those trusses. In the governing members, the following tensile stress is present:

$$\sigma_{t,0,d} = 16.0\ N/mm^2$$

Bending also occurs in these members, in two directions:

$$\sigma_{m,y,d} = 3.0\ N/mm^2$$
$$\sigma_{m,z,d} = 1.4\ N/mm^2$$

And thus, the following unity checks can be carried out (see paragraph 6.3.5):

$$\frac{\sigma_{t,0,d}}{f_{t,0,d}} + \frac{\sigma_{m,y,d}}{f_{m,y,d}} + k_m \cdot \frac{\sigma_{m,z,d}}{f_{m,z,d}} \leq 1$$
$$\frac{16.0}{19.6} + \frac{3.0}{32.7} + 0.7 \cdot \frac{1.4}{32.7} = 0.938 \leq 1 \qquad O.K.$$

$$\frac{\sigma_{t,0,d}}{f_{t,0,d}} + k_m \cdot \frac{\sigma_{m,y,d}}{f_{m,y,d}} + \frac{\sigma_{m,z,d}}{f_{m,z,d}} \leq 1$$
$$\frac{16.0}{19.6} + 0.7 \cdot \frac{3.0}{32.7} + \frac{1.4}{32.7} = 0.923 \leq 1 \qquad O.K.$$

10.4 Steel check

The steel of the trusses also needs to be checked. As they are trusses, they have been modelled with bars that can only take axial loads. The steel bars – with cross section CHSH114.3×8.0 – can be categorised as class 1 sections.

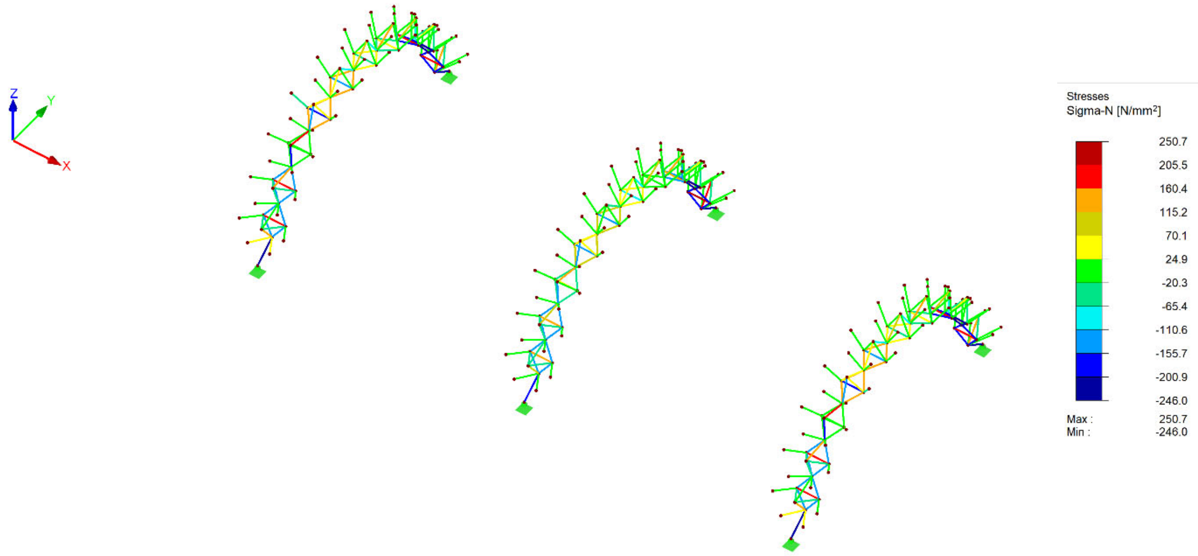

Figure 82: Stresses in the trusses (the timber structure is hidden)

The highest normal stress that occurs is:

$$\sigma_N = 250.7\ N/mm^2$$

The characteristic yield strength of the steel is:

$$f_y = 355\ N/mm^2$$

The Italian code (UNI-EN 1993-1-1, 2007) prescribes the following material factor:

$$\gamma_{M0} = 1.05$$

This results in a design yield strength of:

$$f_{y,d} = 338.1\ N/mm^2$$

And thus, the unity check gives:

$$\frac{\sigma_N}{f_{y,d}} = \frac{250.7}{338.1} = 0.741 \leq 1 \qquad O.K.$$

10.5 Conclusion

The unity checks that have automatically been carried out by Karamba have been checked using the software RFEM. As the unity checks remain below 1.0, all elements have been structurally verified and the Karamba-calculations can be trusted. The next step is the work-out of the joint detail.

11 Connection design

11.1 Introduction

Having defined the top-ranking design and having double-checked its structural validation in Chapter 10, the next step is to detail the connection further and to see it it is feasible. The first step is to structurally design and verify the joint based on the conceptual proposal that has been done. These checks will be followed by extra calculations based on the translational and rotational stiffness of the joints. If the structure needs to be upscaled, iterations can take place in the defined Top 28 (see Figure 79 and Table 14). For elaboration on the determination of the load per bolt, please refer to Appendix H.

11.2 Approach

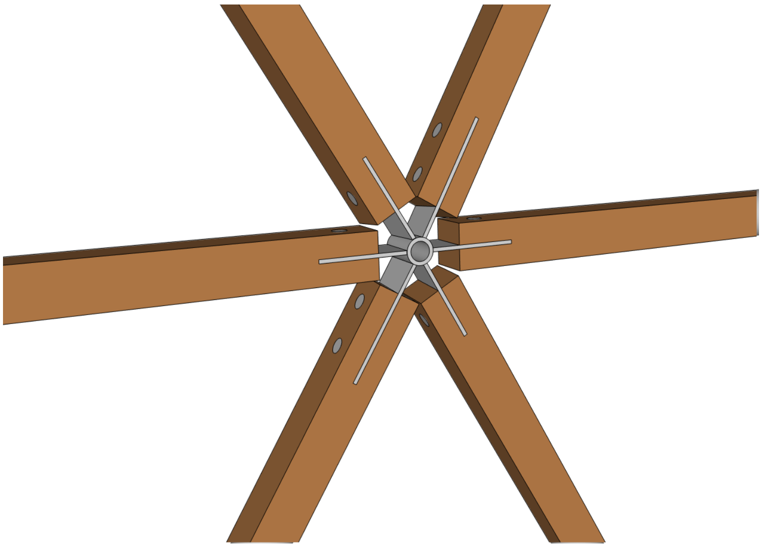

Figure 83: Conceptual joint design

The joint consists out of steel plates, which are welded to a central steel core, which are assumed to be S355. They are connected to the timber elements by bolts. The configuration of the bolts is restricted by the height of the timber profiles, which is 150mm. The goal of the joint design is to pick a configuration that is structurally feasible, which takes into account the available height of the timber elements and which uses as little length of the timber element as possible. Preferable, the same joint design would be applied all over the structure to keep it as simple as possible.

First, a design needs to be chosen that complies with the demands with regard to the minimal distances between the bolts. Second, the rotational stiffness of the members can be calculated which will be used to refine the RFEM-model. Lastly, by applying the rotational stiffness to the RFEM-model, member loads are generated which form the input for unity checks carried out on the bolts, the steel plates and the welds of the design.

11.2.1 Spacing between bolts

When choosing a bolt configuration, it needs to comply with the spacing requirements as prescribed by the Eurocode (EN 1995-1-1, 2011), as presented in Table 15 and Figure 84.

Table 15: Spacing requirements bolts in timber

Spacing and end/edge distances (see Figure 8.7)	**Angle**	**Minimum spacing or distance**
a_1 (parallel to grain)	$0^\circ \leq \alpha \leq 360^\circ$	$(4 + \lvert\cos\alpha\rvert)\, d$
a_2 (perpendicular to grain)	$0^\circ \leq \alpha \leq 360^\circ$	$4\, d$
$a_{3,t}$ (loaded end)	$-90^\circ \leq \alpha \leq 90^\circ$	max (7 d; 80 mm)
$a_{3,c}$ (unloaded end)	$90^\circ \leq \alpha < 150^\circ$ $150^\circ \leq \alpha < 210^\circ$ $210^\circ \leq \alpha \leq 270^\circ$	max([1 + 6 sin α) d; 4d) 4 d max([1 + 6 sin α) d; 4d)
$a_{4,t}$ (loaded edge)	$0^\circ \leq \alpha \leq 180^\circ$	max([2 + 2 sin α) d; 3d)
$a_{4,c}$ (unloaded edge)	$180^\circ \leq \alpha \leq 360^\circ$	3 d

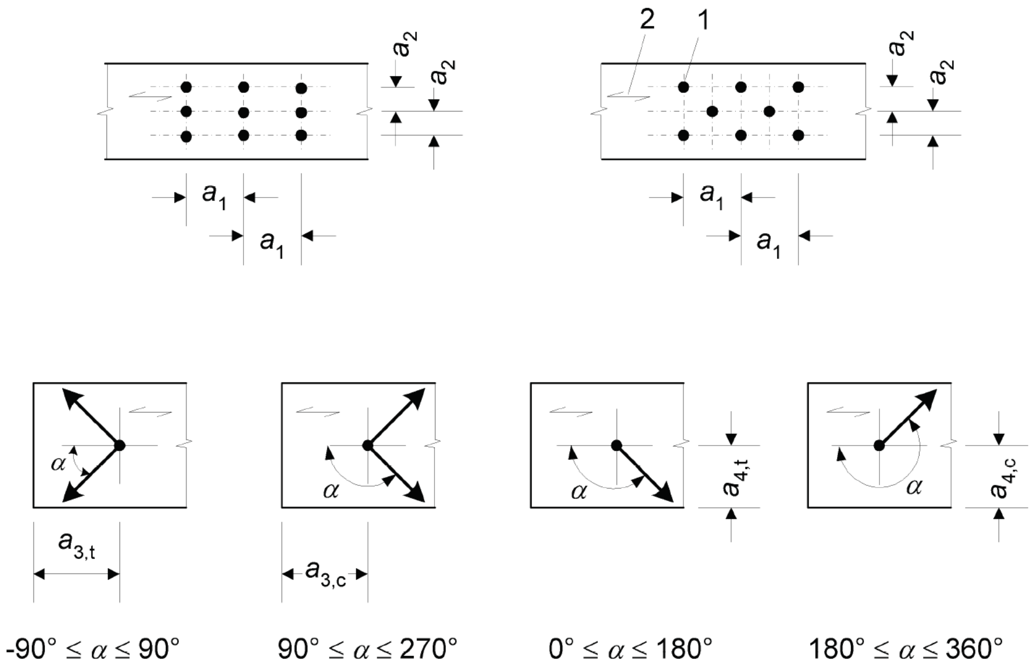

Figure 84: Spacing requirements bolts in timber

11.2.2 Rotational stiffness

The model assumes rigid connections, but depending on the design, there is limited rotational stiffness. Therefore, the rigid connections must be replaced by rotational springs once a connection design has been defined. This influences the stresses in the design. For the calculation of the rotational stiffness, iit is assumed the bolt holes are close-fitting, so movements due to hole clearances have been neglected.

The joint slip modulus can be calculated according to Equation 11 as prescribed by the Eurocode (EN 1995-1-1, 2011), for each shear face in a bolt, in a steel-timber connection.

$$K_{ser} = 2 \cdot \left(\frac{{\rho_{mean}}^{1.5} d}{23} \right) \tag{11}$$

In which:

K_{ser}	joint slip modulus, in N/mm
ρ_{mean}	mean specific weight of the timber, in kg/m³
d	bolt diameter, in mm

As each bolt in this connection has two shear faces, the joint slip modulus per bolt becomes as shown in Equation 12.

$$K_{ser,b} = 2 \cdot K_{ser} \tag{12}$$

The rotational stiffness of the connection can be determined using Equation 13.

$$K_{r,ser} = K_{ser} \sum_{j=1}^{n} {r_j}^2 \tag{13}$$

In which:

$K_{r,ser}$	total rotational stiffness of the connection, in Nmm/rad
r	distance from bolt to rotation centre of the connection, in mm

For connections in ULS calculations, a reduced joint slip modulus must be considered, as shown in Equation 14.

$$K_u = \frac{2}{3} K_{ser} \tag{14}$$

K_u	ultimate joint slip modulus, in N/mm

11.2.3 Check: bolts

The bolts in the connection need to be checked. For the joint design, three bolt failure mechanisms can occur according to the Eurocode (EN 1995-1-1, 2011), as is shown in Figure 85.

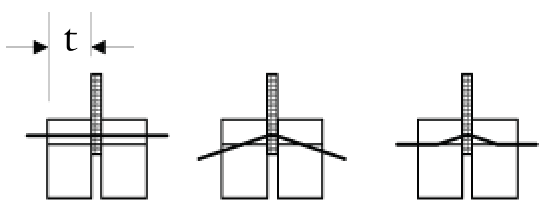

Figure 85: Possible failure mechanisms connection (EN 1995-1-1, 2011)

The accompanying characteristic strength of each bolt per shear face – two per bolt – for each of these mechanisms is expressed in Equation 15.

$$F_{v,Rk} = \min \begin{cases} f_{h,k} \cdot t \cdot d \\ f_{h,k} \cdot t \cdot d \left(\sqrt{2 + \dfrac{4M_{y,Rk}}{f_{h,k} \cdot d \cdot t^2}} - 1 \right) \\ 2.3\sqrt{M_{y,Rk} \cdot f_{h,k} \cdot d} \end{cases} \tag{15}$$

In which:

$F_{v,Rk}$	characteristic strength per shear face per bolt
$f_{h,k}$	characteristic bearing strength of the timber
t	timber thickness on either side of the steel plate
d	bolt diameter
$M_{y,Rk}$	characteristic yield moment of the bolt

The characteristic bearing strength can be calculated according to Equation 16 and, depending on the angle of the load with the grain, Equation 17.

$$f_{h,0,k} = 0.082(1 - 0.01d)\rho_k \tag{16}$$

$$f_{h,\alpha,k} = \frac{f_{h,0,k}}{k_{90} \sin^2 \alpha + \cos^2 \alpha} \tag{17}$$

In which:

$f_{h,0,k}$	characteristic bearing strength of the timber parallel to the grain, in N/mm^2
ρ_k	characteristic volumic mass of the timber, in kg/m^3
$f_{h,\alpha,k}$	characteristic bearing strength of the timber at an angle α with the grain
α	angle of the load with the grain

And in case of hardwood, Equation 18 applies.

$$k_{90} = 0.90 + 0.015d \tag{18}$$

This will result in the unity check as presented by Equation 19.

$$\frac{F_{v,Ed}}{F_{v,Rd}} \leq 1.0 \tag{19}$$

11.2.4 Check: steel plates

The resistance of the steel plate need to be considered, taking into account the bolt holtes. The thickness of the steel plates have a big influence on the weight of the joints elements, which should aim at staying below 40 kg. It is assumed the thickness of the circular steel core in the centre of the joint will be sufficiently thick if the plates have verified. Depending on the location in the model, the loads needed to be transferred are axial loads, shear loads and/or bending loads. Equation 20 shows the unity check that needs to be calculated.

$$\left(\frac{\sigma_{x,Ed}}{f_y/\gamma_M}\right)^2 + 3 \cdot \left(\frac{\tau_{Ed}}{f_y/\gamma_M}\right)^2 \leq 1.0 \tag{20}$$

11.2.5 Check: welds

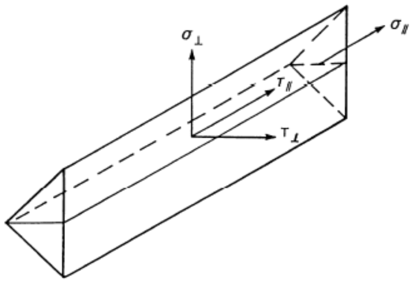

Figure 86: Stresses in weld throat

The resistance of the welds from the plates to the circular core needs to be verified using the formulae in Equation 21 and Equation 22, as prescribed by the Eurocode (EN 1993-1-8, 2011).

$$\frac{[\sigma_\perp{}^2 + 3(\tau_\perp{}^2 + \tau_\parallel{}^2)]^{0.5}}{f_u/\beta_w\gamma_{M2}} \leq 1.0 \tag{21}$$

$$\frac{\sigma_\perp}{0.9 f_u/\gamma_{M2}} \leq 1.0 \tag{22}$$

In which:

$\sigma_\perp$	axial stress perpendicular to the throat section;
$\tau_\perp$	shear stress (in the throat section) perpendicular to the length-axis of the weld;
$\tau_\parallel$	shear stress (in the throat section) parallel to the length-axis of the weld;
f_u	the nominal tensile strength of the weakest connected part;
β_w	correlation factor depending on the steel strength of the connected parts;
γ_{M2}	partial factor regarding the material properties.

The Eurocode (EN 1993-1-8, 2011) prescribes the following partial factor for the bolted connection:

$$\gamma_{M2} = 1.25$$

The correlation factor depends on the material used:

$\beta_w = 0.8$ for steel strength S235

$\beta_w = 0.85$ for steel strength S275

$\beta_w = 0.9$ for steel strength S355

$\beta_w = 1.0$ for steel strength S420

$\beta_w = 1.0$ for steel strength S460

11.3 Model refinement

Before carrying on with the structural checks that need to be carried out, some refinements of the model have been decided upon:

1. In the proposed joint design, there is one axis that has very limited rotational stiffness, namely axis Z – see Figure 87. Therefore, for all members in the RFEM-model, the rotation around this axis has been released. By making this modelling decision, all connections in the basic geometry around the Y-axis need to be rigid. This design choice causes the elimination of some of the structural variations, as shown in Table 16.

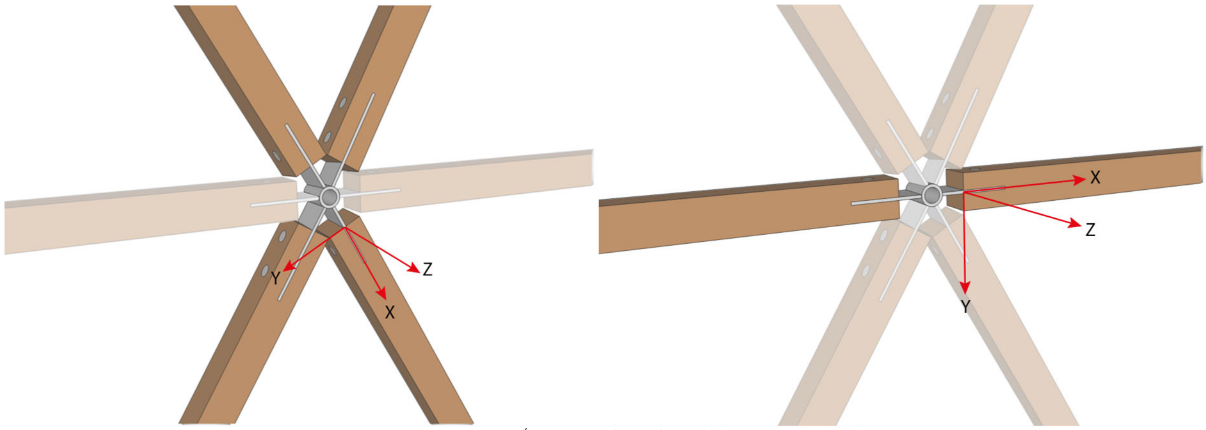

Figure 87: Local axes | Diagonals (left) and horizontals (right)

2. In order to reduce the high tensile stresses that occur in the timber structure around the trusses, the design choice have been made to separate the truss elements from the timber shell – see Figure 88. Apart from a reduction in stresses, this adds to the constructability of the entire structure as the trusses can be constructed separately and replace part of the scaffolding during the erection of the structure.

Figure 88: Redefinition interaction between trusses and main structure

Table 16: Eliminations due to model refinement

Rank	Basic geometry	In-plane variations	Out-of-plane variations	Cross sections main structure	Cross sections trusses	Element length [m]	Element mass [kg]
1	No hinges	Triangles	3 trusses	D70 150.0 × 150.0 mm²	S355 CHSH 114.3 × 8	1.7	30.5
2	No hinges	Triangles	3 trusses	D70 150.0 × 150.0 mm²	S355 CHSH 139.7 × 8	1.7	30.5
3	No hinges	Triangles	3 trusses	D70 150.0 × 150.0 mm²	S355 CHSH 168.3 × 8	1.7	30.5
~~4~~	~~Hinges~~	~~Triangles~~	~~3 trusses~~	~~D70 175.0 × 150.0 mm²~~	~~S355 CHSH 114.3 × 8~~	~~1.7~~	~~35.6~~
5	No hinges	Triangles	3 trusses	D70 175.0 × 150.0 mm²	S355 CHSH 114.3 × 8	1.7	35.6
~~6~~	~~Hinges~~	~~Triangles~~	~~3 trusses~~	~~D70 175.0 × 150.0 mm²~~	~~S355 CHSH 139.7 × 8~~	~~1.7~~	~~35.6~~
7	No hinges	Triangles	3 trusses	D70 175.0 × 150.0 mm²	S355 CHSH 139.7 × 8	1.7	35.6
~~8~~	~~Hinges~~	~~Triangles~~	~~3 trusses~~	~~D70 175.0 × 162.5 mm²~~	~~S355 CHSH 114.3 × 8~~	~~1.7~~	~~38.6~~
9	No hinges	Triangles	3 trusses	D70 175.0 × 162.5 mm²	S355 CHSH 114.3 × 8	1.7	38.6
~~10~~	~~Hinges~~	~~Triangles~~	~~3 trusses~~	~~D70 175.0 × 150.0 mm²~~	~~S355 CHSH 168.3 × 8~~	~~1.7~~	~~35.6~~
11	No hinges	Triangles	3 trusses	D70 175.0 × 150.0 mm²	S355 CHSH 168.3 × 8	1.7	35.6
~~12/14~~	~~Hinges~~	~~Triangles~~	~~3 trusses~~	~~D70 150.0 × 150.0 mm²~~	~~S355 CHSH 114.3 × 8~~	~~1.44~~	~~26~~
13/15	No hinges	Triangles	3 trusses	D70 150.0 × 150.0 mm²	S355 CHSH 114.3 × 8	1.44	26
~~12/14~~	~~Hinges~~	~~Triangles~~	~~3 trusses~~	~~D70 175.0 × 162.5 mm²~~	~~S355 CHSH 139.7 × 8~~	~~1.7~~	~~38.6~~
13/15	No hinges	Triangles	3 trusses	D70 175.0 × 162.5 mm²	S355 CHSH 139.7 × 8	1.7	38.6
16	No hinges	Triangles	3 trusses	D70 150.0 × 150.0 mm²	*Same as main structure*	1.7	30.5
17	No hinges	Triangles	3 trusses	D70 150.0 × 137.5 mm²	*Same as main structure*	1.44	23.8
~~18~~	~~Hinges~~	~~Triangles~~	~~3 trusses~~	~~D70 175.0 × 150.0 mm²~~	~~*Same as main structure*~~	~~1.7~~	~~35.6~~
19	No hinges	Triangles	3 trusses	D70 175.0 × 150.0 mm²	*Same as main structure*	1.7	35.6
~~20~~	~~Hinges~~	~~Triangles~~	~~3 trusses~~	~~D70 150.0 × 150.0 mm²~~	~~*Same as main structure*~~	~~1.44~~	~~26~~
21	No hinges	Triangles	3 trusses	D70 150.0 × 150.0 mm²	*Same as main structure*	1.44	26
~~22~~	~~Hinges~~	~~Triangles~~	~~3 trusses~~	~~D70 175.0 × 162.5 mm²~~	~~*Same as main structure*~~	~~1.7~~	~~38.6~~
23	No hinges	Triangles	3 trusses	D70 175.0 × 162.5 mm²	*Same as main structure*	1.7	38.6
~~24~~	~~Hinges~~	~~Triangles~~	~~3 trusses~~	~~D70 175.0 × 150.0 mm²~~	~~*Same as main structure*~~	~~1.44~~	~~30.3~~
25	No hinges	Triangles	3 trusses	D70 175.0 × 150.0 mm²	*Same as main structure*	1.44	30.3
~~26~~	~~Hinges~~	~~Triangles~~	~~3 trusses~~	~~D70 175.0 × 162.5 mm²~~	~~*Same as main structure*~~	~~1.44~~	~~32.9~~
27	No hinges	Triangles	3 trusses	D70 175.0 × 162.5 mm²	*Same as main structure*	1.44	32.9
28	No hinges	Triangles	3 trusses	S355 CHSH 168.3 × 4	*Same as main structure*	2.05	33.2

11.4 Connection design

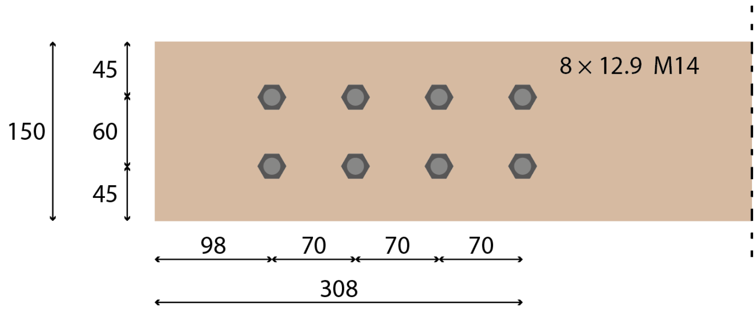

Figure 89: Connection design

11.4.1 Distances between bolts

As the intent of the structural design is to apply the same elements everywhere, this connection design needs to comply in all loading situations; tension, compression, shear and bending. Thus, with regard to the spacing requirements for the bolt configuration, it is necessary to look at the least favourable option to define the demands. As the axial load is a lot higher in all members than any of the transverse loads due to shear and occurring moments, it is assumed that the angle with the grain of the bolt loads remains below $\alpha = 30°$.

In that case, the miminal required spacings become:

$$a_1 = (4 + |\cos\alpha|)d = (4 + 1) \cdot 14 = 70\,mm$$
$$a_2 = 4d = 4 \cdot 14 = 56\,mm$$
$$a_{3,t} = \max(7d; 80) = \max(7 \cdot 14; 80) = 98\,mm$$
$$a_{4,t} = \max((2 + 2\sin\alpha)d; 3d) = 3 \cdot 14 = 42\,mm$$

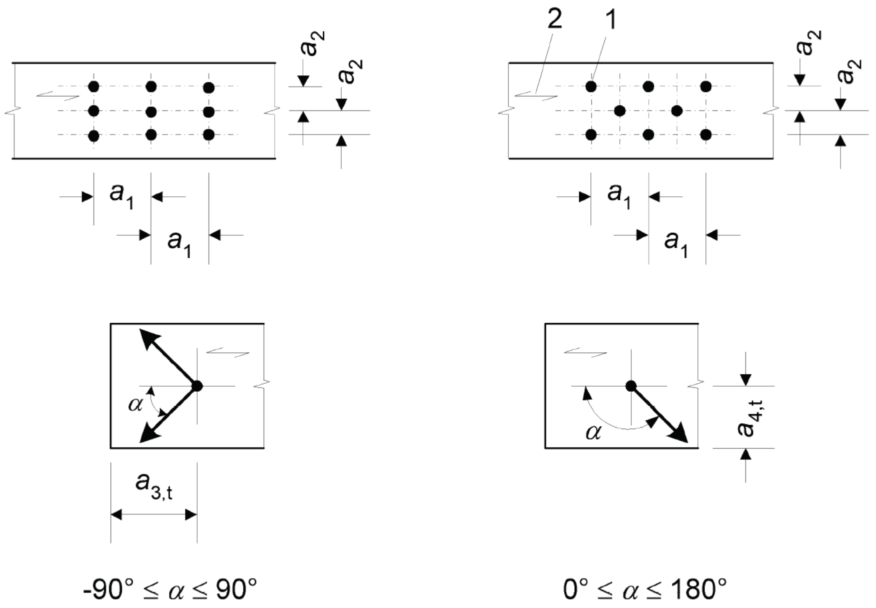

Figure 90: Spacing requirements bolt configuration

The proposed bolt design complies with these requirements.

11.4.2 Rotational stiffness

As shown in Figure 89, the connection consists out of M14 bolts, so the following value applies:

$$d = 14\,mm$$

For D70 timber, the following mean density applies (see paragraph 4.2.2.4):

$$\rho_{mean} = 960\,kg/m^3$$

And thus, the slip modulus per shear face per bolt can be calculated (see Equation 11 and Equation 12):

$$K_{ser,b} = 4 \cdot \left(\frac{\rho_{mean}{}^{1.5} d}{23}\right) = 4 \cdot \left(\frac{960^{1.5} \cdot 14}{23}\right) = 72\,421.4\,N/mm$$

Using Equation 13, the rotational stiffness of the connection can be calculated.

$$K_{r,ser,b} = K_{ser,b} \sum_{j=1}^{n} {r_j}^2 = 72\,421.4 \cdot \left(4 \cdot (35^2 + 30^2) + 4 \cdot (105^2 + 30^2)\right) = 4\,070.1\ kNm/rad$$

For checks in the ULS, the following value for the rotational stiffness needs to be applied (see Equation 15):

$$K_{r,u,b} = \frac{2}{3} K_{r,ser,b} = 2\,713.4\ kNm/rad$$

The rigid connections in the RFEM-model – the rotation around the Y-axis in the diagonals, see Figure 87 - will be carried out as rotational hinges using this stiffness.

11.4.3 Check: bolts

11.4.3.1 Horizontals

The RFEM model generates the following member loads for the governing horizontal member:

$$N_{Ed,hor} = 348.9\ kN$$

$$V_{Ed,hor} = 3.40\ kN$$

This results in a load per bolt of:

$$F_{v,Ed} = 43.6\ kN$$

At an angle with the grain of:

$$\alpha = 0.56°$$

The strength per bolt at this angle with the grain – including both of its shear faces – has been determined:

$$F_{v,Rd} = 47.3\ kN$$

And thus, the unity check is verified.

$$\frac{F_{v,Ed}}{F_{v,Rd}} = \frac{43.6}{47.3} = 0.92 \ \leq 1.0 \qquad O.K.$$

11.4.3.2 Diagonals

The RFEM model generates the following member loads for the governing diagonal member:

$$N_{Ed,diag} = 275.0\ kN$$

$$V_{Ed,diag} = 1.51\ kN$$

$$M_{Ed,diag} = 1.60\ kNm$$

This results in a load per bolt of:

$$F_{v,Ed} = 35.2\ kN$$

At an angle with the grain of:

$$\alpha = 4.6°$$

The strength per bolt at this angle with the grain – including both of its shear faces – has been determined:

$$F_{v,Rd} = 47.3\ kN$$

And thus, the unity check is verified.

$$\frac{F_{v,Ed}}{F_{v,Rd}} = \frac{35.2}{47.3} = 0.74\ \leq 1.0 \qquad O.K$$

11.4.4 Check: steel plates

11.4.4.1 Horizontals

The steel plate needs to transfer the member loads through its reduced cross section. Though close-fit bolt holes are the preferred choice, a bolt hole of 14 + 1 = 15 mm will be assumed for the calculations. A plate thickness of 10 mm will be assumed:

$$t = \ 9\ mm$$

The net area is:

$$A_{net} = t(h - h_{holes}) = 9 \cdot (150 - 2 \cdot 15) = 1080\ mm^2$$

The following loads need to be transferred:

$$N_{Ed,hor} = 348.9\ kN$$
$$V_{Ed,hor} = 3.40\ kN$$

These loads can be transcribed into the following stresses:

$$\sigma_{x,Ed} = \frac{N_{Ed,hor}}{A_{net}} = \frac{348.9 \cdot 10^3}{1080} = 323.1\ N/mm^2$$

$$\tau_{Ed} = \frac{V_{Ed,hor}}{A_{net}} = \frac{3.40 \cdot 10^3}{1080} = 3.15\ N/mm^2$$

Using the material factor of $\gamma_M = 1.05$ as prescribed by the Italian national annex (UNI-EN 1993-1-1, 2007), this results in the following unity check (Equation 20):

$$\left(\frac{\sigma_{x,Ed}}{f_y/\gamma_M}\right)^2 + 3 \cdot \left(\frac{\tau_{Ed}}{f_y/\gamma_M}\right)^2 = \left(\frac{323.1}{355/1.05}\right)^2 + 3 \cdot \left(\frac{3.15}{355/1.05}\right)^2 = 0.91\ \leq 1.0 \qquad O.K.$$

As the unity check is below 1.0, the steel plate complies with the structural demands for the horizontal members.

11.4.4.2 Diagonals

The steel plates needs to transfer the aforementioned axial load through its reduced cross section. The cross section is reduced by two holes with a diameter of 15 mm. The thickness of the plate is:

$$t = 9\ mm$$

The net area is:

$$A_{net} = t(h - h_{holes}) = 9 \cdot (150 - 2 \cdot 15) = 1080\ mm^2$$

Considering both the top and the bottom holes have a vertical distance of 30 mm to the gravitational centre of the cross section, the net moment of intertia and section modulus become:

$$I_{net} = \frac{1}{12}th^3 - 2 \cdot \left(\frac{1}{12}th_{hole}{}^3 + z_{hole}{}^2A\right) =$$
$$\frac{1}{12} \cdot 9 \cdot 150^3 - 2 \cdot \left(\frac{1}{12} \cdot 9 \cdot 15^3 + 30^2 \cdot 9 \cdot 15\right) = 2\ 283\ 187.5\ mm^4$$

$$W_{net} = \frac{I_{net}}{z_{max}} = \frac{2\ 283\ 187.5}{75} = 30\ 442.5\ mm^3$$

The following loads need to be transferred:

$$N_{Ed,diag} = 275.0\ kN$$
$$V_{Ed,diag} = 1.51\ kN$$
$$M_{Ed,diag} = 1.60\ kNm$$

And thus the stresses due to bending and axial tension become:

$$\sigma_{x,Ed} = \frac{N_{Ed,diag}}{A_{net}} + \frac{M_{Ed,diag}}{W_{net}} = \frac{275.0 \cdot 10^3}{1080} + \frac{1.60 \cdot 10^6}{30\ 442.5} = 307.2\ N/mm^2$$

The shear force causes the following stress in the steel plate:

$$\tau_{Ed} = \frac{V_{Ed}}{A_{net}} = \frac{1.51 \cdot 10^3}{1080} = 1.40\ N/mm^2$$

Using the material factor of $\gamma_M = 1.05$ as prescribed by the Italian national annex (UNI-EN 1993-1-1, 2007), the unity check as prescribed by Equation 20 can be carried out:

$$\left(\frac{\sigma_{x,Ed}}{f_y/\gamma_M}\right)^2 + 3 \cdot \left(\frac{\tau_{Ed}}{f_y/\gamma_M}\right)^2 = \left(\frac{307.2}{355/1.05}\right)^2 + 3 \cdot \left(\frac{1.40}{355/1.05}\right)^2 = 0.83 \leq 1.0 \qquad O.K.$$

As the unity check remains below 1.0, the steel plate complies with its structural demands.

11.4.5 Check: welds

11.4.5.1 Horizontals

The steel plates are welded to a circular steel core through two fillet welds, with an assumed throat of $a = 4\ mm$. The total loads that need to be transferred are:

$$N_{Ed,hor} = 348.9\ kN$$
$$V_{Ed,hor} = 3.40\ kN$$

Each fillet weld needs to take the following loads:

$$N_{Ed,weld} = 174.45\ kN$$
$$V_{Ed,weld} = \quad 1.70\ kN$$

The load $N_{Ed,weld}$ can be transcribed into the following weld components:

$$\sigma_{\perp} = \tau_{\perp} = \frac{N_{Ed,weld} \cdot \frac{1}{2}\sqrt{2}}{h \cdot a} = \frac{174.45 \cdot 10^3 \cdot \frac{1}{2}\sqrt{2}}{150 \cdot 4} = 205.6\ N/mm^2$$

The load $V_{Ed,weld}$ can be transcribed into the following component:

$$\tau_{\parallel} = \frac{V_{Ed,weld}}{h \cdot a} = \frac{1.70 \cdot 10^3}{150 \cdot 4} = 2.83\ N/mm^2$$

For this joint consisting of S355 steel parts, the following values apply according to the Eurocode (EN 1993-1-1, 2016):

$$f_u = 490\ N/mm^2$$
$$\beta_w = 0.9$$
$$\gamma_{M2} = 1.25$$

And thus, the following unity checks can be carried out, as prescribed by Equation 21 and Equation 22:

$$\frac{[{\sigma_{\perp}}^2 + 3({\tau_{\perp}}^2 + {\tau_{\parallel}}^2)]^{0.5}}{f_u/(\beta_w \cdot \gamma_{M2})} = \frac{[205.6^{\ 2} + 3(205.6^{\ 2} + 2.83^2)]^{0.5}}{490/(0.9 \cdot 1.25)} = 0.94 \leq 1.0 \quad O.K.$$

$$\frac{\sigma_{\perp}}{0.9 f_u/\gamma_{M2}} = \frac{205.6}{0.9 \cdot 490/1.25} = 0.58 \leq 1.0 \quad O.K.$$

As the unity checks are both below 1.0, the welds are qualified.

11.4.5.2 Diagonals

The steel plates are welded to a circular steel core through two fillet welds, with an assumed throat of $a = 4\ mm$. The total loads that need to be transferred are:

$$N_{Ed,diag} = 275.0\ kN$$
$$V_{Ed,diag} = 1.51\ kN$$
$$M_{Ed,diag} = 1.60\ kNm$$

Each fillet weld needs to take the following loads:

$$N_{Ed,weld} = 137.5\ kN$$
$$V_{Ed,weld} = 0.76\ kN$$
$$M_{Ed,weld} = 0.80\ kNm$$

The load $N_{Ed,weld}$ can be transcribed into the following weld components:

$$\sigma_{\perp,N} = \tau_{\perp,N} = \frac{N_{Ed,weld} \cdot \frac{1}{2}\sqrt{2}}{h \cdot a} = \frac{137.5 \cdot 10^3 \cdot \frac{1}{2}\sqrt{2}}{150 \cdot 4} = 162.0\ N/mm^2$$

The load $V_{Ed,weld}$ can be transcribed into the following component:

$$\tau_{\parallel} = \frac{V_{Ed,weld}}{h \cdot a} = \frac{0.76 \cdot 10^3}{150 \cdot 4} = 1.27\ N/mm^2$$

The load $M_{Ed,weld}$ can be transcribed into the following component:

$$\sigma_{\perp,M} = \tau_{\perp,M} = \frac{M_{Ed,weld} \cdot \frac{1}{2}\sqrt{2}}{\frac{1}{6} \cdot a \cdot h^2} = \frac{0.80 \cdot 10^6 \cdot \frac{1}{2}\sqrt{2}}{\frac{1}{6} \cdot 4 \cdot 150^2} = 37.7\ N/mm^2$$

This results in the following stress components in the welds:

$$\sigma_{\perp} = 199.7\ N/mm^2$$
$$\tau_{\perp} = 199.7\ N/mm^2$$
$$\tau_{\parallel} = 1.27\ N/mm^2$$

For this joint consisting of S355 steel parts, the following values apply according to the Eurocode (EN 1993-1-1, 2016):

$$f_u = 490\ N/mm^2$$
$$\beta_w = 0.9$$
$$\gamma_{M2} = 1.25$$

And thus, the following unity checks can be carried out, as prescribed by Equation 21 and Equation 22:

$$\frac{[\sigma_{\perp}{}^2 + 3(\tau_{\perp}{}^2 + \tau_{\parallel}{}^2)]^{0.5}}{f_u/(\beta_w \cdot \gamma_{M2})} = \frac{[199.7^2 + 3(199.7^2 + 1.27^2)]^{0.5}}{490/(0.9 \cdot 1.25)} = 0.92 \leq 1.0 \quad O.K.$$

$$\frac{\sigma_{\perp}}{0.9 f_u/\gamma_{M2}} = \frac{199.7}{0.9 \cdot 490/1.25} = 0.57 \leq 1.0 \quad O.K.$$

As the unity checks are both below 1.0, the welds are qualified.

11.5 Joint weight

As the design of the joint has been finished, it is relevant to shortly review its approximate weight as the goal for each individual structural element was to remain below 40 kg. The joint consists out of six steel plates of an approximate 400 mm length each. Considering the thickness of 9 mm, the width of 150 mm per plate and the steel density of 7 850 kg/m³, the total weight of the joints sums up to about:

$$m_{joint} = 6 \cdot (0.400 \cdot 0.150 \cdot 0.009) \cdot 7\,850 = 25.4\,kg$$

The weight of the joint remains well below the required 40 kg.

11.6 Conclusion

The initial connection design has been checked fully and lived up to the demands, so no design iterations were necessary. The connection design consists out of eight 12.9 M14 bolts, lined up in two parallel rows of four bolts each. The steel thickness required is 9mm, while the welds need to have a throat size of 4 mm. The total weight of this joint elements remain well below the required 40 kg.

The last step in the design process is to carry out a seismic analysis on the structure including the rotational stiffnesses of this joint design, which will be the topic of Chapter 12.

12 Seismic analysis

12.1 Introduction

In the previous chapter, the joint design has been finalised. The last step to undertake in this design process is a seismic analysis on the finalised structure, including the joint stiffnesses as have been determined Chapter 11. Although static seismic load combinations have been taken into account in the database generation, a more refined seismic analysis shall be carried. This chapter will cover the horizontal response spectrum analysis carried out with RFEM, using the add-on RF-DYNAM Pro, based on the first 250 eigenmodes of the structure.

The elastic response spectrum of L'Aquila for the Italian seismic limit state SLV (UNI-EN 1998-1, 2007) is shown in Figure 91. Please refer to Appendix K for more insight in the seismic properties in the city of L'Aquila. As the ductility of the structure is unknown as it is relatively complex, no reduction of the elastic spectrum will take place for this analysis.

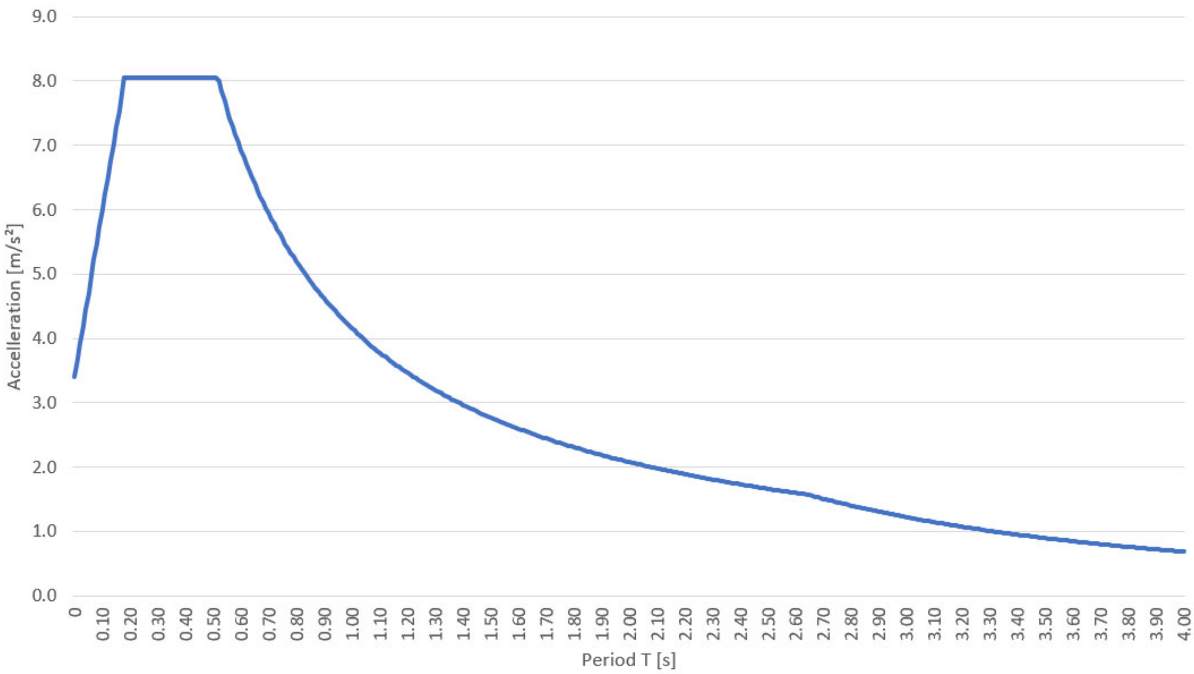

Figure 91: Horizontal elastic response spectrum of L'Aquila, Italy

The RFEM-model has been used for carrying out the modal and response spectrum analyses – this possibility is provided by the RFEM add-on RF-DYNAM Pro.

12.2 Modal analysis

A modal analysis has been carried out on the structure, generating the first 250 eigenmodes and calculating the participating mass in both horizontal directions, X and Y. In this analysis the self-weight of the load-bearing structure as well as the loads from the façades have been included. As the façade loads have been assumed quite high, this generates a total mass of almost 400 000 kg. The total participating mass percentages in both directions sums up to:

$$Participating\ mass\ X = 81.7\%$$
$$Participating\ mass\ Y = 95.4\%$$

The modes in which masses in the X- and Y-directions are active are gathered in Appendix J. The mass participating in the X-direction is fragmented over the different modes. The highest participating mass percentage is found in mode 57, in which 16.4% of the total mass takes part, followed by mode 47, in which 8.7% participates.

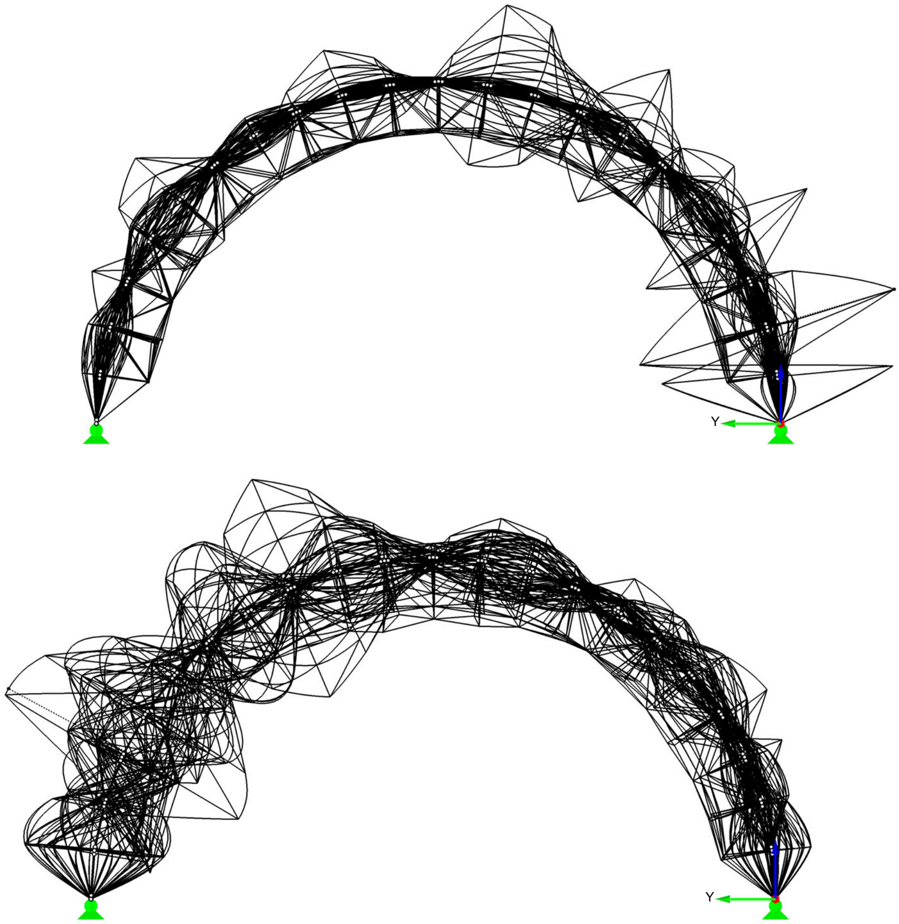

Figure 92: Mode 47 (top) & Mode 57 (bottom)

The mass participating in Y-direction has one very dominant mode, namely the first one. In this mode 90.0% of the total mass partakes.

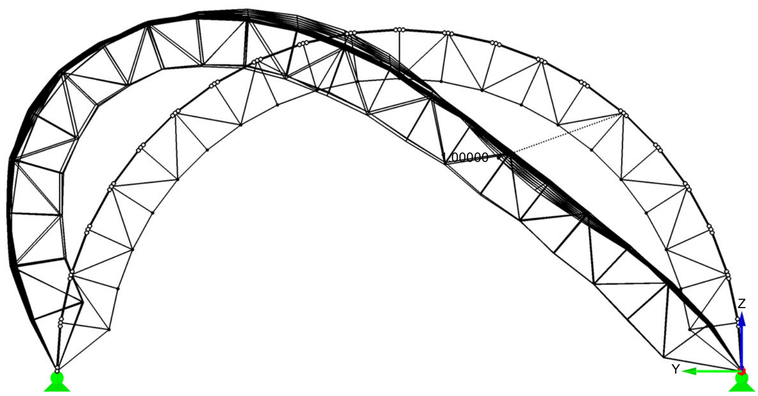

Figure 93: Mode 1

12.3 Response spectrum analysis

The eigenmodes are directly linked to eigenperiods. Using the eigenperiodes per mode, the related accelleration can be determined using the elastic response spectrum of L'Aquila – see Figure 91. The accelerations combined with the respective masses result in loads in the response spectrum analysis, using the basic formulae for loads:

$$F = m \cdot a \tag{23}$$

In which:

F	load, in N
m	mass, in kg
a	acceleration in m/s²

Loads are generated both in X- and Y-direction, using the participating masses per mode, as described in the previous paragraph. The combinations of these loads that will be checked is:

$$1.0X + 0.3Y$$

$$0.3X + 1.0Y$$

The first combination checked in the response spectrum analysis is $1.0X + 0.3Y$. This combination generates a deflection envelope as shown in Figure 94.

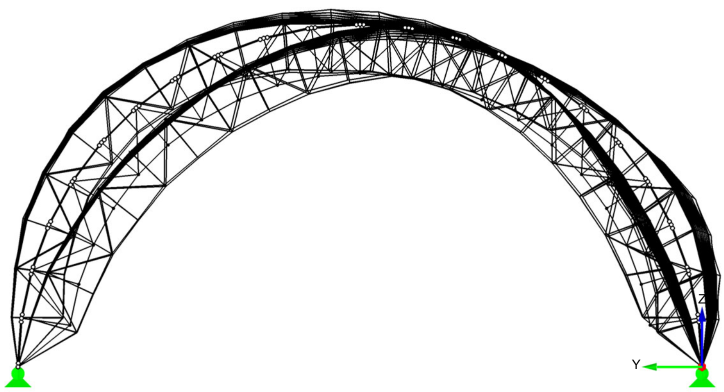

Figure 94: Deflection response spectrum analysis 1

The second combination checked in the response spectrum analysis is $0.3X + 1.0Y$. This combination generates a deflection envelope as shown in Figure 95, which is clearly more extreme.

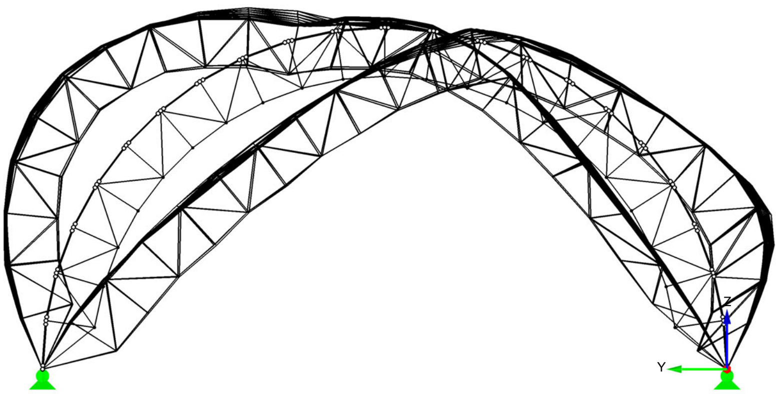

Figure 95: Deflection response spectrum analysis 2

12.4 Structural checks

12.4.1 Steel trusses

The axial load in the governing truss member as a result of the response spectrum analysis is:

$$N_{Ed,truss} = 791.75\ kN$$

The members of the trusses have the following cross section: CHSH 114.3×8.0. The cross-sectional area of this cross section is:

$$A_{truss} = 0.25\pi(114.3^2 - (114.3 - 2 \cdot 8.0)^2) = 2671.6\ mm^2$$

And thus the cross-sectional stresses are:

$$\sigma_N = \frac{N_{Ed,truss}}{A_{truss}} = \frac{791.75 \cdot 10^3}{2671.6} = 296.4\ N/mm^2$$

Using these stresses the following unity check can be carried out:

$$\frac{\sigma_N}{f_y/\gamma_M} = \frac{296.4}{355/1.05} = 0.88 \leq 1.0 \qquad O.K.$$

As the unity check remains below 1.0, the steel trusses comply with the structural demands.

12.4.2 Timber shell

The highest loads occurring in the horizontals of the timber structure is:

$$N_{Ed,hor} = 72.93\ kN$$
$$V_{Ed,hor} = 0\ kN$$

The highest loads occurring in the diagonals of the timber structure is:

$$N_{Ed,diag} = 105.67\ kN$$
$$V_{Ed,diag} = 1.76\ kN$$
$$M_{Ed,diag} = 2.30\ kNm$$

Compared to the loads in Chapter 10 and Chapter 11, these are small. Therefore, it is not necessary to carry out unity checks on the timber members, as this is not the governing load situation.

12.5 Conclusion

A response spectrum analyse has been carried out on the full structure, and the structural elements have been checked. No iterations were needed as the structure complied with all sttructural demands and the resulting design is the highest-ranking design in the list.

IV

CONCLUSION

13 Final design

13.1 Recap

Though iterations where thought necessary before the extra checks on the structure were carried out – connection validations and seismic analyses – it turns out the highest-ranking design has proven to live up to all additional structural demands – see Table 17 and Figure 96.

In this chapter, the final design will be shortly summarised, followed by some potential refinements that could be carried out on this structural design.

Table 17: Final design selection

Rank	Basic geometry	In-plane variations	Out-of-plane variations	Cross sections main structure	Cross sections trusses	Element length [m]	Element mass [kg]
1	No hinges	Triangles	3 trusses	D70 150.0 × 150.0 mm²	S355 CHSH 114.3 × 8	1.7	30.5
2	No hinges	Triangles	3 trusses	D70 150.0 × 150.0 mm²	S355 CHSH 139.7 × 8	1.7	30.5
3	No hinges	Triangles	3 trusses	D70 150.0 × 150.0 mm²	S355 CHSH 168.3 × 8	1.7	30.5
~~4~~	~~Hinges~~	~~Triangles~~	~~3 trusses~~	~~D70 175.0 × 150.0 mm²~~	~~S355 CHSH 114.3 × 8~~	~~1.7~~	~~35.6~~
5	No hinges	Triangles	3 trusses	D70 175.0 × 150.0 mm²	S355 CHSH 114.3 × 8	1.7	35.6
~~6~~	~~Hinges~~	~~Triangles~~	~~3 trusses~~	~~D70 175.0 × 150.0 mm²~~	~~S355 CHSH 139.7 × 8~~	~~1.7~~	~~35.6~~
7	No hinges	Triangles	3 trusses	D70 175.0 × 150.0 mm²	S355 CHSH 139.7 × 8	1.7	35.6
~~8~~	~~Hinges~~	~~Triangles~~	~~3 trusses~~	~~D70 175.0 × 162.5 mm²~~	~~S355 CHSH 114.3 × 8~~	~~1.7~~	~~38.6~~
9	No hinges	Triangles	3 trusses	D70 175.0 × 162.5 mm²	S355 CHSH 114.3 × 8	1.7	38.6
~~10~~	~~Hinges~~	~~Triangles~~	~~3 trusses~~	~~D70 175.0 × 150.0 mm²~~	~~S355 CHSH 168.3 × 8~~	~~1.7~~	~~35.6~~
11	No hinges	Triangles	3 trusses	D70 175.0 × 150.0 mm²	S355 CHSH 168.3 × 8	1.7	35.6
~~12/14~~	~~Hinges~~	~~Triangles~~	~~3 trusses~~	~~D70 150.0 × 150.0 mm²~~	~~S355 CHSH 114.3 × 8~~	~~1.44~~	~~26~~
13/15	No hinges	Triangles	3 trusses	D70 150.0 × 150.0 mm²	S355 CHSH 114.3 × 8	1.44	26
~~12/14~~	~~Hinges~~	~~Triangles~~	~~3 trusses~~	~~D70 175.0 × 162.5 mm²~~	~~S355 CHSH 139.7 × 8~~	~~1.7~~	~~38.6~~
13/15	No hinges	Triangles	3 trusses	D70 175.0 × 162.5 mm²	S355 CHSH 139.7 × 8	1.7	38.6
16	No hinges	Triangles	3 trusses	D70 150.0 × 150.0 mm²	*Same as main structure*	1.7	30.5
17	No hinges	Triangles	3 trusses	D70 150.0 × 137.5 mm²	*Same as main structure*	1.44	23.8
~~18~~	~~Hinges~~	~~Triangles~~	~~3 trusses~~	~~D70 175.0 × 150.0 mm²~~	~~*Same as main structure*~~	~~1.7~~	~~35.6~~
19	No hinges	Triangles	3 trusses	D70 175.0 × 150.0 mm²	*Same as main structure*	1.7	35.6
~~20~~	~~Hinges~~	~~Triangles~~	~~3 trusses~~	~~D70 150.0 × 150.0 mm²~~	~~*Same as main structure*~~	~~1.44~~	~~26~~
21	No hinges	Triangles	3 trusses	D70 150.0 × 150.0 mm²	*Same as main structure*	1.44	26
~~22~~	~~Hinges~~	~~Triangles~~	~~3 trusses~~	~~D70 175.0 × 162.5 mm²~~	~~*Same as main structure*~~	~~1.7~~	~~38.6~~
23	No hinges	Triangles	3 trusses	D70 175.0 × 162.5 mm²	*Same as main structure*	1.7	38.6
~~24~~	~~Hinges~~	~~Triangles~~	~~3 trusses~~	~~D70 175.0 × 150.0 mm²~~	~~*Same as main structure*~~	~~1.44~~	~~30.3~~
25	No hinges	Triangles	3 trusses	D70 175.0 × 150.0 mm²	*Same as main structure*	1.44	30.3
~~26~~	~~Hinges~~	~~Triangles~~	~~3 trusses~~	~~D70 175.0 × 162.5 mm²~~	~~*Same as main structure*~~	~~1.44~~	~~32.9~~
27	No hinges	Triangles	3 trusses	D70 175.0 × 162.5 mm²	*Same as main structure*	1.44	32.9
28	No hinges	Triangles	3 trusses	S355 CHSH 168.3 × 4	*Same as main structure*	2.05	33.2

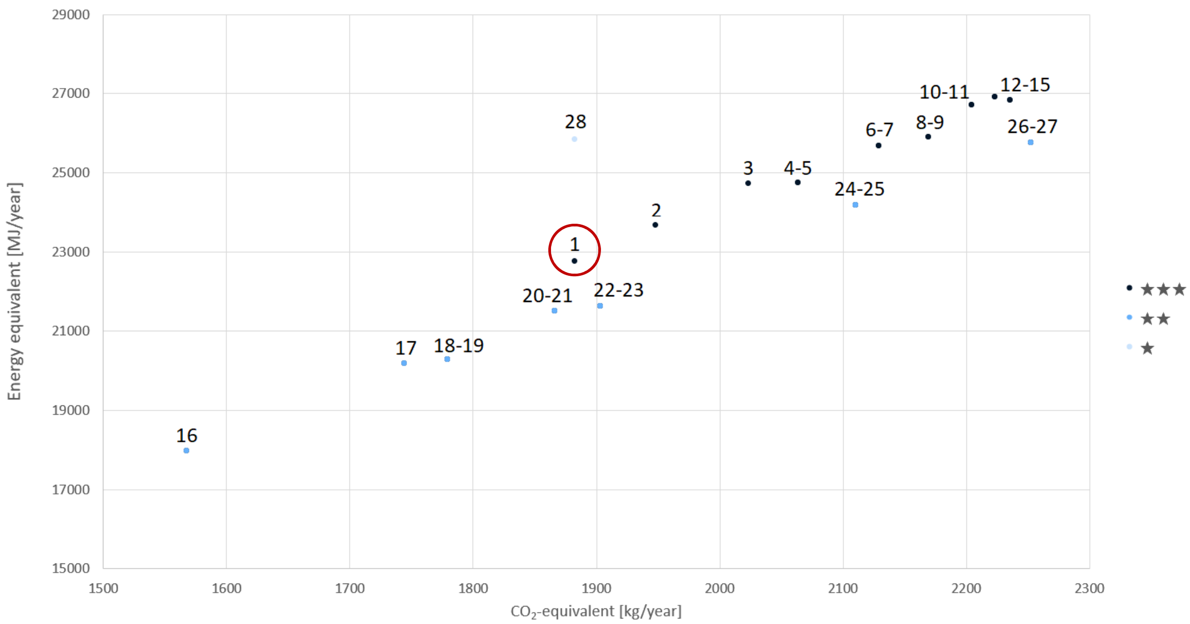

Figure 96: Final design selection

13.2 Structural design

The top 1 design that followed from the exclusion and sorting of the database entries (see Chapter 0) has been selected as the final structural design, as it also passed all the other checks that have been carried out. Its properties are shortly gathered below.

Optimised design:	Number-1 ranking structure
Elements main structure:	D70 timber (azobé), 150×150mm², 1.7m long, 30.6 kg per piece
Elements trusses:	S355 steel, CHSH114.3×8.0, 31.8 to 41.9 kg per piece
Joint:	S355, plate thickness 9 mm, 8 × 12.9 M14 bolts, 25.4 kg per piece
Connection:	8 × 12.9 M14 bolts

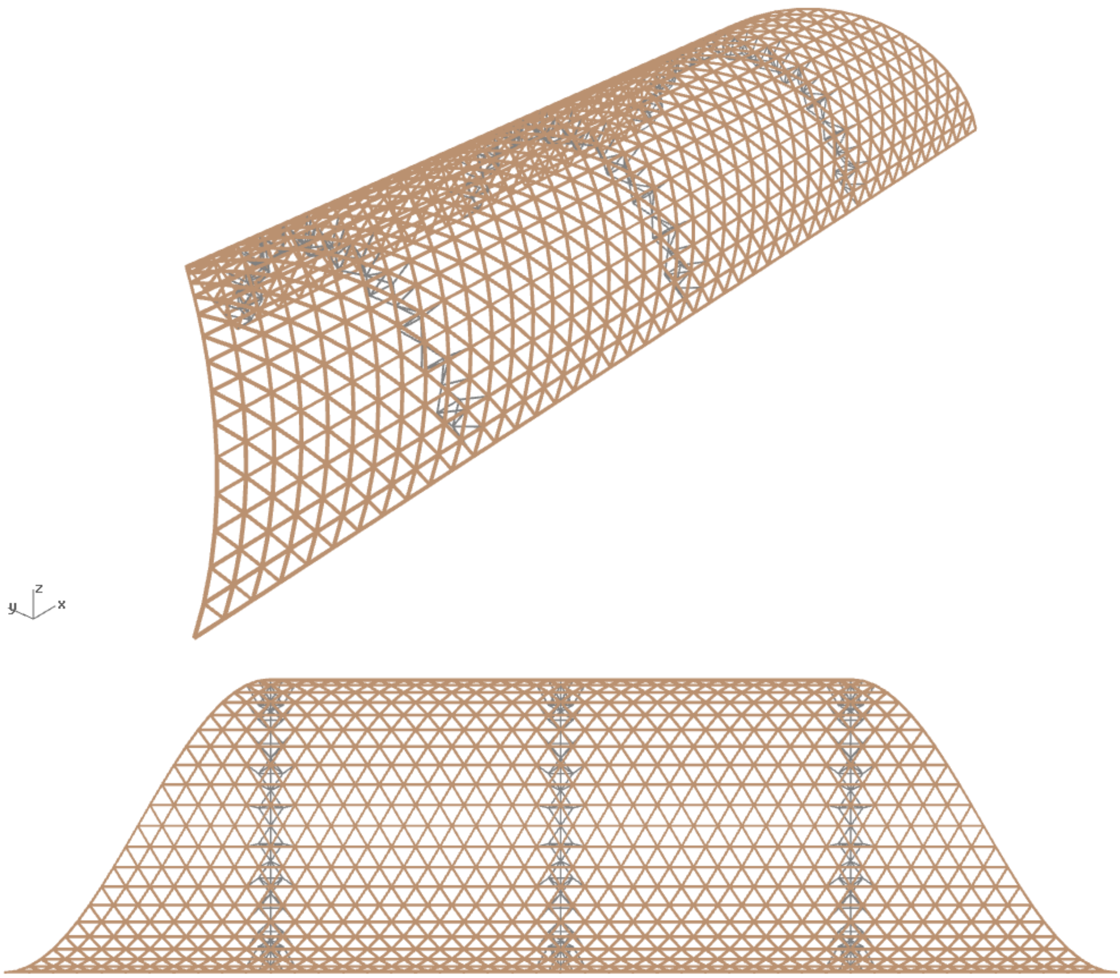

Figure 97: Final structural design | Perspective (top) & top view (bottom)

13.3 Potential refinements

Some further structural refinements could be considered, to reduce the structural mass even more. These were shortly be discussed in the following paragraph, followed by a short discussion on the advantages and disadvantages of these refinements.

13.3.1 Joint and element design

The joint design has been structurally verified based on the governing structural members in the structure. As it turns out, these high loads only occur very locally, namely around the trusses and near the rim of the structure. The pattern is shown in Figure 98.

A design choice that could be made is to make two different joint elements: heavy ones where they are required, and lighter ones where they are not. This way, for more than 750 joints, the plate thickness could be reduced as well as the number of bolts and consequently the dimensions of the joint element.

The same goes for the elements: these could potentially be cross-sectionally optimised. The elements could be reduced in size at the locations that are less heavily loaded.

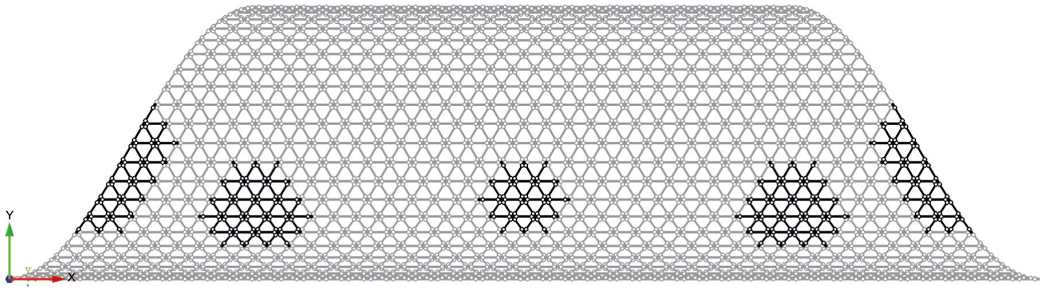

Figure 98: High loads (black) vs. low loads (grey)

13.3.2 Truss design

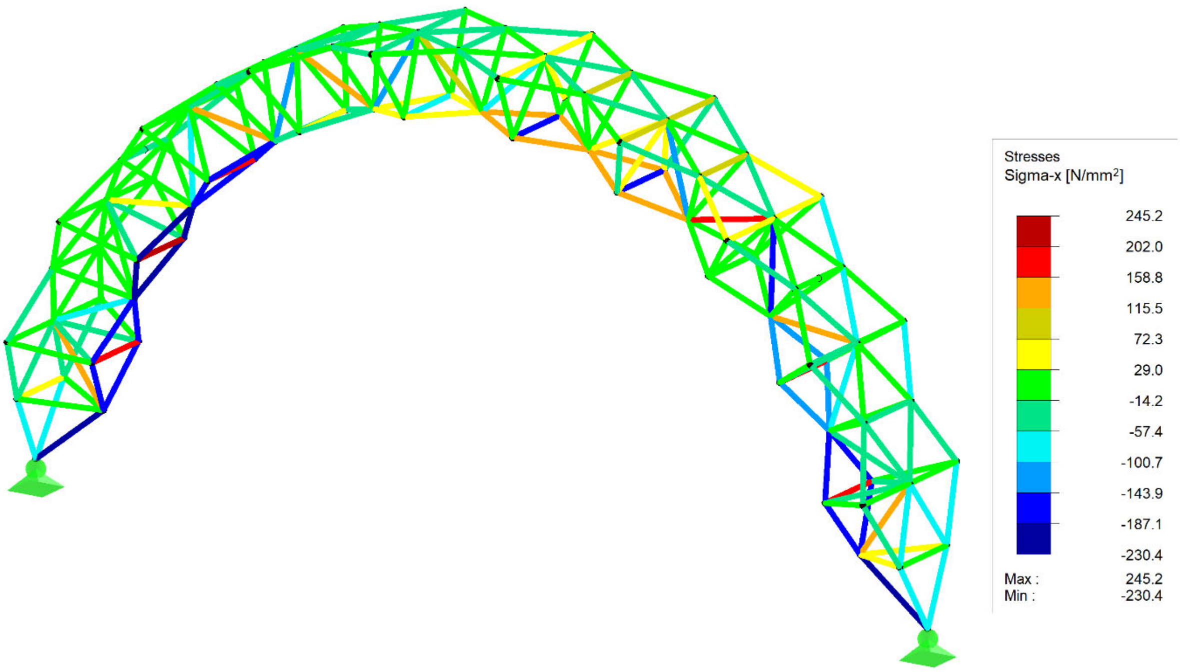

Figure 99: Stresses in truss

The stresses that occur in the trusses are different depending on the function of each member. A distinction has been made between 5 different parts of the truss, as shown in Figure 100, Figure 101 and Figure 102.

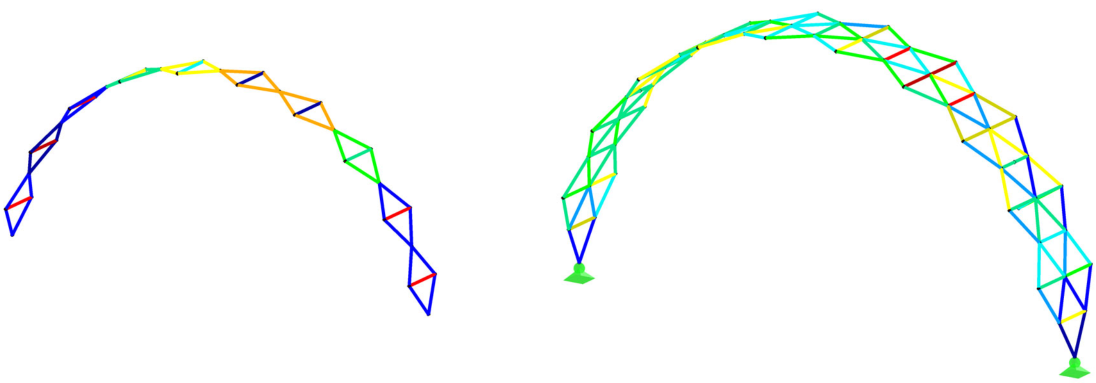

Figure 100: Truss | Members inner layer (left) & outer layer (right)

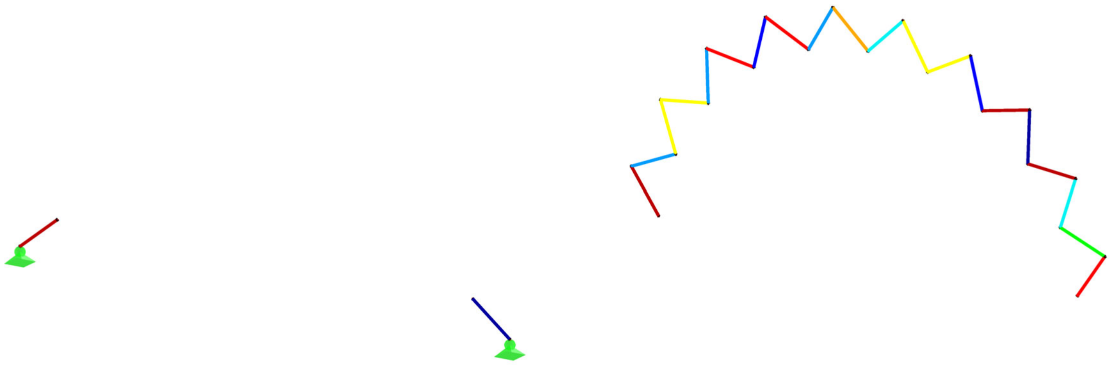

Figure 101: Truss | Supporting members (left) and connecting members A (right)

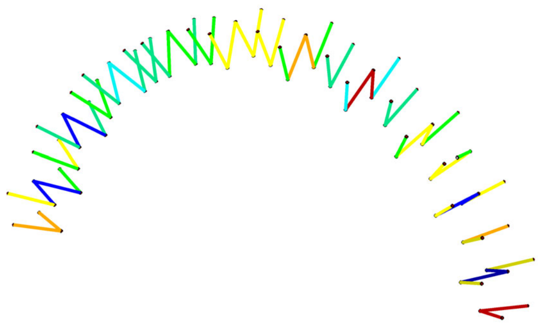

Figure 102: Truss | Connecting members B

The minimal and maximal stresses that occur in each of these parts are presented in Table 18. Depending on the occurring loads, a design choice could be made to carry out the different parts of the truss in different cross sections.

Table 18: Maximal stresses per part of the truss

Members	**Highest absolute stress [N/mm^2]**
Inner layer	245.2
Outer layer	106.1
Supporting	230.4
Connecting A	177.6
Connecting B	37.2

13.3.3 Discussion

The advantage of these model refinements is that the material use can be further minimised. However, it is questionable whether this is necessarily an environmentally friendlier solution, as the production of materials of different sizes might cost more effort and energy. Moreover, the structure would become more complex as making structural exceptions throughout the design makes the construction less understandable, especially for non-experts. This could complicate its erection. Based on current knowledge, the suggestion is to keep the design as simple as possible. However, it would be interesting to research if refining the structure further and reducing its structural weight would have a significant enough impact on the environmental footprints to accept the added complexity.

14 Conclusion

14.1 Introduction

The architectural design for the community centre on the Piazza del Duomo in L'Aquila, Italy, and the underlying social concept contain many objectives that have had a great influence on the structural design: such as sustainability, participation of the local population (resulting in striving for simplicity and lightweight structural elements) and minimal use of material. That these aims led to contradictions proved both complicated and fascinating. For example: when minimising the weight of each structural element by reducing their size, the total amount of elements and structural joints grows significantly, which has an undesirable effect on the environmental impact. Another question raised is whether a simplistic design – which aims at the participation of local laymen in its construction – is well-suited for a seismic context.

In these apparent contradictions lies the core of this research: is it possible to find a golden mean or do tough choices need to be made? On that basis, the following central research question has been formulated at the beginning of this project:

Given the architectural design, how can the main load-bearing structure be optimised for seismic contexts using parametric modelling, considering the following objectives: maximal demountability and structural simplicity, minimal material use and environmental impact, and limited weight per structural element?

In the previous chapters, the final structural design has been presented. Now it is of interest to reflect on the results of this project: what are the accomplishments, what are the limitations and where lie the possibilities for future research?

The project has two aspects that need to be elaborated upon. First is the design itself: what are the strengths, where is room for improvement, and how do I reflect on my choices as the architect after having worked out the structural design? Second is the method applied for the structural optimisation. How does this method fit next to the available optimisation tools, what are the advantages and where lie the pitfalls?

14.2 Design

The architectural design that formed the basis for this graduation project in structural engineering includes a temporary structure that can be constructed multiple times in different regions. The context chosen for the structural development of the design is a severely damaged historic town centre in Central Italy, in the city of L'Aquila. In 2009, the region was hit by an intense earthquake, killing over 300 people, wounding over 1500 and rendering more than 65000 inhabitants homeless. The town centre of L'Aquila was heavily affected. The after-disaster policy resulted in the fact that the town centre is still a ghost town 10 years after the earthquake. It is covered in scaffolding in a forest of cranes and a cloud of concrete, without any perspective on restoration on short term, to the citizens' absolute frustration. There are multiple gaps in the policy, but one of the most important once is the lack of local participation (Alexander, 2010).

The architectural design proposes an alternative after-disaster policy, in which a community centre is constructed in the middle of the affected town centre and will remain there during its recovery. This multi-purpose centre can fulfil many of the city's lost functions after the earthquake and give urban life the possibility to continue even when the town is being reconstructed. Above all, it provides a platform for all-round participation and discussion about the city's restoration.

In short, an expressly social concept underlies the design: participation of the local population. This manifests itself in the structural design, aiming to be as simple as possible with lightweight and portable structural elements. This way, the local population is given the opportunity to actively take part in the recovery of their own city, in order to give them some pride back after the earthquake has deprived them of so much. This social concept forms a guiding principle during the structural optimisation.

Figure 103 shows the structural concept resulting from the architectural design, and the final structural design proposal after this project's optimisation.

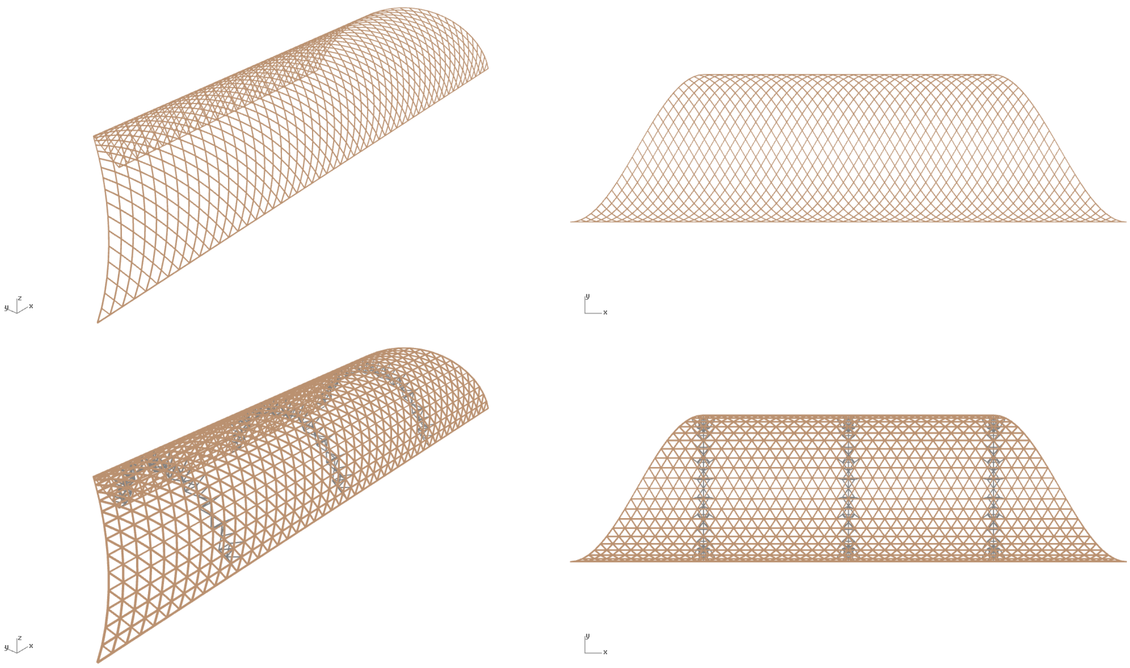

Figure 103: Perspective and top view of the structural concept (top) and the final structural design (bottom)

Comparing the 'before' and 'after' structures shows that alterations have been made. In the transition from concept to reality, it soon became clear that the original structure did not meet the structural requirements. The timber elements – with a cross section of 100×100mm² – turned out to be too small to bridge the span of 20m as well as unsuitable for the proposed joint design. The timber elements have therefore been upscaled to cross sections of 150×175mm². The length of the elements has increased from 1.5m to 1.7m.

Another significant different between concept and final design is the addition of three trusses underneath the structure. The original choice for a single-curved structure resulted in one weak structural direction, in which large deflections occur (see Figure 104), especially in case of horizontally acting loads during earthquakes. To establish more stiffness in this direction without having to significantly upscale the timber elements, trusses have been applied. In order not to undermine the aesthetical simplicity of the curved timber plane, these trusses are constructed in steel. Moreover, this choice in material creates a very easy-to-understand structure, also for the laymen of the local population.

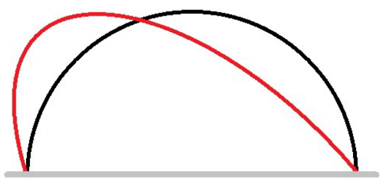

Figure 104: Weak direction

A third important different between concept and final design is the addition of horizontal timber elements, resulting in a triangular pattern instead of a diamond pattern. These horizontals cause the structure to become stiffer and the loads to be more equally distributed. Though there are feasible structural variants which have the diamond pattern, the addition of the horizontals reduces required cross sections and the total structural mass and thus, the environmental impact.

Lastly, a few adaptations have been made during the refinement of the design. The applied trusses resulted in very high stresses in the timber structure. These stresses have been reduced by separating the truss structures from the timber structure, as shown in Figure 105. By doing so, the constructability of the entire structure has also improved, as the trusses can be erected separately and provide stability during the erection of the timber shell.

Figure 105: Integrated trusses (left) & separate trusses (right)

Despite the structural separation of the trusses and the timber – resulting in a significant decrease in stresses – there are certain spots in the structure where peak stresses occur. As the joints have been designed for the governing members – which are located around these peak stresses, see Figure 106 – the joints are over-dimensioned for over 700 connections. A way to reduce the over-dimensioning would be to work with two different-sized joints, but this makes the structure more complex than envisioned. It would be recommended to research whether a decrease in material by applying different joints in the structure – or even different member elements – has a significant influence on the environmental impact, as this could potentially overrule the desire of keeping the structure as simple as possible.

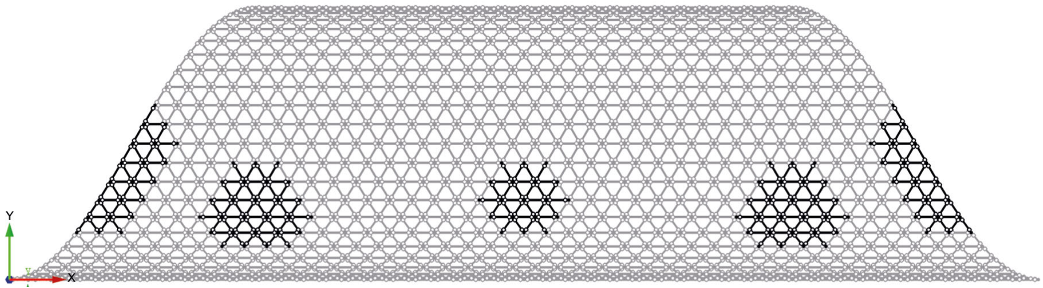

Figure 106: Big joints (black) vs. small joints (grey)

Reality has dictated the architectural design to be adjusted in a number of ways. Though it has been proven that the desired structure is practically possible and that the design balances the required objectives quite well, the question arises to what extent this design still lives up to the underlying conceptual demands. After all, the aim was to create a structure as simple and light-weight as possible; has this aim been reached? The shape chosen in the architectural design has caused the structure to be more complex than deemed desirable considering its core concept. In my opinion a double-curved structure would potentially be a better solution, or even more specific, in its purest form: a dome-shaped structure. Considering the goal to create a structure as simple as possible, such a structure would comply more neatly with the conceptual demands.

The single-curved structure does have advantages, e.g. it is easily extendable on both sides. This same flexibility is not possible in a dome-shaped structure, but one could think of other solutions, such as linking multiple domes together. On top of that, one can research the possibilities to create a flexible joint so that multiple spans can be created using the same element. This flexibility is more conceivable in dome-shaped than single-curved structures. It is recommended to carry out more research into different structural shapes – among which a dome – in order to achieve a more efficient and in the end simpler structural design.

Regardless of the choice in structural shape, it is recommended to carry out more research into:

- the design of the joint and the slip of the joints, as this can accumulate greatly in a grid-like structure with such numerous joints;
- the dynamic behaviour of the structure during an earthquake, as the modal analysis in the end results in a static load, which may be too much of a simplification for deviant structures;
- the structural interaction between the two different materials that have been applied in the structural design – timber and steel – under the influence of their different properties, such as thermal behaviour;
- variation of cross sections and joints throughout the structure, to determine whether complicating the structure further would have a positive effect on its environmental impact;
- the long-term structural effects – such as creep and fatigue – as these have not yet been taken into consideration.

Finally, attention needs to be paid to the fact that by concluding the design of the main load-bearing roof structure, the design of the community centre is far from finalised. Another important structural element is the elevated floor that ties the structural design together; how can this floor be designed modularly, while containing enough mass for keeping the structure grounded in its lifetime and being able to take the loads applied to it by the roof structure? And let's not forget one of the most important aspects of the community centre: it needs to be able to function fully off-the-grid, as it has been designed for a post-disaster context in which facilities as electricity and water are not a given. How can an off-the-grid community centre be created which provides its users with a pleasant environment, equipped with all basic conveniences (e.g. lavatories)?

Summarising all aforementioned conclusions, I recommend to carry out more research into the following points in order to get to a coherent and complete design:

(1) more efficient load-bearing shape, in order to create a structure as simple as possible;
(2) possibilities to make the structure flexible in size, so it can be constructed in numerous different contexts;
(3) more refined design and analysis of the structural joints;
(4) design and analysis of the rest of the load-bearing structure, mostly the elevated floor;
(5) dynamic analysis of the main load-bearing structure in case of a seismic event;
(6) off-the-grid design of the community centre, mainly focussing on building physics;
(7) long-term effects, such as creep and fatigue.

14.3 Method

For the optimisation of the main load-bearing structure, a combination of an automated process and manual iteration has been chosen: through an automated process a database has been generated of around 11000 structural variants, after which the variants have been excluded and sorted manually. Through extra analyses, iterations have been carried out in the remaining list of structural models.

For the software Grasshopper – a plug-in for the 3D-platform Rhino, which focusses on parametric design – multiple tools have already been developed which carry out automated optimisation. Where does the applied method stand in this framework of optimisation process? What are the advantages and disadvantages of the chosen method and what are the recommendations for future developments?

Various plug-ins have been designed that generate an optimum in a list of possibilities in Grasshopper using several algorithmic methods. Galapagos (Rutten, 2013), which is integrated in Grasshopper already, is one of them, or the externally developed tool Goat (Rechenraum, 2019). Both optimisation plug-ins have a single-objective solver, which uses one output value to generate an optimum based on mathematical genetic algorithms. An alternative single-objective tool is Opossum (Wortmann, 2017). This tool is based on a different calculation method, relying on model-based optimisation, in which parametric models form the basis for calculation.

The downside of these optimisation plug-ins is, as the name suggests, that they are single-objective. This means that only one output value is taken into consideration, which is either minimised or maximised. For instance, one could maximise the gain of heat by optimising the location of windows in a building, or one could minimise the total distance from all rooms to a WiFi-modem by optimising its location. It is possible to combine multiple output values into one value, for instance by multiplication, and one could even influence the weighting of the several values by increasing them by certain factors. However, by using these single-objective optimisation tools, a significant sense of control is lost.

An alternative would be the use of a multi-objective optimisation tool and these are available on the market as well. One of these tools is Octopus (Vierlinger, 2018), developed by the Eidgenössische Technische Hochschule (ETH) in Zurich. This tool also uses genetic algorithms to find an optimum – the same as the aforementioned Galapagos and Goat – and on top of that, it provides the possibility to select multiple objectives. The outcome is a series of optimised solutions between different extremes.

This tool lies closer to what was necessary for this project, as there is more control over the different objectives. Unfortunately, the downside of this tool is – which is also the case for the aforementioned single-objective ones – that it is only possible to minimise or maximise the chosen objectives; the tool either strives for the absolute minimum or the absolute maximum of an output value. In this design project, not all objectives are this black-and-white, there is actually a lot of grey area. For example: one could set the maximum allowed deflection to be 300mm; whether the deflection of the optimised design is 200mm or 100mm is irrelevant. It is not possible to provide such input in the plug-in. Furthermore, it is quite complex to quantify certain aspects of the design – such as the aesthetical value – and to assign correct weighting to the different objectives.

Therefore, the main reason the applied optimisation method has been chosen – in which a database is generated before manual exclusion, sorting and iteration takes place – is the extensive insight it provides and the control that can be exercised over the optimisation process and outcome. In case of fully automated optimisation in complex design situations, it is necessary to be sufficiently familiar with the underlying mathematics to fully comprehend the outcome. In addition, everything needs to be determined and quantified upfront, while in case of manual iteration a lot of room is available for adjustments during the entire process. It is human nature to adjust an opinion and approach based on new insights, and that was not any different during this project. For example, only once the sorting process was carried out, did the weighting of the aesthetics compared to the weighting of the environmental impact come forward; this weighting was strongly dependent on the remainder of models, which was not known upfront. Thus, for a project in which the designer can be surprised by certain outcomes along the way, fully automated optimisation is quite difficult to establish.

In this context, one more available Grasshopper optimisation tool should be mentioned, namely modeFrontier (Esteco SpA, 2019). This plug-in offers more freedom of input and sense of control than the aforementioned ones, but unfortunately it is not freely available and it is therefore undefined if it would have been a suitable tool for this project. It would be valuable to carry out the same optimisation using this plug-in and to compare its outcome to the outcome of this research in order to understand its potential and to see whether this tool does provide the sense of control that the others were lacking.

It is recommended to improve the Grasshopper-script, through which the database was generated, in certain respects. Firstly, one can question if and why it was necessary to generate 11000 models, while only around 400 models passed the exclusion phase of the optimisation process. However, the choice for a low success rate has been a conscious one during the selection of steel and timber cross sections. As the cross section increases in size, the success rate of the geometrical variations increases, as is visualised in Figure 107.

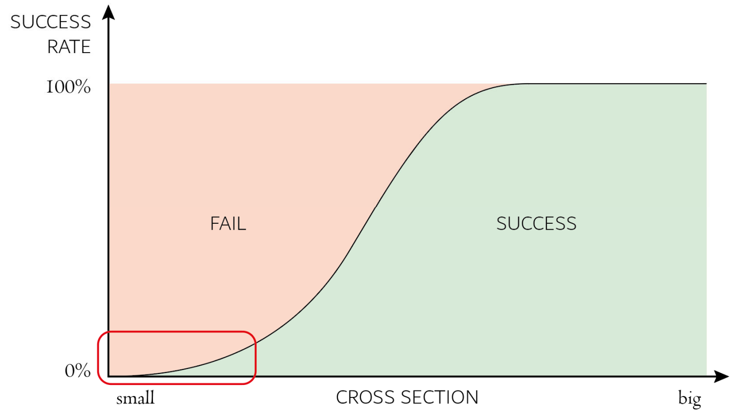

Figure 107: Success rate of different cross sections

As one of the objectives is a low environmental impact – a value directly related to the total structural mass – it is relevant to minimise the size of the cross section. A higher success rate will therefore not generate a different final result as it will always lie in the circled region (see Figure 107). Following up on that, the database could by simplified by filtering the failing models from its generation, only storing successful designs.

Secondly, apart from Rhino and Grasshopper, other software and calculation techniques have been applied extensively to conduct this research. For the determination of the environmental impact, CES EduPack 2018 has been used, while RFEM has carried out the seismic analyses and the structural checks of the joints have been mostly calculated manually. Further integration of all these calculations in the Grasshopper-script would be desirable in order to save time. In some cases, that is not yet possible, since the tools or the interoperability between Grasshopper and these tools are either not available or too limited. Further research in this regard is recommended.

In summary, the method applied during this graduation project has proven very successful, giving the designer a high sense of control, and resulting in a well-balanced structural design. However, for further development of this optimisation method, it is recommended to carry out the following points:

(1) research into advanced optimisation software (e.g. modeFrontier), which allows more control on combining the objectives of multi-objective optimisation algorithms, possibly as a basis for the design of a new multi-objective optimisation tool which provides a good sense of control and input flexibility;
(2) improvement of the Grasshopper-script to generate a database more time-efficiently, e.g. by automated exclusion of failing models from its generation;
(3) research into expanding the usability of existing environmental database-querying Grasshopper tools (e.g. Bombyx, Tortuga, BEETLE^2), possibly in order to develop new tools to this end;
(4) research into the potential of interoperability between Grasshopper and the software in which analyses have been carried out separately, namely RFEM – detailed software for structural analysis based on the finite element method, in which seismic analyses have been carried out – and CES EduPack 2018 – software for performing a database-querying environmental analysis; interoperability between these programs would allow the calculation of all necessary objectives with only one algorithm, carrying out fully integrated optimisation loops.

REFERENCES & APPENDICES

References

Advameg. (2018). *Nations Encyclopedia.* Retrieved December 12, 2018, from https://www.nationsencyclopedia.com/

Alexander, D. E. (2010). The L'Aquila Earthquake of 6 April 2009 and Italian Government Policy on Disaster Response. *Journal of Natural Resources Policy Research, 2*(4), 325-342.

CES EduPack. (2018). Retrieved from Granta Design: grantadesign.com/education/ces-edupack/

Dhingra, R., Overly, J. G., & Davis, G. A. (1999). *Life-Cycle Environmental Evaluation of Aluminum and Composite Intensive Vehicles.* University of Tennessee.

Durability Class. (2018). Retrieved from Wood Solutions: www.woodsolutions.com.au/glossary/Durability-Class

Ecoinvent v2.2. (2010). Retrieved from Ecoinvent: www.ecoinvent.com

EN 1912. (2012). *Structural Timber - Strength classes - Assignment of visual grades and species.*

EN 1990. (2011). *Eurocode: Basis of structural design.*

EN 1991-1-3. (2011). *Actions on structures - Part 1-3: General actions - Snow loads.*

EN 1991-1-4. (2011). *Eurocode 1: Actions on structures - Part 1-4: General actions - Wind actions.*

EN 1993-1-1. (2016). *Eurocode 3: Design of steel structures - Part 1-1: General rules and rules for buildings.*

EN 1993-1-8. (2011). *Eurocode 3: Design of steel structures - Part 1-8: Design of joints.*

EN 1995-1-1. (2011). *Eurocode 5: Design of timber structures – Part 1-1: General - Common rules and rules for buildings.*

EN 338. (2016). *Structural timber - Strength classes.*

EN 350. (2016). *Durability of wood and wood-based products - Testing and classification of the durability to biological agents of wood and wood-based materials.*

EN-ISO 12944-2. (2018). *Paints and varnishes - Corrosion protection of steel structures by protective paint systems - Part 2: Classification of environments.*

Esteco SpA. (2019). *modeFrontier: Process automation and optimization in the engineering design process.* Retrieved from Esteco: www.esteco.com/modefrontier

Hammond, G., & Jones, C. (2008). *Inventory of Carbon and Energy (ICE).* Bath: University of Bath.

Koning, L. (2018). *Digital Fabrication of a Timber Bridge: Design, optimisation, fabrication and testing at global and connection level.* Delft: Delft University of Technology.

Matsuzaki, R., Ueda, M., Namiki, M., Jeong, T., Asahara, H., Horiguchi, K., . . . Hirano, Y. (2016). Three-dimensional printing of continuous-fibre composites by in-nozzle impregnation. *Scientific Reports.*

Olshansky, R. B. (2005). How do Communities Recover from Disaster? A Review of Current Knowledge and an Agenda for Future Research. Kansas City: University of Illinois.

Preisinger, C. (2018, August 9). *Karamba3D parametric engineering; User manual (version 1.3.1).* Retrieved from Karamba3D: www.karamba3d.com

Rechenraum. (2019). *Goat: Free optimization solver component for Rhino's Grasshopper.* Retrieved from Rechenraum e.U.: www.rechenraum.com/en/goat.html

Rutten, D. (2013, March/April). Galapagos: On the Logic and Limitations of Generic Solvers. *Architectural design, Special Issue; Computation Works: The Building of Algorithmic Thought, 83*(2), 132-135.

UNI-EN 1990. (2007). *Criteri generali di progettazione strutturale.*

UNI-EN 1990. (2007). *Criteri generali di progettazione strutturale.*

UNI-EN 1991-1-3. (2007). *Azioni sulle costruzioni Parte 1-3: Carichi della neve.*

UNI-EN 1991-1-4. (2007). *Azioni sulle costruzioni – Parte 1-4: Azioni in generale – Azioni del vento.*

UNI-EN 1993-1-1. (2007). *Progettazione delle strutture in acciaio: Regole generali e regole per gli edifici.*

UNI-EN 1995-1-1. (2007). *Progettazione delle strutture di legno: Regole generali e regole per gli edifici*.

UNI-EN 1998-1. (2007). *Progetto delle strutture in zona sismica - Parte 1 - Regole generali, azione sismica e regole per gli edifici*.

Vega, A., Arriaga, F., Guaita, M., & Baño, V. (2013). Proposal of visual grading criteria of structural timber of Sweet Chestnut from Spain. *Holz als Roh- und Werkstoff*.

Vierlinger, R. (2018). *Octopus*. Retrieved from Food4Rhino: Apps for Rhino and Grasshopper: www.food4rhino.com/app/octopus

Voet, E. v., Oers, L. v., & Nikolic, I. (2008). Dematerialization: Not Just a Matter of Weight. *Journal of Industrial Ecology, 8*(4), 121-137.

Wortmann, T. (2017). Opossum: Introducing and Evaluating a Model-based Optimization Tool for Grasshopper. *CAADRIA 2017* (pp. 283-293). Hong Kong: The Association for Computer-Aided Architectural Design Research in Asia (CAADRIA).

Xia, L., Xia, Q., Huang, X., & Xie, Y. (2016). Evolutionary Structural Optimization on Advanced Structures and Materials: A Comprehensive Review. *Archives of computational Methods in Engineering, 25*(2), 437–478.

Appendix A

Circular Hollow Sections Hot-rolled (CHSH)

Main structure: S235

CHSH139.7x4.0
CHSH139.7x6.0
CHSH139.7x8.0
CHSH139.7x10.0
CHSH139.7x12.0
CHSH168.3x4.0
CHSH168.3x6.0
CHSH168.3x8.0
CHSH168.3x10.0
CHSH168.3x12.0
CHSH177.8x6.0
CHSH177.8x8.0
CHSH177.8x10.0
CHSH177.8x12.0
CHSH193.7x6.0
CHSH193.7x8.0
CHSH193.7x10.0

Main structure: S355

CHSH101.6x4.0
CHSH101.6x6.0
CHSH101.6x8.0
CHSH101.6x10.0
CHSH139.7x4.0
CHSH139.7x6.0
CHSH139.7x8.0
CHSH139.7x10.0
CHSH139.7x12.0
CHSH168.3x4.0
CHSH168.3x6.0
CHSH168.3x8.0
CHSH168.3x10.0
CHSH168.3x12.0
CHSH177.8x6.0
CHSH177.8x8.0
CHSH177.8x10.0
CHSH177.8x12.0
CHSH193.7x6.0
CHSH193.7x8.0
CHSH193.7x10.0

Trusses under timber structure: S355

CHSH114.3x8.0
CHSH139.7x8.0
CHSH168.3x8.0

Appendix B

Timber cross sections

100.0×100.0	150.0×125.0	175.0×162.5	200.0×200.0
125.0×100.0	150.0×137.5	175.0×175.0	225.0×200.0
125.0×112.5	150.0×150.0	200.0×175.0	225.0×212.5
125.0×125.0	175.0×150.0	200.0×187.5	225.0×225.0

Appendix C

Wind loads

<u>General wind pressure</u>

For Abruzzo in Italy, zone 3: $\bar{v}_{b,0} = 27\ m/s$

$a_0 = 500\ m$

$k_0 = 0.020\ s^{-1}$

The height of the location: $a_s = 721\ m$

So that: $v_{b,0} = \bar{v}_{b,0} + k_0(a_s - a_0)$

$v_{b,0} = 27 + 0.020(721 - 500)$

$v_{b,0} = 31.42\ m/s$

According to the Italian annex: $c_{dir} = 1.0$ and $c_{season} = 1.0$

So that: $v_b = c_{dir} * c_{season} * v_{b,0}$

$v_b = 31.42\ m/s$

Terrain category IV gives: $z_0 = 1.0\ m$

$z_{min} = 10\ m$

$z_{0,II} = 0.05\ m$

$z_{max} = 200\ m$

$k_r = 0.19\left(\frac{z_0}{z_{0,II}}\right)^{0.07} = 0.234$

As the structure is below z_{min}: $c_r(z) = c_r(z_{min}) = k_r ln\left(\frac{z_{min}}{z_0}\right) = 0.234\ln\left(\frac{10}{1.0}\right)$

$c_r(z) = 0.539$

The Italian annex gives: $c_0(z) = 1.0$

$k_t = 1.0$

Up to 10 m height: $v_m = c_r(z) * c_0(z) * v_b = 0.539 * 1.0 * 31.42$

$v_m = 16.94\ m/s$

The Eurocode gives: $\sigma_v = k_r * v_b * k_t = 0.234 * 31.42 * 1.0$

$\sigma_v = 7.35$

$I_v = \frac{\sigma_v}{v_m} = \frac{7.35}{16.95} = 0.434$

The Italian annex gives: $\rho = 1.25\ kg/m^3$

Giving the general wind pressure: $q_p(z) = (1 + 7 * I_v) * \frac{1}{2} * \rho * {v_m}^2$

$$q_p(z) = (1 + 7 * 0.434) * \frac{1}{2} * 1.25 * 16.94^2$$

$$q_p(z) = 0.724\ kN/m^2$$

<u>Building with curved roof</u>

For the determination of the wind factors on the curved roof of a closed building, see Figure 108. For the community centre in questions, h = 0, and f/d = 0,5.

This gives the following factors: $c_{pe,10,A} = +0.8$

$$c_{pe,10,B} = -1.2$$

$$c_{pe,10,C} = -0.4$$

The internal pressure coefficients: $c_{pi} = +0.2 \ / -0.3$

This gives: $c_{p,net,A} = +0.8 - -0.3 = +1.1$

$$c_{p,net,B} = -1.2 - +0.2 = -1.4$$

$$c_{p,net,C} = +0.4 - +0.2 = -0.6$$

The wind pressure in these zones is: $w_p = c_{p,net} * q_p$

And thus: $w_{p,A} = +1.1 * 0.724 = +0.80\ kN/m^2$

$$w_{p,B} = -1.4 * 0.724 = -1.01\ kN/m^2$$

$$w_{p,C} = -0.6 * 0.724 = -0.43\ kN/m^2$$

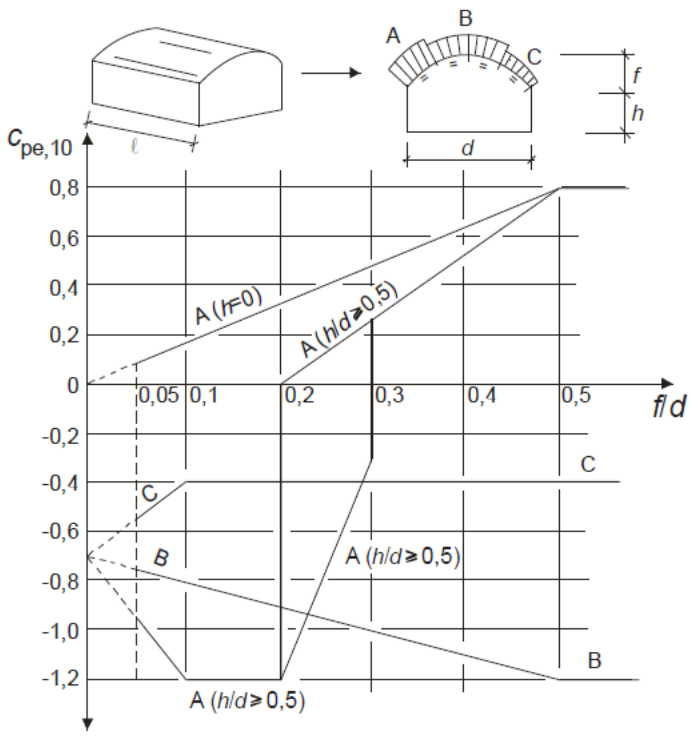

Figure 108: Determination $c_{pe,10}$ for curved roofs (Eurocode 1, Fig. 7.11)

Open roof

Table 19: $c_{p,net}$ values for open roof structures (Eurocode 1, Table 7.7)

Dakhelling α [°]	Blokkering φ	Globale kracht-coëfficiënt c_f	Nettodrukcoëfficiënten $c_{p,net}$ Zone-indeling 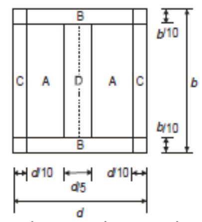 Zone A	Zone B	Zone C	Zone D
- 20	Maximaal voor alle φ	+ 0,7	+ 0,8	+ 1,6	+ 0,6	+ 1,7
	Minimaal voor φ = 0	- 0,7	- 0,9	- 1,3	- 1,6	- 0,6
	Minimaal voor φ = 1	- 1,3	- 1,5	- 2,4	- 2,4	- 0,6
- 15	Maximaal voor alle φ	+ 0,5	+ 0,6	+ 1,5	+ 0,7	+ 1,4
	Minimaal voor φ = 0	- 0,6	- 0,8	- 1,3	- 1,6	- 0,6
	Minimaal voor φ = 1	- 1,4	- 1,6	- 2,7	- 2,6	- 0,6
- 10	Maximaal voor alle φ	+ 0,4	+ 0,6	+ 1,4	+ 0,8	+ 1,1
	Minimaal voor φ = 0	- 0,6	- 0,8	- 1,3	- 1,5	- 0,6
	Minimaal voor φ = 1	- 1,4	- 1,6	- 2,7	- 2,6	- 0,6
- 5	Maximaal voor alle φ	+ 0,3	+ 0,5	+ 1,5	+ 0,8	+ 0,8
	Minimaal voor φ = 0	- 0,5	- 0,7	- 1,3	- 1,6	- 0,6
	Minimaal voor φ = 1	- 1,3	- 1,5	- 2,4	- 2,4	- 0,6
+ 5	Maximaal voor alle φ	+ 0,3	+ 0,6	+ 1,8	+ 1,3	+ 0,4
	Minimaal voor φ = 0	- 0,6	- 0,6	- 1,4	- 1,4	- 1,1
	Minimaal voor φ = 1	- 1,3	- 1,3	- 2,0	- 1,8	- 1,5
+ 10	Maximaal voor alle φ	+ 0,4	+ 0,7	+ 1,8	+ 1,4	+ 0,4
	Minimaal voor φ = 0	- 0,7	- 0,7	- 1,5	- 1,4	- 1,4
	Minimaal voor φ = 1	- 1,3	- 1,3	- 2,0	- 1,8	- 1,8
+ 15	Maximaal voor alle φ	+ 0,4	+ 0,9	+ 1,9	+ 1,4	+ 0,4
	Minimaal voor φ = 0	- 0,8	- 0,9	- 1,7	- 1,4	- 1,8
	Minimaal voor φ = 1	- 1,3	- 1,3	- 2,2	- 1,6	- 2,1
+ 20	Maximaal voor alle φ	+ 0,6	+ 1,1	+ 1,9	+ 1,5	+ 0,4
	Minimaal voor φ = 0	- 0,9	- 1,2	- 1,8	- 1,4	- 2,0
	Minimaal voor φ = 1	- 1,3	- 1,4	- 2,2	- 1,6	- 2,1
+ 25	Maximaal voor alle φ	+ 0,7	+ 1,2	+ 1,9	+ 1,6	+ 0,5
	Minimaal voor φ = 0	- 1,0	- 1,4	- 1,9	- 1,4	- 2,0
	Minimaal voor φ = 1	- 1,3	- 1,4	- 2,0	- 1,5	- 2,0
+ 30	Maximaal voor alle φ	+ 0,9	+ 1,3	+ 1,9	+ 1,6	+ 0,7
	Minimaal voor φ = 0	- 1,0	- 1,4	- 1,9	- 1,4	- 2,0
	Minimaal voor φ = 1	- 1,3	- 1,4	- 1,8	- 1,4	- 2,0
OPMERKING Positieve waarden duiden op een netto neerwaartse windbelasting, negatieve waarden duiden op een netto opwaartse windbelasting.						

For an open roof, the $c_{p,net}$ values are presented in Table 19. For an estimation of the coefficients on the open structure in the East and West zone during south wind (see 5.3.2), it is assumed that φ = 1, as shown in Figure 109.

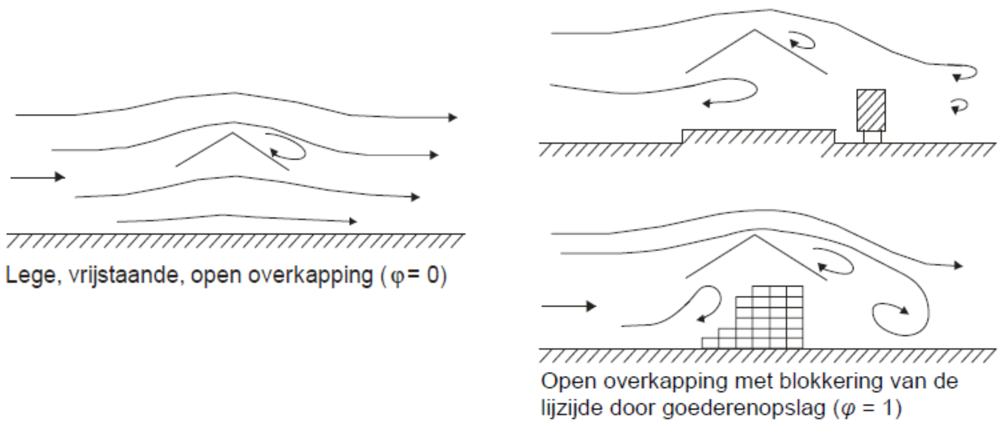

Figure 109: Open roofs (Eurocode 1, Fig. 7.15)

Free-standing walls

For the coefficient determination, the $c_{p,net}$ values for free-standing walls have also been taken into account, as shown in Table 20. As the façade consists out of separate, layered ETFE-parts, it is assumed there are a lot of openings, so that φ = 0.8.

Table 20: $c_{p,net}$ values for free-standing walls (Eurocode 1, Table 7.9)

Dichtheid	Zone		A	B	C	D
φ = 1	Zonder omgezette einden	$\ell/h \leq 3$	2,3	1,4	1,2	1,2
		$\ell/h = 5$	2,9	1,8	1,4	1,2
		$\ell/h \geq 10$	3,4	2,1	1,7	1,2
	Met omgezette einden met lengte $\geq h$ [a]		2,1	1,8	1,4	1,2
φ = 0,8			1,2	1,2	1,2	1,2

[a] Er mag lineair worden geïnterpoleerd bij omgezette einden met een lengte tussen 0,0 en *h*.

Building sides

The wind coefficients for vertical building facades have also been taken into account, especially for the side wind situation (see paragraph 5.3.4) – refer to Table 21 and Figure 110.

Table 21: $c_{pe,10}$ values for vertical sides of buildings (Eurocode 1, Table 7.1)

Zone	A		B		C		D		E	
h/d	$c_{pe,10}$	$c_{pe,1}$	$c_{pe,10}$	$c_{pe,1}$	$c_{pe,10}$	$c_{pe,1}$	$c_{pe,10}$	$c_{pe,1}$	$c_{pe,10}$	$c_{pe,1}$
5	-1,2	-1,4	-0,8	-1,1	-0,5		+0,8	+1,0	-0,7	
1	-1,2	-1,4	-0,8	-1,1	-0,5		+0,8	+1,0	-0,5	
≤ 0,25	-1,2	-1,4	-0,8	-1,1	-0,5		+0,7	+1,0	-0,3	

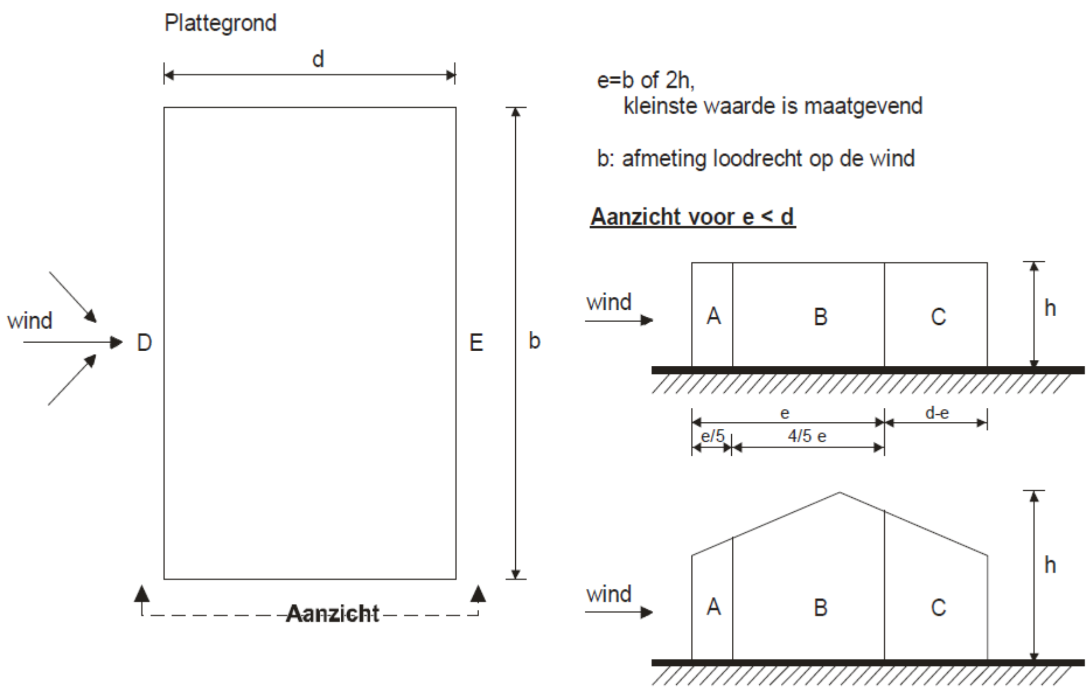

Figure 110: Zoning of vertical sides of buildings (Eurocode 1, Fig. 7.5)

Appendix D

Snow loads

Formula for the snow load: $s = \mu_i C_e C_t s_k$

In which: $C_e = 1.0$

$C_t = 1.0$

$$s_k = (0.498 * Z - 0.209) * \left(1 + \left(\frac{A}{452}\right)^2\right)$$

The zone number of the location: $Z = 2$

And the height above sea level: $A = 721 + 10 = 731\ m$

So that: $$s_k = (0.498 * 2 - 0.209) * \left(1 + \left(\frac{731}{452}\right)^2\right) = 2.85\ kN/m^2$$

The determination of the snow load coefficients μ_i is prescribed by Figure 111.

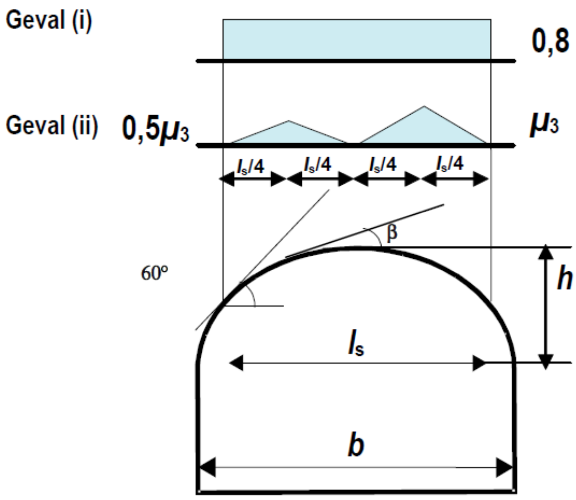

Figure 111: Snow load coefficients for cylinder roofs (Eurocode 1, Fig. 5.6)

The load configuration needs to be assessed for two situations, (i) in which the snow is distributed evenly, and (ii) in which the snow has been redistributed on top of the roof.

For β > 60° $\mu_3 = 0$

For β < 60° $\mu_3 = 0.2 + 10\ h/b < 2.0$

$\mu_3 = 0.2 + 10 * 10/20 = 5.2 > 2.0$

$\mu_3 = 2.0$

Case (i) $\mu = 0.8$

$s = \mu_i C_e C_t s_k = 0.8 * 1.0 * 1.0 * 2.85$

$s = 2.28\ kN/m^2$

Case (ii) $s_{peak,1} = 0.5\mu_3 s_k = 0.5 * 2.0 * 2.85 = 2.85\ kN/m^2$

$s_{peak,2} = \mu_3 s_k = 2.0 * 2.85 = 5.70\ kN/m^2$

Appendix E

Static seismic loads

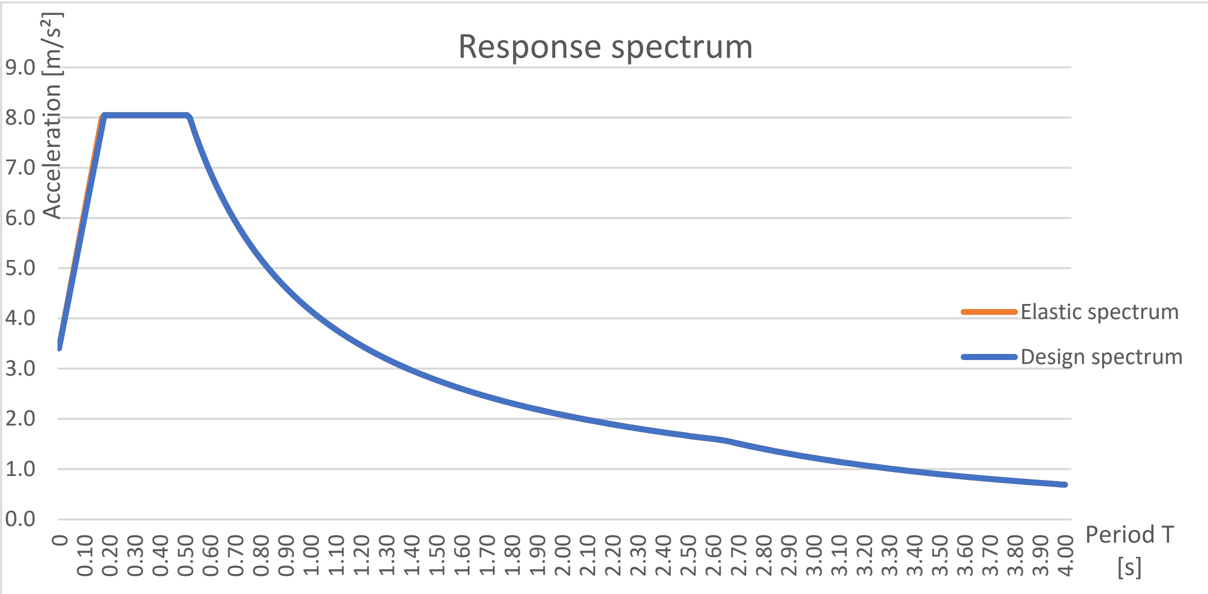

INPUT

Peak ground acceleration $a_g = 0.261\ g = 2.56\ m/s^2$

For L'Aquila: $F_o = 2.364$
$T_C{}^* = 0.347$

Categories C & T1: $S_T = 1.0$
$C_C = 1.49$
$S_S = 1.50$

Soil factor $S = S_S \cdot S_T = 1.5$

Viscous damping ratio $\xi = 5$

Damping factor $\eta = \sqrt{10/(5+\xi)} = 1$

Lower limit constant acc. branch $T_B = \frac{T_C}{3} = 0.172\ s$

Higher limit constant acc. branch $T_C = C_C \cdot T_C{}^* = 0.517\ s$

Beginning constant displ. response $T_D = 4.0 \cdot a_g + 1.6 = 2.644\ s$

To get from the elastic response spectrum to the design response spectrum for checks in the ULS/SLV, a factor of q_{lim} = 4.0 is used.

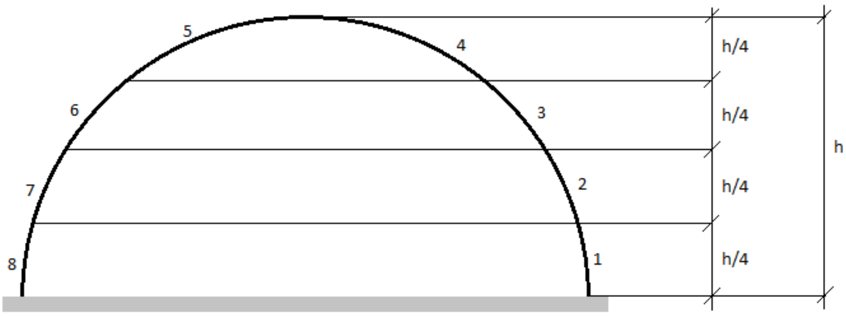

A_{tot} = 1885.1 m^2

100%

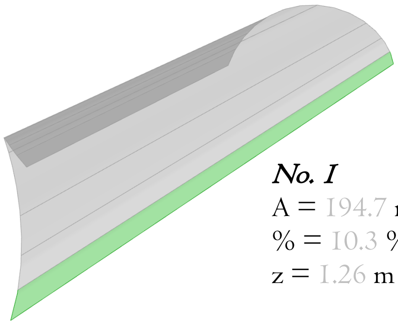

No. 1
A = 194.7 m²
% = 10.3 %
z = 1.26 m

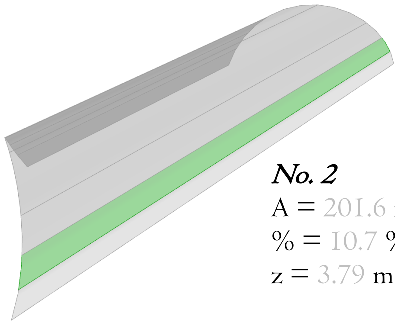

No. 2
A = 201.6 m²
% = 10.7 %
z = 3.79 m

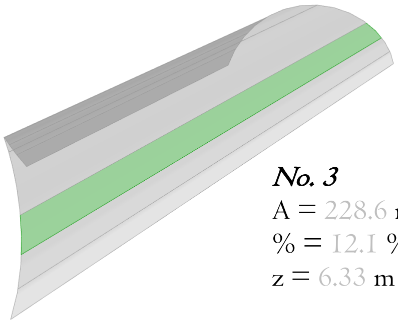

No. 3
A = 228.6 m²
% = 12.1 %
z = 6.33 m

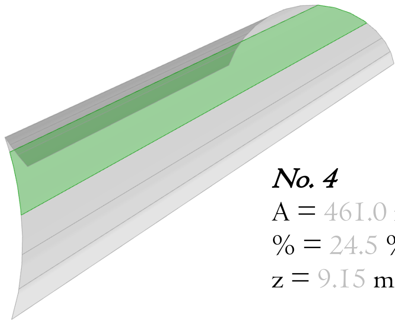

No. 4
A = 461.0 m²
% = 24.5 %
z = 9.15 m

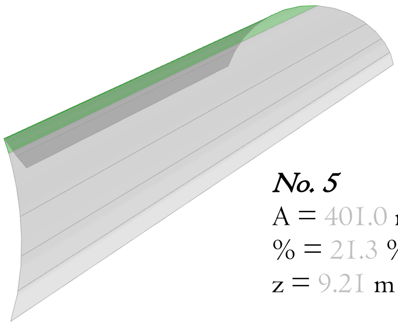

No. 5
A = 401.0 m²
% = 21.3 %
z = 9.21 m

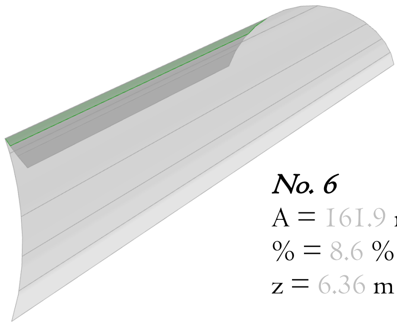

No. 6
A = 161.9 m²
% = 8.6 %
z = 6.36 m

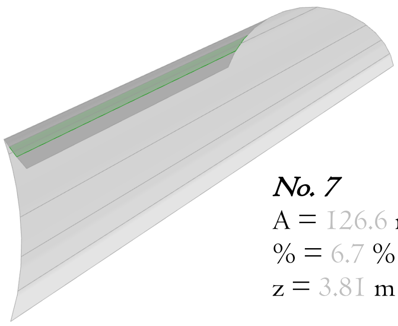

No. 7
A = 126.6 m²
% = 6.7 %
z = 3.81 m

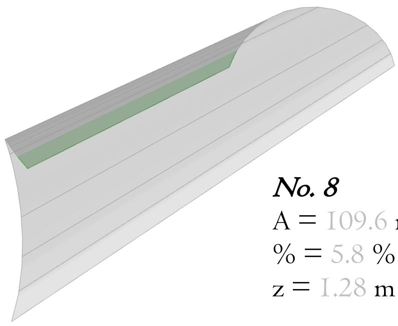

No. 8
A = 109.6 m²
% = 5.8 %
z = 1.28 m

LOAD FORMULA PER FRACTION

$$q_i = \frac{F_i}{A_i} = \frac{S_e(T) \cdot W_{tot} \cdot \frac{W_i \cdot z_i}{\sum W_j \cdot z_j}}{A_i}$$

Total weight structure $W_{tot} = \text{Grasshopper output}$

Weight per structure fraction $W_i = \%_i \cdot W_{tot}$

Natural frequency $T = \text{Grasshopper output}$

EXAMPLE

Element length: 1 m (7537 pieces). No hinges in basic geometry. Horizontals. Three trusses. CHSH193.7×10.0, S355.

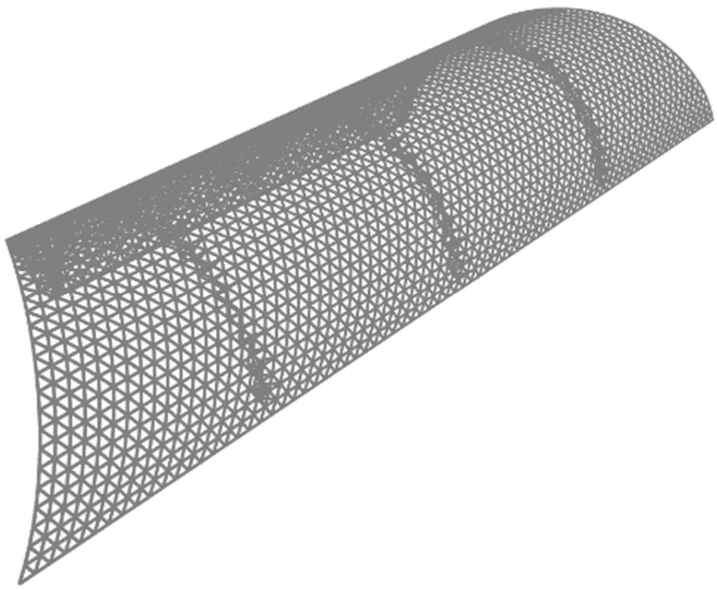

$W_{tot} = 341\,825\ kg$ (GH output)

$W_1 = 35\,642\ kg$

$W_2 = 36\,677\ kg$

$W_3 = 41\,745\ kg$

$W_4 = 84\,368\ kg$

$W_5 = 72\,741\ kg$

$W_6 = 28\,931\ kg$

$W_7 = 22\,365\ kg$

$W_8 = 19\,356\ kg$

$T = 0.578\ s$ (GH output)

$S_e = 1.798\ m/s^2$ (GH output)

$$\sum W_j \cdot z_j = 2\,278\,900\ kgm$$

No. 1

$$q_1 = \frac{S_e(T) \cdot W_{tot} \cdot \frac{W_i \cdot z_i}{\sum W_j \cdot z_j}}{A_i} = \frac{1.798 \cdot 341\,825 \cdot \frac{35\,642 \cdot 1.26}{2\,278\,900}}{194.7} = 0.062\ kN/m^2$$

No. 2

$$q_2 = \frac{S_e(T) \cdot W_{tot} \cdot \frac{W_i \cdot z_i}{\sum W_j \cdot z_j}}{A_i} = \frac{1.798 \cdot 341\,825 \cdot \frac{36\,677 \cdot 3.78}{2\,278\,900}}{201.6} = 0.187\ kN/m^2$$

No. 3

$$q_3 = \frac{S_e(T) \cdot W_{tot} \cdot \frac{W_i \cdot z_i}{\sum W_j \cdot z_j}}{A_i} = \frac{1.798 \cdot 341\,825 \cdot \frac{41\,745 \cdot 6.33}{2\,278\,900}}{228.6} = 0.313\ kN/m^2$$

No. 4

$$q_4 = \frac{S_e(T) \cdot W_{tot} \cdot \frac{W_i \cdot z_i}{\sum W_j \cdot z_j}}{A_i} = \frac{1.798 \cdot 341\,825 \cdot \frac{84\,368 \cdot 9.15}{2\,278\,900}}{461.0} = 0.453\ kN/m^2$$

No. 5

$$q_5 = \frac{S_e(T) \cdot W_{tot} \cdot \frac{W_i \cdot z_i}{\sum W_j \cdot z_j}}{A_i} = \frac{1.798 \cdot 341\,825 \cdot \frac{72\,741 \cdot 9.21}{2\,278\,900}}{401.0} = 0.457\ kN/m^2$$

No.

$$q_6 = \frac{S_e(T) \cdot W_{tot} \cdot \frac{W_i \cdot z_i}{\sum W_j \cdot z_j}}{A_i} = \frac{1.798 \cdot 341\,825 \cdot \frac{28\,931 \cdot 6.36}{2\,278\,900}}{161.9} = 0.314\ kN/m^2$$

No. 7

$$q_7 = \frac{S_e(T) \cdot W_{tot} \cdot \frac{W_i \cdot z_i}{\sum W_j \cdot z_j}}{A_i} = \frac{1.798 \cdot 341\,825 \cdot \frac{22\,365 \cdot 3.81}{2\,278\,900}}{126.6} = 0.188\ kN/m^2$$

No. 8

$$q_8 = \frac{S_e(T) \cdot W_{tot} \cdot \frac{W_i \cdot z_i}{\sum W_j \cdot z_j}}{A_i} = \frac{1.798 \cdot 341\,825 \cdot \frac{19\,356 \cdot 1.28}{2\,278\,900}}{109.6} = 0.063\ kN/m^2$$

The same method is carried out in the X-direction, for which the eigenperiod is slightly lower (stiffer).

Appendix F

Load combinations

The Eurocode (EN 1990, 2011) and the Italian national annex (UNI-EN 1990, 2007) prescribed the following load combinations:

SLS combination

$$G_1 + G_2 + \psi_{11} \cdot Q_{k1} + \psi_{22} \cdot Q_{k2} + \psi_{23} \cdot Q_{k3} + \cdots$$

Assumed in the SLS combinations, is that there won't be any maintenance on the roof during heavy roof loading due to snow and/or wind.

ULS combination

$$\gamma_{G1} \cdot G_1 + \gamma_{G2} \cdot G_2 + \gamma_{Q1} \cdot Q_{k1} + \gamma_{Q2} \cdot \psi_{02} \cdot Q_{k2} + \gamma_{Q3} \cdot \psi_{03} \cdot Q_{k3} + \cdots$$

SLV combinations

$$E + G_1 + G_2 + \psi_{21} \cdot Q_{k1} + \psi_{22} \cdot Q_{k2} + \cdots$$

In which:

G	permanent load
Q	imposed load
E	earthquake load
ψ	combination factor
γ	partial factor

Appendix G

Environmental impact analysis

CES EduPack 2018: Eco-values AISI 1020 (≈S235)

Primary material production: energy, CO2 and water

Embodied energy, primary production	30.8	-	33.9	MJ/kg

Sources

19.4 MJ/kg (Dhingra, Overly Davis, 1999); 23 MJ/kg (Norgate, Jahanshahi, Rankin, 2007); 27.9 MJ/kg (Ecoinvent v2.2); 29.2 MJ/kg (Hammond and Jones, 2008); 32.8 MJ/kg (Hammond and Jones, 2008); 34.7 MJ/kg (Hammond and Jones, 2008); 35.4 MJ/kg (Hammond and Jones, 2008); 37.2 MJ/kg (Sullivan and Gaines, 2010); 38 MJ/kg (Hammond and Jones, 2008); 45.4 MJ/kg (Hammond and Jones, 2008)

CO2 footprint, primary production	2.26	-	2.49	kg/kg

Sources

0.396 kg/kg (Voet van der and Oers, van, 2003); 1.75 kg/kg (Ecoinvent v2.2); 1.81 kg/kg (Voet, van der and Oers, van, 2003); 2.23 kg/kg (Voet, van der and Oers, van, 2003); 2.3 kg/kg (Norgate, Jahanshahi, Rankin, 2007); 2.74 kg/kg (Hammond and Jones, 2008); 2.77 kg/kg (Hammond and Jones, 2008); 2.87 kg/kg (Hammond and Jones, 2008); 2.89 kg/kg (Hammond and Jones, 2008); 3.03 kg/kg (Hammond and Jones, 2008); 3.27 kg/kg (Hammond and Jones, 2008)

Water usage	* 43.1	-	47.7	l/kg

Processing energy, CO2 footprint & water

Casting energy	* 11	-	12.2	MJ/kg
Casting CO2	* 0.826	-	0.913	kg/kg
Casting water	* 20.9	-	31.3	l/kg
Roll forming, forging energy	* 2.65	-	2.93	MJ/kg
Roll forming, forging CO2	* 0.199	-	0.22	kg/kg
Roll forming, forging water	* 2.69	-	4.03	l/kg
Extrusion, foil rolling energy	* 5.02	-	5.55	MJ/kg
Extrusion, foil rolling CO2	* 0.377	-	0.416	kg/kg
Extrusion, foil rolling water	* 3.7	-	5.55	l/kg
Wire drawing energy	* 18	-	19.9	MJ/kg
Wire drawing CO2	* 1.35	-	1.5	kg/kg
Wire drawing water	* 6.8	-	10.2	l/kg
Metal powder forming energy	* 38.9	-	42.8	MJ/kg
Metal powder forming CO2	* 3.11	-	3.43	kg/kg
Metal powder forming water	* 42.4	-	63.5	l/kg
Vaporization energy	* 1.09e4	-	1.2e4	MJ/kg
Vaporization CO2	* 815	-	901	kg/kg
Vaporization water	* 4.53e3	-	6.8e3	l/kg
Coarse machining energy (per unit wt removed)	* 0.83	-	0.918	MJ/kg
Coarse machining CO2 (per unit wt removed)	* 0.0623	-	0.0688	kg/kg
Fine machining energy (per unit wt removed)	* 4.03	-	4.45	MJ/kg
Fine machining CO2 (per unit wt removed)	* 0.302	-	0.334	kg/kg
Grinding energy (per unit wt removed)	* 7.58	-	8.38	MJ/kg
Grinding CO2 (per unit wt removed)	* 0.568	-	0.628	kg/kg
Non-conventional machining energy (per unit wt removed)	* 109	-	120	MJ/kg
Non-conventional machining CO2 (per unit wt removed)	* 8.15	-	9.01	kg/kg

CES EduPack 2018: Eco-values AISI 1040 (≈S355)

Primary material production: energy, CO2 and water

Embodied energy, primary production	30.8	-	33.9	MJ/kg

Sources

19.4 MJ/kg (Dhingra, Overly Davis, 1999); 23 MJ/kg (Norgate, Jahanshahi, Rankin, 2007); 27.9 MJ/kg (Ecoinvent v2.2); 29.2 MJ/kg (Hammond and Jones, 2008); 32.8 MJ/kg (Hammond and Jones, 2008); 34.7 MJ/kg (Hammond and Jones, 2008); 35.4 MJ/kg (Hammond and Jones, 2008); 37.2 MJ/kg (Sullivan and Gaines, 2010); 38 MJ/kg (Hammond and Jones, 2008); 45.4 MJ/kg (Hammond and Jones, 2008)

CO2 footprint, primary production	2.26	-	2.49	kg/kg

Sources

0.396 kg/kg (Voet, van der and Oers, van, 2003); 1.75 kg/kg (Ecoinvent v2.2); 1.81 kg/kg (Voet, van der and Oers, van, 2003); 2.23 kg/kg (Voet, van der and Oers, van, 2003); 2.3 kg/kg (Norgate, Jahanshahi, Rankin, 2007); 2.74 kg/kg (Hammond and Jones, 2008); 2.77 kg/kg (Hammond and Jones, 2008); 2.87 kg/kg (Hammond and Jones, 2008); 2.89 kg/kg (Hammond and Jones, 2008); 3.03 kg/kg (Hammond and Jones, 2008); 3.27 kg/kg (Hammond and Jones, 2008)

Water usage	* 43.6	-	48.2	l/kg

Processing energy, CO2 footprint & water

Casting energy	* 10.9	-	12.1	MJ/kg
Casting CO2	* 0.819	-	0.906	kg/kg
Casting water	* 20.7	-	31	l/kg
Roll forming, forging energy	* 3.11	-	3.44	MJ/kg
Roll forming, forging CO2	* 0.233	-	0.258	kg/kg
Roll forming, forging water	* 2.88	-	4.32	l/kg
Extrusion, foil rolling energy	* 5.94	-	6.57	MJ/kg
Extrusion, foil rolling CO2	* 0.446	-	0.492	kg/kg
Extrusion, foil rolling water	* 4.09	-	6.14	l/kg
Wire drawing energy	* 21.5	-	23.8	MJ/kg
Wire drawing CO2	* 1.61	-	1.78	kg/kg
Wire drawing water	* 8.1	-	12.2	l/kg
Metal powder forming energy	* 38.1	-	42	MJ/kg
Metal powder forming CO2	* 3.05	-	3.36	kg/kg
Metal powder forming water	* 41.5	-	62.2	l/kg
Vaporization energy	* 1.09e4	-	1.2e4	MJ/kg
Vaporization CO2	* 815	-	901	kg/kg
Vaporization water	* 4.53e3	-	6.8e3	l/kg
Coarse machining energy (per unit wt removed)	* 0.899	-	0.994	MJ/kg
Coarse machining CO2 (per unit wt removed)	* 0.0674	-	0.0745	kg/kg
Fine machining energy (per unit wt removed)	* 4.72	-	5.21	MJ/kg
Fine machining CO2 (per unit wt removed)	* 0.354	-	0.391	kg/kg
Grinding energy (per unit wt removed)	* 8.96	-	9.9	MJ/kg
Grinding CO2 (per unit wt removed)	* 0.672	-	0.743	kg/kg
Non-conventional machining energy (per unit wt removed)	* 109	-	120	MJ/kg
Non-conventional machining CO2 (per unit wt removed)	* 8.15	-	9.01	kg/kg

CES EduPack 2018: Eco-values Chestnut

Primary material production: energy, CO2 and water

Embodied energy, primary production	11.6	-	12.8	MJ/kg
Sources 0.5 MJ/kg (Ximenes, 2006); 2 MJ/kg (Ximenes, 2006); 9.1 MJ/kg (Hammond and Jones, 2008); 11.6 MJ/kg (Hubbard and Bowe, 2010); 23.7 MJ/kg (Ecoinvent v2.2); 26 MJ/kg (Ecoinvent v2.2)				
CO2 footprint, primary production	0.574	-	0.633	kg/kg
Sources 0.229 kg/kg (Ecoinvent v2.2); 0.412 kg/kg (Ecoinvent v2.2); 0.862 kg/kg (Hammond and Jones, 2008); 0.909 kg/kg (Hubbard and Bowe, 2010)				
Water usage	* 665	-	735	l/kg

Processing energy, CO2 footprint & water

Coarse machining energy (per unit wt removed)	* 1.2	-	1.33	MJ/kg
Coarse machining CO2 (per unit wt removed)	* 0.0901	-	0.0995	kg/kg
Fine machining energy (per unit wt removed)	* 7.73	-	8.55	MJ/kg
Fine machining CO2 (per unit wt removed)	* 0.58	-	0.641	kg/kg
Grinding energy (per unit wt removed)	* 15	-	16.6	MJ/kg
Grinding CO2 (per unit wt removed)	* 1.12	-	1.24	kg/kg

CES EduPack 2018: Eco-values Azobé

Primary material production: energy, CO2 and water

Embodied energy, primary production	* 11.6	-	12.8	MJ/kg
CO2 footprint, primary production	* 0.574	-	0.633	kg/kg
Water usage	* 665	-	735	l/kg

Processing energy, CO2 footprint & water

Coarse machining energy (per unit wt removed)	* 1.35	-	1.49	MJ/kg
Coarse machining CO2 (per unit wt removed)	* 0.101	-	0.112	kg/kg
Fine machining energy (per unit wt removed)	* 9.19	-	10.2	MJ/kg
Fine machining CO2 (per unit wt removed)	* 0.689	-	0.762	kg/kg
Grinding energy (per unit wt removed)	* 17.9	-	19.8	MJ/kg
Grinding CO2 (per unit wt removed)	* 1.34	-	1.48	kg/kg

Determination eco-values joint steel structure

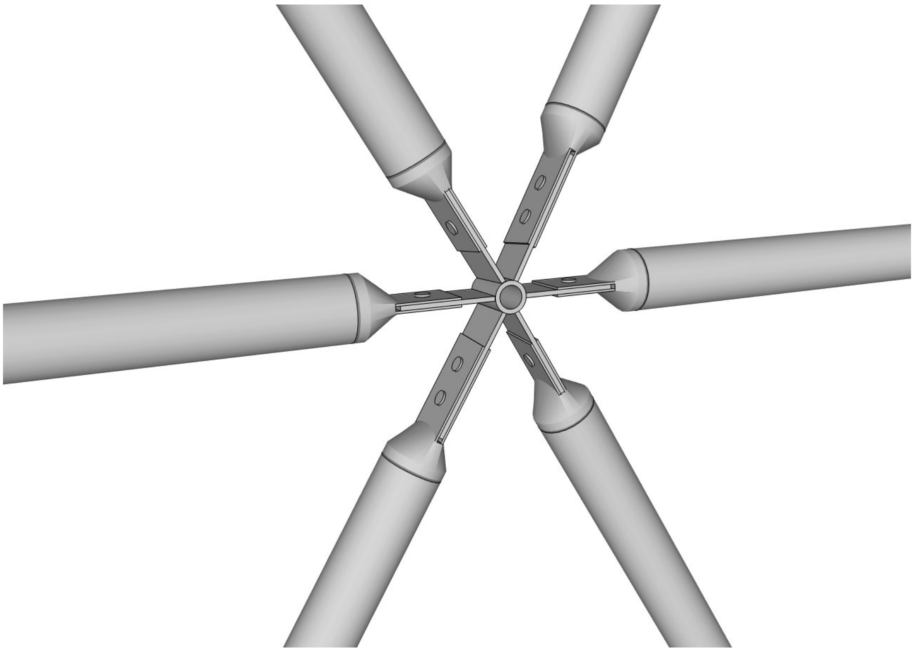

Assumed steel:	AISI 1040 (≈ S355)					
Average cross section:	168.3 mm					
Plates (t = 8 mm)	*Rigids*	*2×(168.3×300×8)*	=	*0.00081m³*		
	Hinges	*4×(168.3×200×8)*	=	*0.00108m³*		
	Circular core	*(60π)×8×168.3*	=	*0.00025m³*		
	TOTAL		=	*0.00214m³*		
	Density		=	*7850 kg/m³*		
				TOTAL	=	*16.8 kg*
	Manufacturing method:	roll forming				
	End of life potential:	66.7% for both energy and CO_2				
Cast elements	Assumption based on models' volume:			*TOTAL*	=	*30 kg*
	Manufacturing method:	casting				
	End of life:	66.7% for both energy and CO_2				
Welds:	*Joint piece*	*6×2×168.3*	=	*2.02m*		
	Elements	*6×(163.8π)*	=	*3.17m*		
				TOTAL	=	*5.19 m*
Fasteners:	Large fasteners			*TOTAL*	=	*8 pieces*
Transport:	600 km					

Determination eco-values joint timber structure

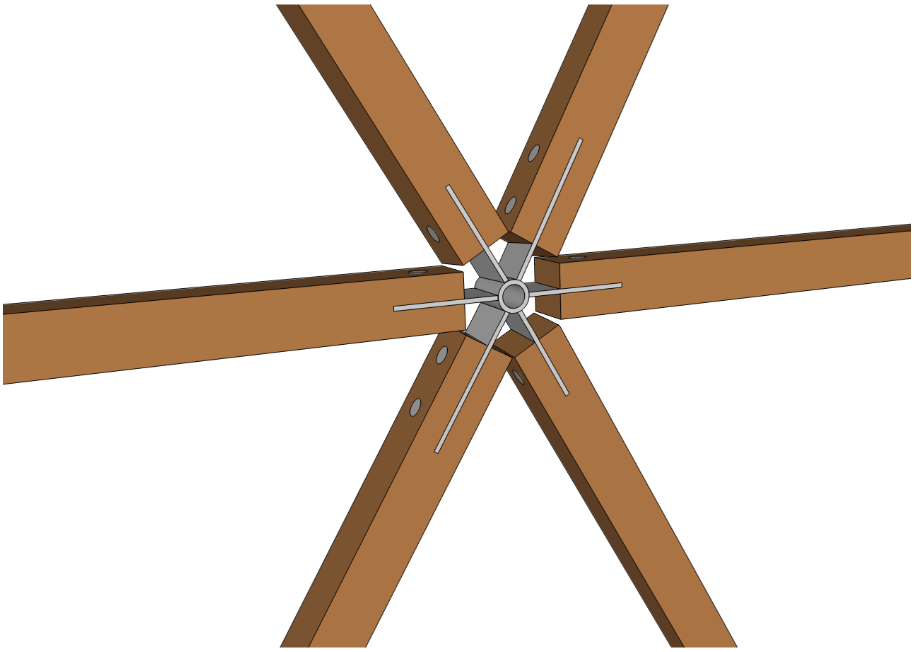

Assumed steel:	AISI 1040 (≈ S355)					
Average cross section:	175 mm					
Plates (t = 8 mm)	*Rigids*	$2\times(175\times300\times8)$	=	$0.00084 m^3$		
	Hinges	$4\times(175\times200\times8)$	=	$0.00112 m^3$		
	Circular core	$(60\pi)\times8\times175$	=	$0.00026\ m^3$		
	TOTAL		=	$0.00222\ m^3$		
	Density		=	$7850\ kg/m^3$		
				TOTAL	=	*17.4 kg*

Manufacturing method: roll forming

End of life potential: 66.7% for both energy and CO_2

Welds:	*Joint piece*	$6\times2\times175$	=	$2.1 m$		
				TOTAL	=	*2.1 m*
Fasteners:	Large fasteners			*TOTAL*	=	*8 pieces*
Transport:	600 km					

Appendix H

Determination of load per bolt

<u>Axial loads</u>

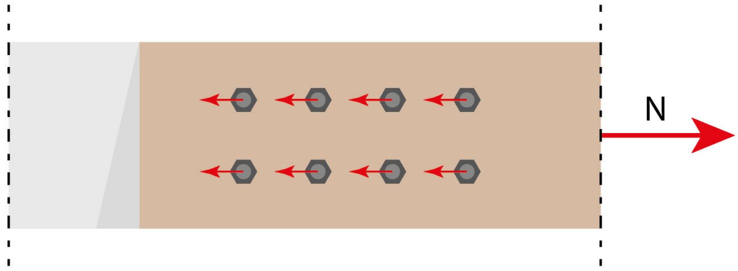

Figure 112: Distribution axial loads among bolts

In case of a bolt distribution with bolts of equal sizes, axial loads have been assumed to be evenly divided over the number of bolts n:

$$F_{bolt,N} = \frac{N}{n} \tag{24}$$

In which:

$F_{bolt,N}$	bolt load due to axial load
N	axial load

<u>Shear loads</u>

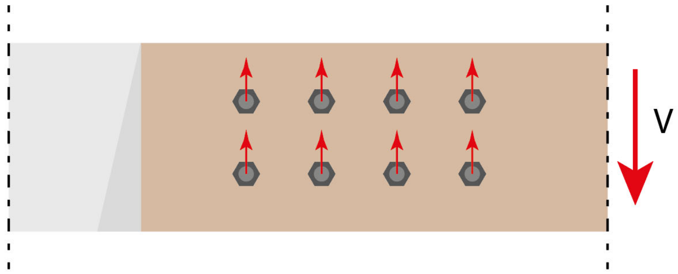

Figure 113: Distribution shear loads among bolts

In case of a bolt distribution with bolts of equal sizes, shear loads have been assumed to be evenly divided over the number of bolts n:

$$F_{bolt,V} = \frac{V}{n} \tag{25}$$

In which:

$F_{bolt,V}$	bolt load due to shear load
V	shear load

Bending loads

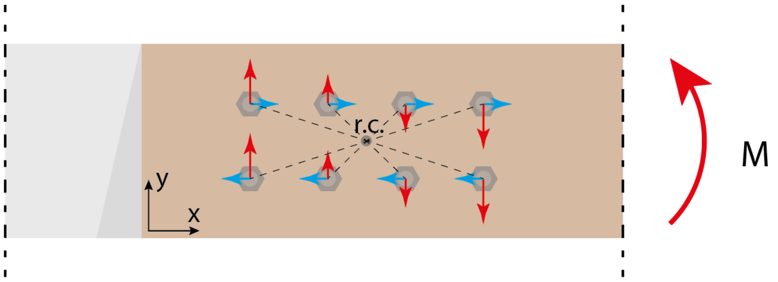

Figure 114: Distribution bending loads among bolts

The loads occuring in the bolts due to a bending moment M are a little less straight-forward. They need to be calculated using the polar moment of inertia of the bolt group.

$$I_p = \sum_{i=1}^{n} {r_i}^2 A_i \tag{26}$$

In which:

I_p	polar moment of inertia of the bolt group
r_i	distance from the bolt to the rotational centre (r.c.)
A_i	bolt area

The horizontal and vertical load component per bolt can be calculated using the polar moment of inertia:

$$F_{bolt,M,x} = \frac{A_i M c_y}{I_p} \tag{27}$$

$$F_{bolt,M,y} = \frac{A_i M c_x}{I_p} \tag{28}$$

In which:

$F_{bolt,M,x}$	horizontal bolt load component due to moment
$F_{bolt,M,y}$	vertical bolt load component due to moment
$c_{y,i}$	vertical distance from bolt to the rotational centre (r.c.)
$c_{x,i}$	horizontal distance from bolt to the rotational centre (r.c.)

Resulting load and angle with grain

$$F_{bolt,tot} = \sqrt{\left(F_{bolt,N} + F_{bolt,M,x}\right)^2 + \left(F_{bolt,V} + F_{bolt,M,y}\right)^2} \tag{29}$$

$$\alpha = \tan^{-1}\left(\frac{F_{bolt,V} + F_{bolt,M,y}}{F_{bolt,N} + F_{bolt,M,x}}\right) \tag{30}$$

Appendix J

Eigenmodes with active masses

Mode	Natural frequency	Natural period	Effective Modal Mass Factor	
No.	f [Hz]	T [s]	f_{meX} [-]	f_{meY} [-]
1	1.630	0.613	0.000	**0.900**
2	3.292	0.304	0.005	0.000
3	3.410	0.293	0.000	0.005
4	3.776	0.265	0.024	0.000
5	4.233	0.236	0.003	0.000
7	4.669	0.214	0.003	0.000
9	5.122	0.195	0.000	0.004
10	5.338	0.187	0.003	0.000
11	5.427	0.184	0.000	0.011
13	5.560	0.180	0.013	0.000
14	5.805	0.172	0.000	0.007
15	6.365	0.157	0.041	0.000
19	7.133	0.140	0.018	0.000
22	7.808	0.128	0.002	0.000
23	7.965	0.126	0.001	0.000
24	8.098	0.123	0.000	0.002
27	8.323	0.120	0.000	0.002
28	8.449	0.118	0.004	0.000
29	8.527	0.117	0.000	0.004
31	8.776	0.114	0.002	0.000
32	8.797	0.114	0.000	0.006
36	9.427	0.106	0.023	0.000
37	9.554	0.105	0.000	0.001
38	9.774	0.102	0.050	0.000
39	9.959	0.100	0.019	0.000
41	10.102	0.099	0.005	0.000
43	10.193	0.098	0.000	0.001
44	10.545	0.095	0.009	0.000
46	10.800	0.093	0.000	0.002
47	10.849	0.092	0.087	0.000
49	10.983	0.091	0.052	0.000
51	11.171	0.090	0.030	0.000
52	11.262	0.089	0.015	0.000
54	11.564	0.086	0.057	0.000
57	11.846	0.084	**0.164**	0.000
59	12.071	0.083	0.004	0.000

Mode	Natural frequency	Natural period	Effective Modal Mass Factor	
No.	f [Hz]	T [s]	f_{meX} [-]	f_{meY} [-]
64	12.324	0.081	0.028	0.000
65	12.428	0.080	0.073	0.000
66	12.556	0.080	0.040	0.000
69	12.687	0.079	0.001	0.000
73	13.066	0.077	0.004	0.000
76	13.328	0.075	0.002	0.000
81	13.742	0.073	0.002	0.000
84	13.882	0.072	0.004	0.000
85	13.894	0.072	0.000	0.001
90	14.363	0.070	0.001	0.000
94	14.657	0.068	0.000	0.001
96	14.702	0.068	0.003	0.000
98	14.829	0.067	0.000	0.001
99	14.902	0.067	0.000	0.001
101	15.090	0.066	0.001	0.000
102	15.123	0.066	0.001	0.000
103	15.144	0.066	0.000	0.001
106	15.310	0.065	0.001	0.000
108	15.483	0.065	0.001	0.000
112	15.654	0.064	0.002	0.000
113	15.784	0.063	0.001	0.000
115	15.827	0.063	0.003	0.000
118	15.984	0.063	0.002	0.000
120	16.060	0.062	0.001	0.000
123	16.247	0.062	0.001	0.000
126	16.376	0.061	0.001	0.000
132	16.615	0.060	0.002	0.000
133	16.660	0.060	0.001	0.000
138	16.800	0.060	0.001	0.000
149	17.227	0.058	0.001	0.000
150	17.257	0.058	0.001	0.000
Sum	---	---	0.817	0.954

Appendix K

Elastic spectra of L'Aquila per limit state

Table 22: Properties elastic response spectra, L'Aquila, Italy

SLO: Elastic Spectra			
a_g [g]	0.079	S	1.500
F_0	2.399	α	0.5
T^*_c [s]	0.272	η	1.00
C_u	1	T_B	0.135
V_N [years]	50	T_c	0.405
V_R [years]	50	T_D	1.916
P_{VR} [%]	81		
T_R [years]	30		
Cat. di sottosuolo	C		
Cat. di topografica	T1		
S_S	1.500		
S_T	1		
C_c	1.490		
ξ [%]	5		

SLD: Elastic Spectra			
a_g [g]	0.104	S	1.500
F_0	2.332	α	0.5
T^*_c [s]	0.281	η	1.00
C_u	1	T_B	0.140
V_N [years]	50	T_c	0.419
V_R [years]	50	T_D	2.016
P_{VR} [%]	63		
T_R [years]	50		
Cat. di sottosuolo	C		
Cat. di topografica	T1		
S_S	1.500		
S_T	1		
C_c	1.490		
ξ [%]	5		

SLV: Elastic Spectra			
a_g [g]	0.261	S	1.500
F_0	2.364	α	0.5
T^*_c [s]	0.347	η	1.00
C_u	1	T_B	0.172
V_N [years]	50	T_c	0.517
V_R [years]	50	T_D	2.644
P_{VR} [%]	10		
T_R [years]	475		
Cat. di sottosuolo	C		
Cat. di topografica	T1		
S_S	1.500		
S_T	1		
C_c	1.490		
ξ [%]	5		

SLC: Elastic Spectra			
a_g [g]	0.334	S	1.500
F_0	2.400	α	0.5
T^*_c [s]	0.364	η	1.00
C_u	1	T_B	0.181
V_N [years]	50	T_c	0.542
V_R [years]	50	T_D	2.936
P_{VR} [%]	5		
T_R [years]	975		
Cat. di sottosuolo	C		
Cat. di topografica	T1		
S_S	1.500		
S_T	1		
C_c	1.490		
ξ [%]	5		

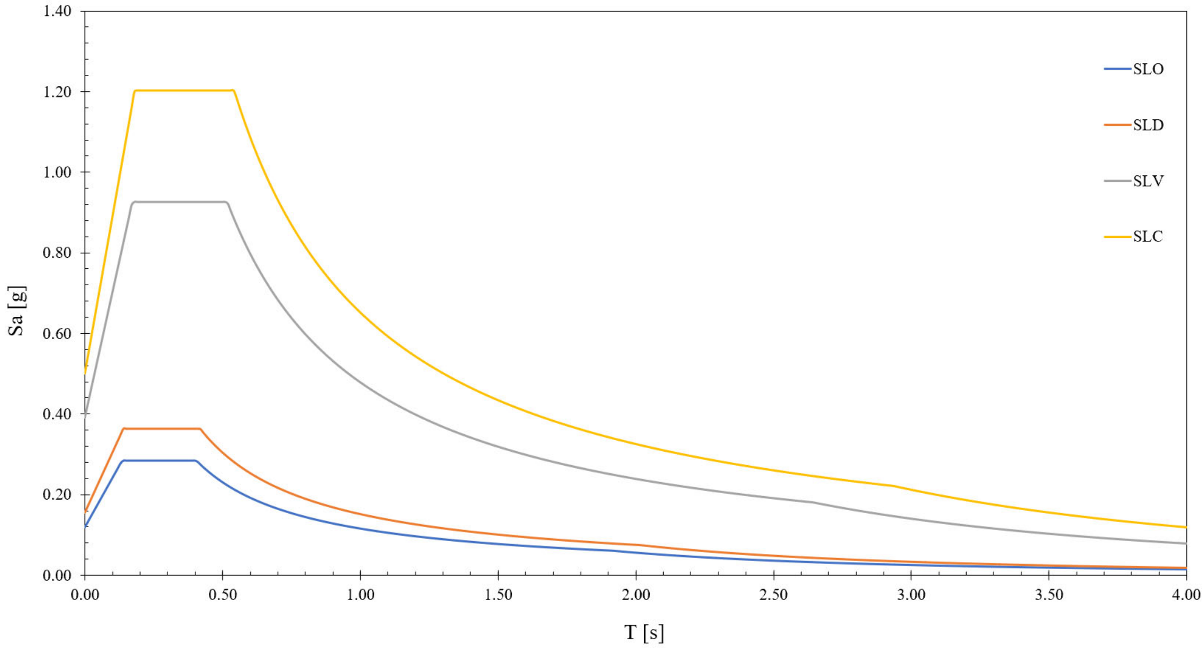

Figure 115: Elastic response spectra, L'Aquila, Italy